Queen Charlotte Sound / Tōtaranui and

Tory Channel / Kura Te Au (HS51) Survey

What lies beneath?

Guide to Survey Results and Graphical Portfolio

Part 2

Surveyed for Land Information New Zealand and Marlborough District Council

Prepared by:
NIWA
Neil H.L., Mackay K., Wilcox S., Kane T., Lamarche G., Wallen B., Orpin A., Steinmetz T., Pallentin A. 2018. What lies beneath? Guide to Survey Results and Graphical Portfolio, Queen Charlotte Sound/Tōtaranui and Tory Channel/Kura Te Au (HS51) Survey. NIWA Client Report 2018085WN.

For any information regarding this report please contact:

Helen Neil
National Projects Manager
+64-4-386 0375
helen.neil@niwa.co.nz

National Institute of Water & Atmospheric Research Ltd
Private Bag 14901
Kilbirnie, Wellington 6241

NIWA CLIENT REPORT No: 2018085WN
Report date: 30 May 2018
NIWA Project: LIN17301

Revision	Description	Date
Original 1.0	Report rendered to client	30 May 2018

Quality Assurance Statement		
H.L. Neil	Compiled By	Helen Neil
Alan Orpin	Reviewed by:	Alan Orpin Geoffroy Lamarche International reviewers: Margaret Doolan (Geological Survey of Norway) Vanessa Lucieer (Institute of Marine and Antarctic Studies, University of Tasmania) Xavier Lurton (Ifremer, France)
H.L. Neil	Formatting checked by:	Helen Neil
Andrew Laing	Approved for release by:	Andrew Laing

Front cover image: Queen Charlotte Sound/Tōtaranui and Tory Channel/Kura Te Au. NIWA Chart, Miscellaneous Series 101. Neil H.L., Mackay K., Mackay E.J., Wilcox S., Smith R. 2018.

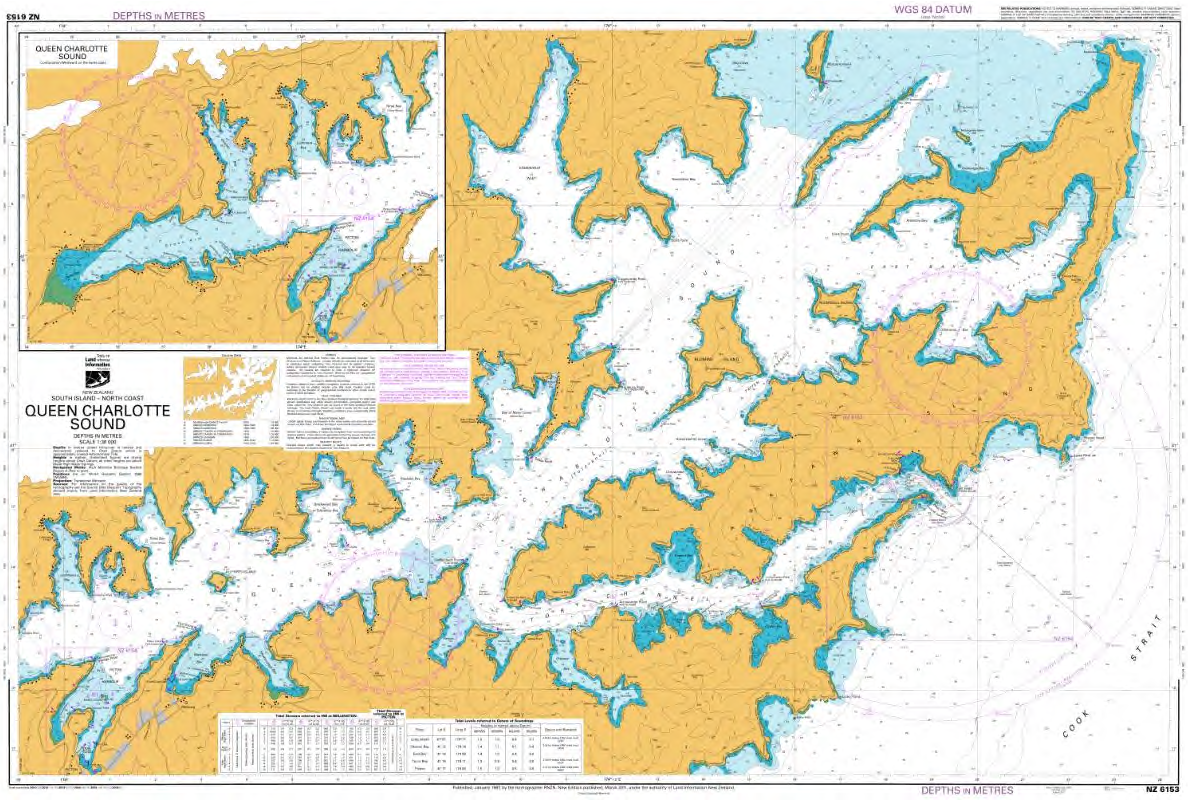

Frontispiece Figure 1: Chart NZ6153 – Queen Charlotte Sound.

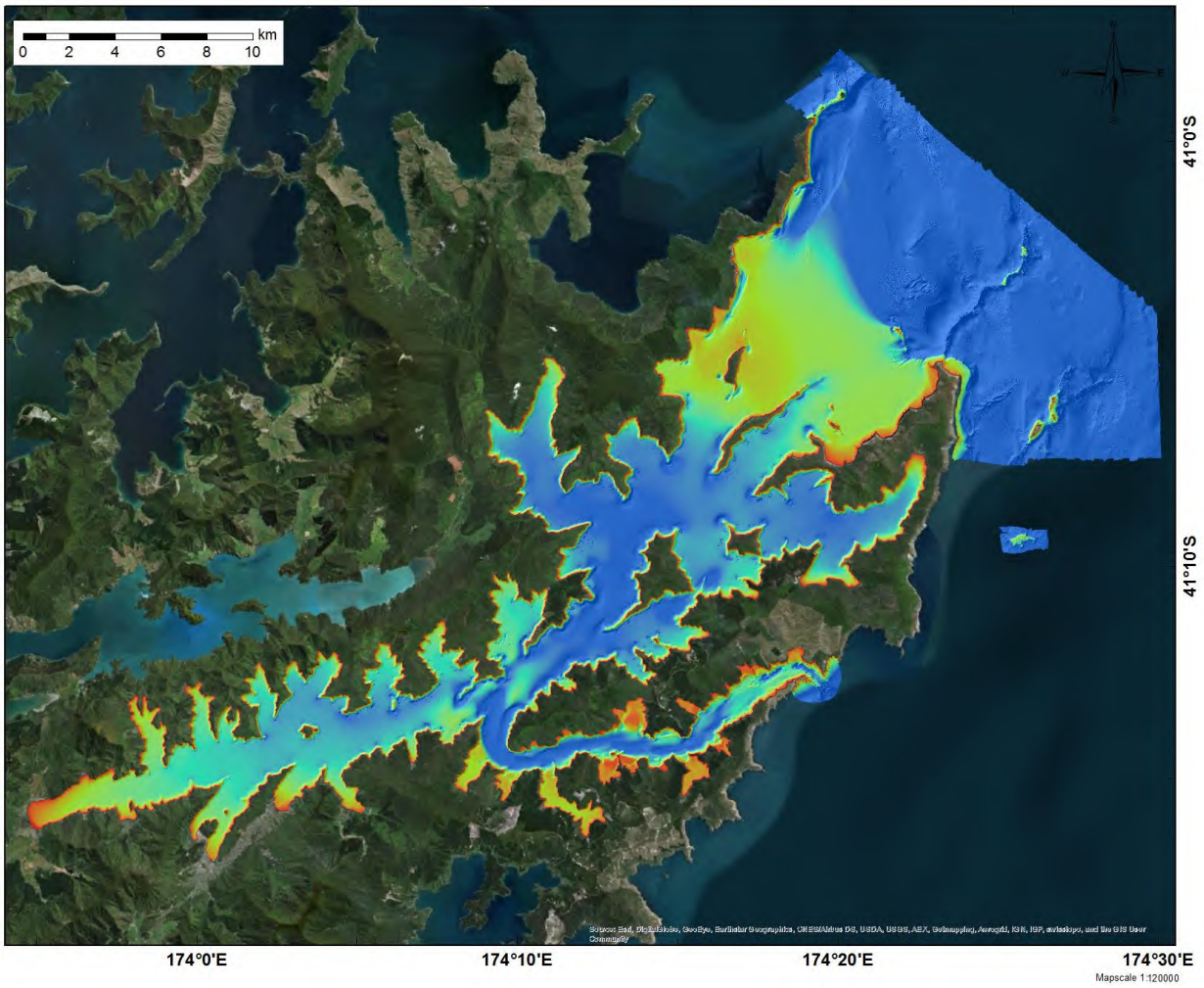

Frontispiece Figure 2: Queen Charlotte Sound / Tōtaranui and Tory Channel / Kura Te Au Hydrographic Survey (HS51) Survey Coverage. (2 m sun-illuminated digital elevation model)

Contents

Tables

Part 2

Appendices

Figures

Part 2

Appendices

Executive summary

The National Institute of Water and Atmospheric Research Ltd (NIWA) was contracted in October 2016 by Land Information New Zealand (LINZ) to undertake hydrographic surveying services for the Queen Charlotte Sound / Tōtaranui and Tory Channel / Kura Te Au Hydrographic Survey (HS51). This work was commissioned by a partnership between LINZ and the Marlborough District Council (MDC).

The commissioned survey comprises both hydrographic (LINZ) and habitat mapping (MDC), requirements which are met by a NIWA-led partnership with Discovery Marine Limited (DML) under LINZ project HYD-2016/17-01 (HS51) Contract No 20058.

This Guide to Survey Results and Graphical Portfolio accompanies the final deliverables and is submitted in accordance with the HS51 Services Agreement Contract and MDC Specifications for Science Component.

The seafloor mapping campaign for HS51 comprised 280 days on the water. On 224 days soundings were acquired using two vessel platforms. An additional 67 days were completed for observational (coastal, seabed, and navigation aids) and tide gauge installation. This survey has gathered more than 30 terabytes (Tb) of digital information, with an estimated 5,549,300,000 depth-data points collected by the multibeam systems across a coverage of 433 km^2. The portfolios and this accompanying guide to the science encompass the entirety of the datasets collected, including over 15 Tb of water column soundings. Additionally, these documents are in support of a substantial digital-data delivery that captures all the field and value-added products.

Two NIWA vessels were used in the survey: the RV *Ikatere* for all but the shallowest extents of the sounds; and the smaller RV *Rukuwai* for shoals, embayments and shorelines. The RV *Ikatere* was fitted with a multibeam survey system that gives seafloor coverage of up to 5-times the water depth. It produces a fan-shaped array of 800 acoustic beams that result in a very high-density of soundings. It also logs water column and backscatter data. The smaller RV *Rukuwai* was fitted with a new specialist shallow-water system which allows bottom coverage of up to 12 times in water depth <5 m. It was used along coastline areas not surveyed by the larger vessel.

Collectively, the deliverables comprise the following documents and digital data:

- A guide document that summarises the acoustic dataset and identified features, which are illustrated in detail in the accompanying portfolio set. Part 1 (separate document) of the guide summarises essential results and field interpretations arising from the survey, and briefly highlights how these data could be used in future benthic surveys and resource planning. For the most part, Part 1 can be read independently of Part 2, sufficient for the end user that does not require specific details around acquisition and post-processing methodologies.

  Part 2 (this document) of the guide includes post-processing methodologies, as well as technical information and specifications already provided to LINZ and MDC for HS51 which was included within the following documents and datasets: Report of Survey (RoS), Tidal Data Pack (TDP), Quality Assurance Data Pack (QADP), Mobilisation Report, Geodetic Data Pack (GDP), 23 standard and ancillary sheets as well as digital contours and coastline and 13 Tb of Raw Multi-Beam Echo Sounder (MBES) data, 1.7 Tb of processed GSF and ASCII data, 1.7 Mb of plotted depth ASCII.

- A set of thirteen A2 portfolios, each comprising 28 map sets. Each map set portrays a full suite of data visualisations, including: bathymetry, backscatter, benthic-terrain class outputs, seafloor classification, water-column features, modelled-benthic habitats, and marine farm subsets where applicable.

- Six new NIWA Miscellaneous Chart Series: – maps of the region that illustrate the bathymetry and are produced primarily for the purposes of public engagement.

- Digital delivery – ESRI feature database (fgdb and accompanying mxd's), that includes all processed datasets and tabulated data.

This final package of deliverables provides MDC with NIWA's appraisal of the coastal marine area, which will assist MDC, industry and the community to better understand, sustainably manage and protect resources and important coastal marine ecosystems of the Queen Charlotte Sound/ Tōtaranui and Tory Channel / Kura Te Au region. It provides a data-rich foundation and point of reference that will support future initiatives across a range of spatial, logistical, social, and resourcing scales.

Key outcomes

- A total coverage of 433 km^2 of bathymetric data were acquired and these data collectively illustrate the seafloor complexity of Queen Charlotte Sound/Tōtaranui and Tory Channel/Kura Te Au. Bathymetry is illustrated as a sun-illuminated digital elevation model (DEM), produced from a 2-m resolution dataset.

- Four notable features are: (a) the sill in outer Queen Charlotte Sound that separates the relatively quiescent inner Queen Charlotte Sounds from the tidally dominated deeper Cook Strait; (b) the seafloor depression/scour that occurs throughout Tory Channel and is flanked by shallow bays; (c) the extensive rocky ridges extending into Cook Strait, and the extensive flat areas of seafloor plains; (d) the marginal bays and inlets of Queen Charlotte Sound, that, while shoaling at their heads, are similar depths to those of central Queen Charlotte Sound. In contrast, the marginal bays of Tory Channel are shallower than central Tory Channel.

- Eight terrain attributes were produced from the new bathymetric data to aid in defining the geomorphic complexity (shape and depth), including: Depth; Depth range; Standard deviation of depth; Slope; Standard deviation of Slope; Curvature; Aspect; and Rugosity. In the benthic environment, ecological diversity can generally be correlated with the complexity of the physical environment, and can help identify areas where high biodiversity may exist on the seafloor.

- The backscatter intensity is a measure of the reflected-sound signal returned from the seafloor. The intensity of the backscatter signal provides a semi-quantitative indication of the nature of the seabed substrate. Seafloor backscatter (for >5 m water depth) was segmented into four classes representative of the substrate or sediment types. The resultant classification indicates: ~49% of the area comprises low reflectivity mud, ~36% of the area comprises high reflectivity coarse sand or gravel, 8% of the area low-medium reflectivity fine sand, and ~6% of the area is medium-high reflectivity medium sand.

- Thirteen significant seafloor features are highlighted in the new bathymetry data, including:

- Prominent sediment wave fields comprising coarse sand and gravel linear ridges, up to 20 m high and 300 m apart; often associated with fine-scaled rippled sands;
- Seafloor depressions: (a) small pockmarks 0.5–1 m deep and 2–15 m wide attributed to freshwater seeps, (b) large scours along the coastline and headlands, and (c) deep-water scours tens of metres deep and kilometres long with gravel- to cobble-sized substrates;
- Anthropogenic seafloor structures captured distinctly in the bathymetry including: mooring blocks, pipelines, propeller wash, anchor drag marks and seabed cable features;
- Significant areas of rocky reefs and ridges occuring in outer Queen Charlotte Sound and Tory Channel. These steep-sided features rise above the surrounding seafloor and exhibit complex topography;
- Flat seafloor plains dominating the middle and inner Queen Charlotte Sound. Here, the seafloor is generally featureless with bioturbated fine-grained mud, low backscatter reflectivity, rugosity, and slope. The sill at the outer Queen Charlotte Sound, which separates the relatively quiescent inner Queen Charlotte Sounds from the tidally dominated deeper Cook Strait, is a significant flat plain within the survey area. The axis of Tory Channel has many sections with low slopes and rugosity, although the substrate is generally coarse sand and gravels.

- Various objects through the water column can scatter the emitted sound, and this acoustic-backscatter echo from the water column was recorded. These data were used to image features such as: seeps, kelp beds, mooring lines, marine farms, wharf structures, and submerged shipwrecks. Seep plumes were identified within the water column at numerous locations throughout the survey area, and were more active following periods of heavy rain, after which they diminished. Kelp features identified in the water column were classified according to their height above the seafloor. Kelp observed in the water column data generally occurred over, or proximal to, rocky shoals and ridges with high occurrences in Tory Channel, as well around Pickersgill Island, Arapawa Island and Cape Jackson.
- Using aerial imagery, the seafloor was successfully classified to provide coverage across areas of water depths <5 m not included in the backscatter seafloor classification. Three seafloor classes occur within the survey area: vegetated seafloor, which is either seagrass or algae; hardbottom; and unconsolidated sediment. Of particular interest are the areas of vegetated seafloor which correspond to records of kelp and algae from water-column data and from coastal observations.
- The information from the depth, slope, rugosity and other measures of shape are used to create a classification scheme for the benthic terrain. The resultant classification suggests that Queen Charlotte Sound and Tory Channel have the following proportion of geomorphic habitats: 63% flat plains, 17% broad slopes, 7% broad platforms or depressions, and 4% narrow slopes and rock outcrop highs. This classification scheme underpins a benthic-habitat map, with each class predicted to have distinct environmental conditions, and can inform future targeted photographic and bottom-sampling programmes.

- The co-collection of bathymetric and water-column data allows the three-dimensional investigation of features that extend from the seabed into the water column. The utility of this dataset allows characterisation of marine farms and their relationship with physical habitats, such as rocky reefs. This survey programme offered the opportunity to undertake a regionally integrated and relatively cost-effective assessment of these at a bay- and sound-wide scale which can inform the consenting process for marine farms by providing fundamental environmental data.

- HS51 survey followed established international best practise for scientific-data acquisition and processing and will provide a valuable baseline record for future reference. This full-scale coverage of combined and processed datasets provides a wealth of information that will underpin future management of the survey area, and lends itself to further resource evaluation and development of applied products. This guide provides a list of suggestions.

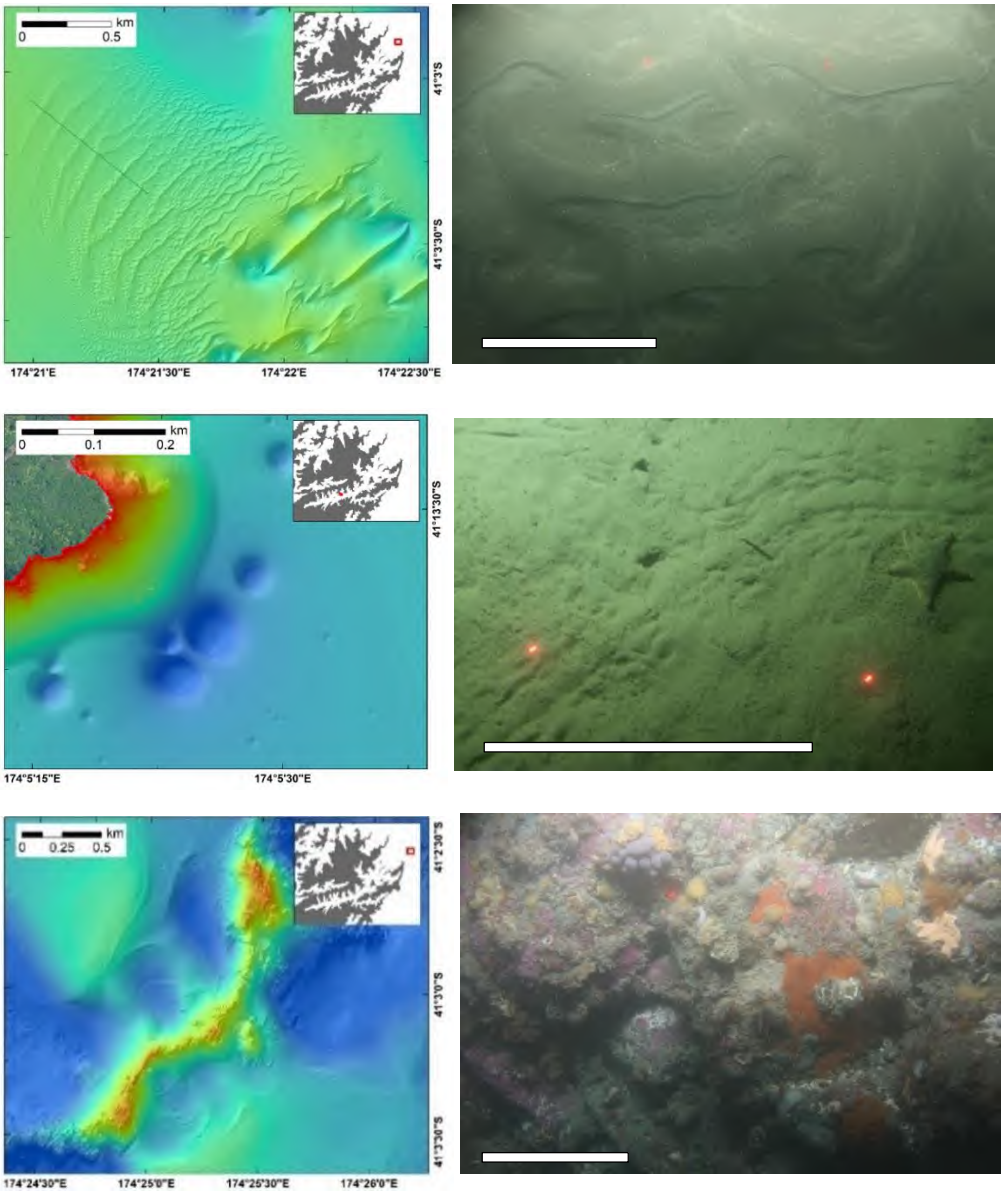

Frontispiece Figure 3: Bathymetry illustrating sediment waves (upper), pockmarks (middle) and rocky ridges (lower) in Queen Charlotte Sound / Tōtaranui and Tory Channel / Ku. Representative seafloor images for each feature are illustrated to the right. Seafloor images, white scale = 20 cm.

Part 2 – Technical Specifications and Methods

1 Introduction

1.1 Background to HS51 survey

Land Information New Zealand (LINZ) partnered with Marlborough District Council (MDC) to commission a comprehensive seabed survey (Sounds Survey – HS51) of Queen Charlotte Sound/Tōtaranui and Tory Channel/Kura Te Au.

LINZ will use the information gathered to update its nautical charts, making it safer for the increasing number of vessels – from dinghies to cruise liners – that use these waterways. The survey will also provide MDC with an appraisal of the coastal marine area, to assist MDC, industry and the community to better understand, sustainably manage and protect resources and important coastal marine ecosystems.

1.2 Data acquisition

The survey was carried out by the National Institute of Water & Atmospheric Research Limited (NIWA) and Discovery Marine Limited (DML), both experts in environmental science and hydrographic surveying, respectively. NIWA has been heavily involved in the mapping of more than 1,500,000 km² of New Zealand's seafloor using multibeam echosounder equipment.

A suite of digital systems was used to acquire and process the multibeam MBES data, which includes bathymetry, seafloor backscatter, and water column data. Multibeam data can be used to assess the type of substrate and bedforms, along with other seafloor features such as dredge marks, wrecks and pockmarks. More specifically, backscatter intensity can help identify the type of seafloor substrate; whether it is hard rock or soft mud, or sediments are coarse- or fine-grained. Various objects through the water column can also scatter the emitted sound pulse from the MBES, and this acoustic backscatter echo from the water column was recorded and analysed. Examples include kelp beds, marine farms, pipelines, and freshwater seeps.

Two NIWA vessels were used in the survey: the RV *Ikatere* for all but the shallowest extents of the sounds; and the smaller RV *Rukuwai* for shoals, embayments and shorelines. The RV *Ikatere* was fitted with a Kongsberg EM2040 MBES, which gives seafloor coverage of up to 5-times the water depth. It produces a fan-shaped array of 800 acoustic beams that result in a very high-density of soundings. The EM2040 MBES also logs water column and backscatter data. The RV *Rukuwai* was fitted with a Kongsberg Geoswath Plus system to acquire geo-referenced side scan and bathymetric information in water depths less than 5 m, as well as along coastline areas not surveyed by the EM2040 multibeam. The Geoswath system is an interferometric multibeam which allows bottom coverage of up to 12 times the water depth.

In addition, these acoustic data are supported by ground-truth data obtained during the survey, which includes seabed substrate samples, bottom video and photographs, and aerial photographs.

1.3 Purpose of this guide and portfolio

This guide provides an overview of the acoustic dataset and identified features, illustrated in detail in the accompanying portfolio. It is accompanied by 3D visualisations which can be viewed with iView4D software and data used to generate the portfolio images are supplied as an ESRI file geodatabase. This guide also summarises essential results and field interpretations arising from the survey. Finally, the guide highlights how these data could be used in future benthic surveys and resource planning. The portfolio comprises 28 map sets as shown on the portfolio index map (Figure 1-1), with localities shown on Figure 1-2. Each map set comprises a full suite of visualisations of bathymetry, backscatter, benthic terrain class outputs, seafloor classification, water column features, modelled benthic habitats, and where applicable marine farm subsets.

Part 2 (this document) of the guide includes post-processing methodologies, as well as technical information and specifications already provided to LINZ and MDC for HS51

1.4 HS51 survey objectives

Queen Charlotte Sound/Tōtaranui, Tory Channel/Kura Te Au Hydrographic Survey (HS51) comprised a survey of the areas A, B, C, D and E indicated in Figure 1-1. These areas are in Queen Charlotte Sound/Tōtaranui, Tory Channel/Kura Te Au and offshore areas of the Marlborough Sounds (Cook Strait), New Zealand.

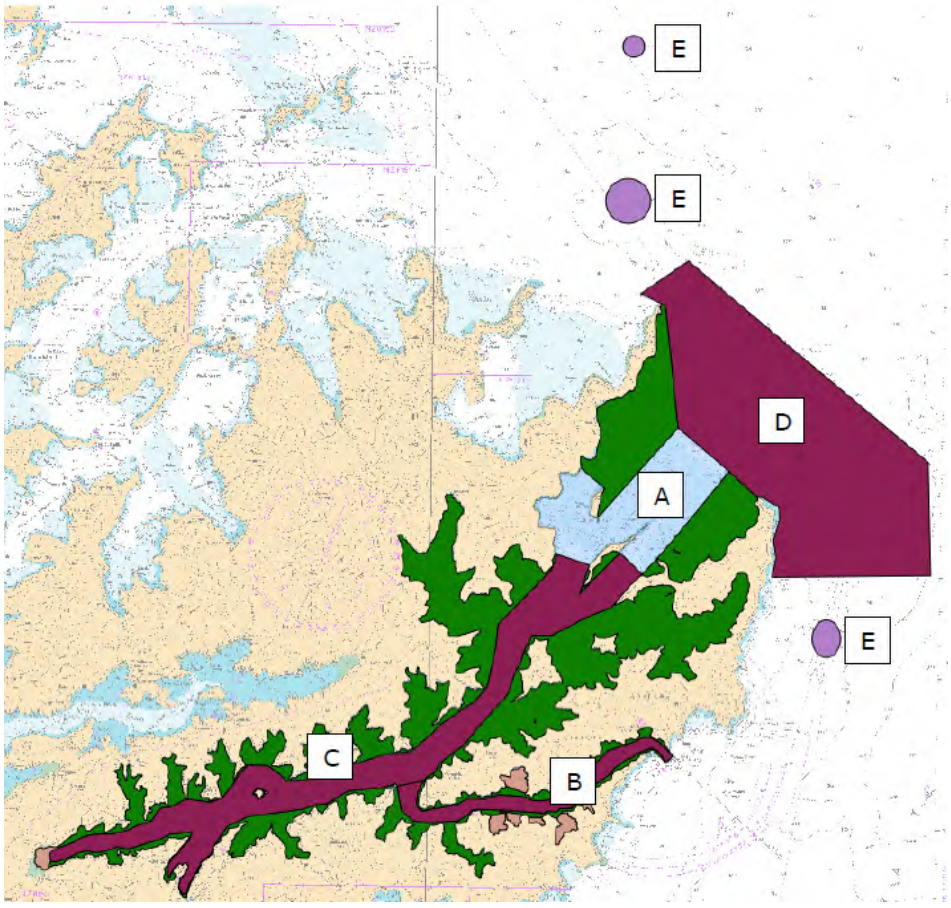

Figure 1-1: Overview of HS51 Survey Areas. (from LINZ, 2016a).

HS51 includes the following hydrographic and scientific objectives:

- Hydrographic Objectives
  - The delineation of all low water drying rocks and islets; and
  - Full area search to locate and determine the least depths over significant bathymetric features, known shoals/reef areas and any listed dangers.
- Science Objectives
  - Characterisation and mapping of seabed features, derived from bathymetry;
  - Seafloor Classifications and Benthic Terrain Modelling to aid classification of habitats; and
  - Identification of potential biological habitats important for biodiversity assessment.

The specifications required the following survey data to be obtained:

- MBES full seafloor bathymetric coverage with a depth accuracy of LINZ 1 in depths greater than 5m;
- MBES backscatter coverage in depths greater than 5m;
- Minimum of SBES and side-scan data, (a Geoswath Plus was deployed) in depths less than 5m;
- A multibeam solution to characterise marine farms and underlying seabed; and
- Water column data for significant features to be collected.

1.4.1 HS51 Statistical and Reporting Summary

Table 1-1 lists the key dates and statistics relevant to the survey. Deliverables are highlighted with bold text.

Table 1-1: HS51 Key dates and statistical summary.

Key date and deliverable	Dates
Preparations and pre-deployment calibrations	1 – 12 October 2016
Commence fieldwork on site (Mobilisation)	12 October 2016
Marine Future Initiatives Launch and RV *Ikatere* dignitary tour, information marque at **Picton Open Day**	21-22 October 2016
LINZ Mobilisation Visit	10 November 2016
Kaikoura Earthquake occurs early am. Progress on HS51 paused whilst checks carried out.	14 November 2016
Break off site over Christmas/New Year	16 Dec 2016 – 7 Feb 2017
Mobilisation Report (Report 2016149WN)	30 January 2017
HS51 Provisional Data and Reports for Area A Rendered (Report 2017014WN)	3 February 2017 LINZ/MDC

Key date and deliverable	Dates
Recommence Survey Operations	8 February 2017
LINZ day and visit of Hon Mark Mitchell, Minister	7 April 2017
Geodetic Control (Ayson Survey Plus)	11 April – 2 May 2017 LINZ
HS51 Area A1/A2 Data and Reports Rendered (Report 2017014WN), including **Final HS51 Geodetic Data Pack** (Report 2017122WN)	27 May 2017 LINZ
Fieldwork End Date (Demobilisation)	22 June 2017
Marine Mammal Observations Report (Report 2017208WN) OBIS at https://nzobisipt.niwa.co.nz/resource?r=hs51marinemammalobs&v=1.0, GBIF at https://doi.org/10.15468/s7ctpf. doi:10.15468/s7ctpf.	29 June 2017
East Bay Seafloor Habitat Maps: A2 folio series and 3D visualisations of marine farm structures (Report 2017353WN)	30 October 2017
East Bay Seafloor Habitat Maps MDC Environment Committee **Presentation** and MDC Council **Workshop**	23 November 2017
HS51 Tidal Data Pack complete for all stations rendered/accepted (Report 2017305WN)	3 November 2017 LINZ
HS51 Draft Report of Survey Deliverables (Report 2017408WN) and **Quality Assurance Data Pack** completed (Report 2017128WN)	20 December 2017 LINZ
HS51 Report of Survey Deliverables review work completed (Report 2017408WN)	6 April 2018 LINZ
HS51 Science deliverables (**Portfolio** - 2018084WN; **This Guide** - 2018085WN; **Digital delivery** – ESRI fgdb and accompanying mxds; and **NIWA Miscellaneous Chart Series** 101 – Queen Charlotte Sound/Tōtaranui and Tory Channel/ Kura Te Au; 102 – Outer Queen Charlotte Sound/Tōtaranui, 103 – Middle Queen Charlotte Sound/Tōtaranui, 104 – Inner Queen Charlotte Sound/Tōtaranui, 105 – Tory Channel/Kura Te Au, 106 - Picton)	June 2018 LINZ/MDC

Activities	Statistics
MBES sounding days with RV *Ikatere*	136 days
Geoswath sounding days with RV *Rukuwai*. Data used during SBES work	44days
SBES sounding days with RV *Rukuwai*	44 days
Tidal Control days, BM installation, levelling, gauge installations checks and recovery during the survey, includes using Water Taxi	43 days - Includes checks arising from earthquake
Ancillary Observations, coastline, lights, positioning sectors, seabed sampling using either RV *Ikatere or* RV *Rukuwai*	24 days
Downtime in field due to weather, equipment delays	22 days
Total Days on Survey Ground between 12 October 2016 to 22 June 2017	195 days
Post fieldwork processing and delivery to LINZ of HS51 hydrographic data complete 3 July 2017 to 20 December 2017	125 days
Post fieldwork processing and delivery to LINZ/MDC of HS51 science data complete May 2018	160 days

1.5 Survey Platforms

Two NIWA owned and operated vessels were used for HS51, RV *Ikatere* and RV *Rukuwai.* Key vessel parameters and full descriptions of the mobilisation and equipment setup are included in the hydrographic deliverable suite of products: namely the Mobilisation Report, which is part of the Quality Assurance Data Pack (QADP), accompanying the Report of Survey (ROS).

The RV *Ikatere* is a 14m Teknicraft design alloy catamaran, built by Q-West Ltd in Whanganui and is fitted with Hamilton Jet drives (Figure 1-2). She is fitted with an industry leading Kongsberg EM2040 MBES which is deployed through a centrally positioned moonpool. The RV *Ikatere* was used for most of the survey in water depths >5 m, to survey areas of navigational significance covering greater than 70% of the survey area.

Figure 1-2: RV *Ikatere*.

The RV *Rukuwai* is a McLay 680, trailerable alloy mono hull, built by McLay Boats in Milton (Figure 1-3). This 6.8 m vessel was used for shallow water (<5m) MBES operations and as a support vessel for ancillary work. The RV *Rukuwai* was fitted with the latest generation Kongsberg Geoswath Plus Compact multibeam which had a dual transducer head and integrated Seapath 134 system, and with a motion sensor mounted on a custom built retractable frame. Used in this configuration, the Geoswath system provided a bathymetric and backscatter dataset significantly exceeding the hydrographic requirement for sidescan sonar and singlebeam coverage in water depths < 5m.

Figure 1-3: RV *Rukuwai*.

1.6 Survey Acquisition Systems

A suite of digital systems was used to collect and process the soundings obtained during the survey. Full details of the acquisition and digital systems used for HS51 are included in the Report of Survey, the Mobilisation Report, and in the Quality Assurance Data Pack. A summary is provided below.

1.6.1 Data Acquisition Systems RV *Ikatere*

The Ikatere was fitted with a EM2040 0.4° x 0.7° MBES which can be operated at 200, 300 or 400 kHz. In 300 kHz mode it obtains optimum swath width with a maximum beam angle of 70°/70°, giving a seafloor coverage of up to 5-times water depth. It produces up to 800 beams per ping resulting in a very high-density data set.

The system has dual swath capability, which doubled the along-track resolution, resulting in 1600 soundings per ping. Line spacing was planned such that 100% of the seafloor is ensonified. The system collects backscatter and bathymetry concurrently.

The EM2040 MBES logged water column and backscatter data which the sonar operator monitored so as to be aware of any degradation in data quality due to factors such as vessel speed or weather. The operator also ensured that the multibeam acquisition settings were suitable for both hydrographic and backscatter data collection (Table 1-2). All EM2040 depth data was acquired using Kongsberg SIS software v432 Build No. 31. This software is installed on the acquisition computer on board RV *Ikatere.*

1.6.2 Data Acquisition Systems RV *Rukuwai*

A Geoswath Plus compact system was used to acquire co-registered geo-referenced side scan and bathymetric information in water depths less than 5m, as well as along coastline areas not surveyed by the EM2040 multibeam. The Geoswath system is an interferometric multibeam which allows bottom coverage of up to 12 times the water depth compared with up to 6 times with a beam forming multibeam. The transmitted signal is similar to a side-scan sonar, but the reception of the scattered signal is through a sonar array where the phase difference of the received signal is used to calculate the grazing angle. The Geoswath sonar receives information up to an angle of 120° either side of the sonar which allowed it to survey up to the drying line (when survey conducted in upper half of tidal cycle).

Geoswath data, position and motion were logged directly into the GS4 acquisition module of the laptop. Transducer draft was measured daily when alongside and depth data was corrected for sound velocity (SV) by daily and frequent sound velocity probe (SVP) dips which were enetered into the Geoswath software. Checks of Geoswath data quality were carried out during weekly patch tests over the calibration surface in Grove Arm.

Attitude and motion were provided by an integrated Seapath 134 GNSS positioning system with Seatex MRUH. Positioning was provided by a Seastar 8200 GNSS receiver with Marinestar VBS WADGNSS. The Geoswath installation on the RV *Rukuwai* is shown in Figure 1-4.

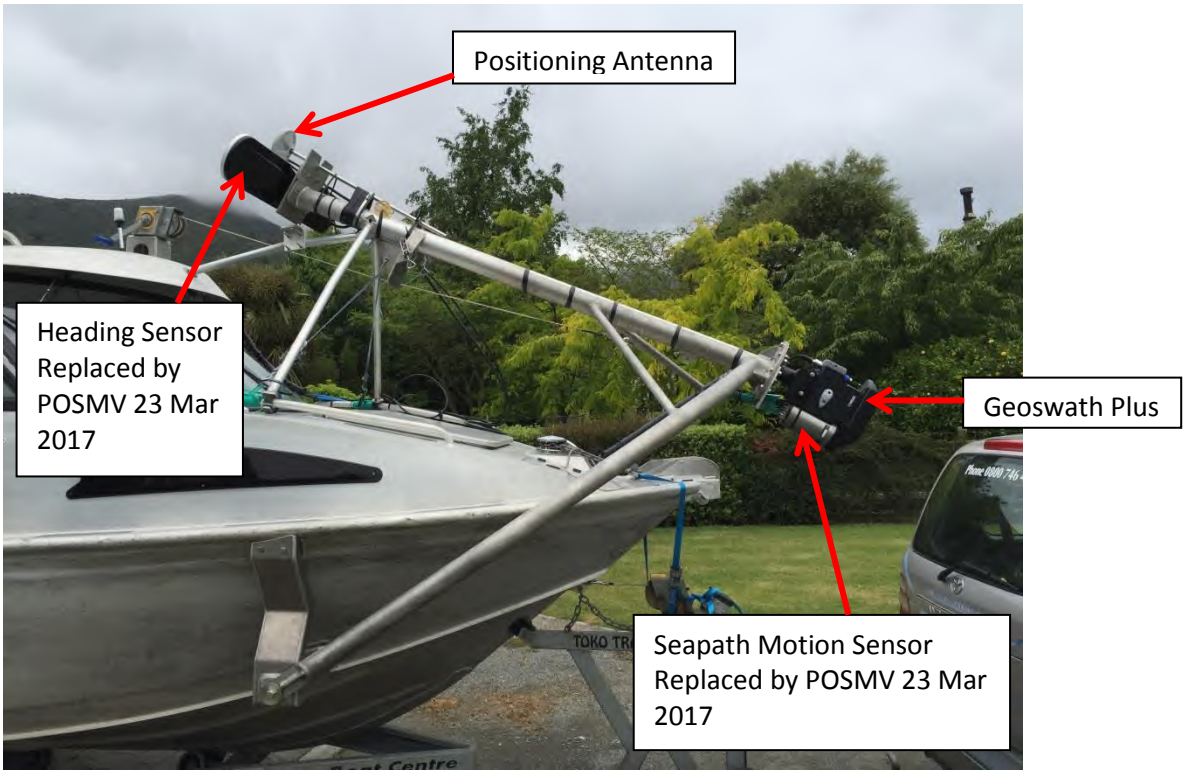

Figure 1-4: RV *Rukuwai*, Sensors and Mounting Frame for Sonar Acquisition.

1.6.3 MBES System Checks and Calibrations

Initial MBES system checks and a patch test were undertaken in Wellington before the survey commenced (October 2016). On arrival in Queen Charlotte Sound/Tōtaranui two suitable areas for patch tests/reference surfaces were located and used for patch testing:

- Grove Arm for Geoswath; and
- Waikawa Bay for MBES.

These two areas were used for Reference Surface and Patch Tests throughout the 2016 period of the survey. In 2017 the Waikawa Bay reference surface and an area in deeper water with better features for Yaw offset determination (off Ngatawhetawheta Point), were used for EM2040 patch testing.

To ensure system accuracy and consistency the MBES system was checked at weekly intervals. The checks comprised a positioning comparison against a known mark, a patch test followed by a line over the reference surface, then specific backscatter calibration lines also over the reference surface. The results of all positioning and patch tests are included in the Quality Assurance Data Pack.

Following each replacement/repair of the EM2040 transducer a full calibration and reference surface check was undertaken with results reported to LINZ. Copies of each calibration report are included in the Quality Assurance Data Pack.

1.6.4 EM2040 Operating Parameters

During the initial quality control process, it was observed that data gaps were present in the acquired dataset. A set of operating guidelines for were adopted for the unique seafloor topography and tidal stream and current conditions of the Queen Charlotte Sound/Tōtaranui and Tory Channel/Kura Te Au area. These guidelines are detailed in Table 1-2.

Table 1-2: HS51 Operating Guidelines for EM2040.

Depths	Swath Max	MAX Speed over Ground	Frequency/Ping Rates	Comments
Coast lining	+/-75-45 deg Gen +/-65 deg.	As required	300 /set to 15 max	May swing swath shoreward on inshore line (coastline). Overlap into 5m (green) colour band from RV *Rukuwai* work.
< 25m	+/-65 deg.	6.5 knots	300 /15 max	
Increasing beyond 25-30m	+/-60 deg.	6.5 knots	300 />12	Where depth is continuing to increase then reduce the swath width.
25-65	+/-60deg	6-6.5	300 />10	
60-110	+/-55	5.5	300 />8	
110 – 150	+/-45	4-5	200 />5	Change freq. to 200kHz over 100m and deeper.
150-220	+/-40	3-4	200 />3	
200-300	+/-40	5	200/ Change to FM Mode at depth 200 m	Change mode once deeper than 200m.
300-400	+/-40	4-5	200/FM Mode	

The realtime depth data was corrected for draft, motion and sound velocity so that actual depth below the surface and across the swath could be displayed. This was considered important for vessel and personnel safety in view of the shallow nature of the near shore area and to enable real time QA of swath overlap areas to be undertaken.

Figure 1-5: Interior of RV *Ikatere* looking aft to POS/PC and SIS PU, and forward to the operator workstation.

Figure 1-6: EM2040 transducers being deployed through the moonpool.

Coastal Geoswath data was imported into the EM2040 operating software (SiS) to allow EM2040 surveying close to the shoreline. The images in Figure 1-7 are an example of the colour banded depth and sonar mosaic images for the southern part of Long Island.

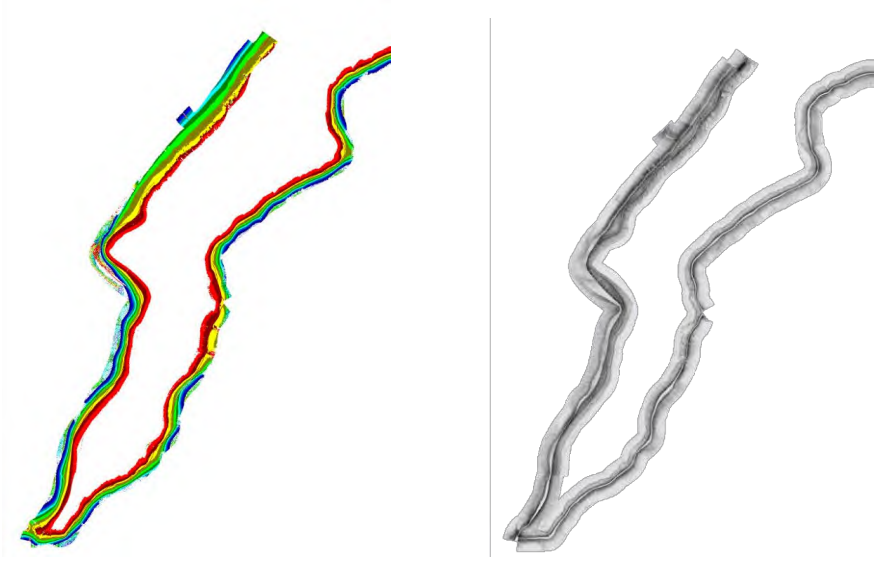

Figure 1-7: Geoswath Derived Depth Colour Banded Imagery (left) and Side Scan Sonar Mosaic (right), Long Island Area.

1.7 Data Processing Systems

HS51 utilised several software suites for data processing which are listed below:

- EM2040 bathymetry processing using QIMERA;
- Geoswath GS4 software for initial Geoswath bathymetric processing (coastline and areas less than 5 m);
- CARIS for merging Geoswath and EM2040 bathymetric surfaces;
- Geoswath backscatter processing using Geotexture;
- EM2040 backscatter processing using Fledermaus FMGT;
- Geospatial and seafloor classification ESRI Arc GIS.

The MBES system and data workflow for hydrographic acquisition and processing, and science processing is depicted in Figure 1-8.

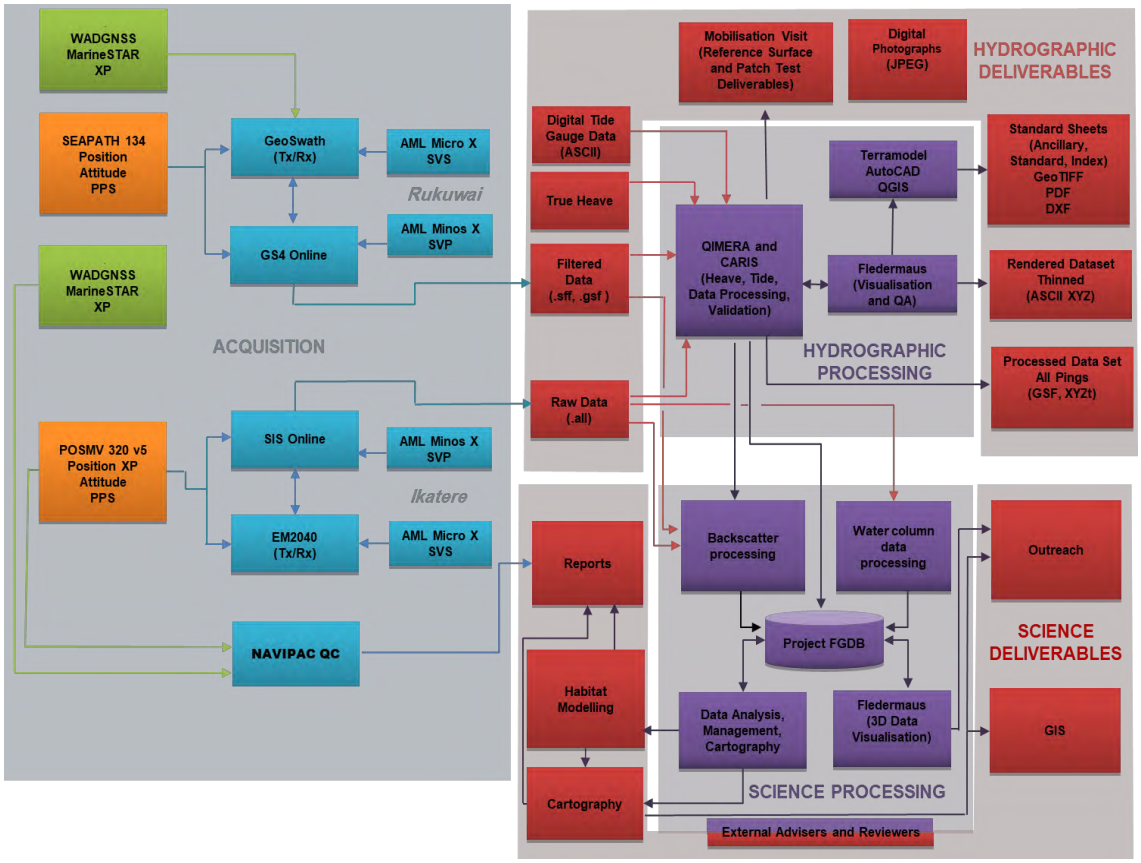

Figure 1-8: MBES system and data workflow.

1.7.1 Data quality control

The results of calibrations and checks of the sounding system used for each vessel are summarised in the Report of Survey, fully described in the Mobilisation Report and Quality Assurance Data Pack.

The acquired seafloor backscatter and water column data was also checked following the weekly offsite data backup to check the survey coverage, and examine for irregular and unexplained changes in the backscatter which could be indicative of system errors. The observations from this quality control process were fed back to the field team to ensure coverage, and if required check the system performance.

1.8 Bathymetric Processing

1.8.1 Tidal correction

The reduction of soundings for HS51 was undertaken using the observed tidal data adjusted to the Sounding Datum (SD) for the seven tidal stations. The reduced tidal data were applied as block corrections within the eight discrete tidal block areas. These tidal block areas are closed polygons as indicated in Figure 1-9. The tides for virtual station TEWH were generated using reduced data from ANAK-1 adjusted by co tidal factors. Tidal corrections are fully described in the Tidal Data Pack.

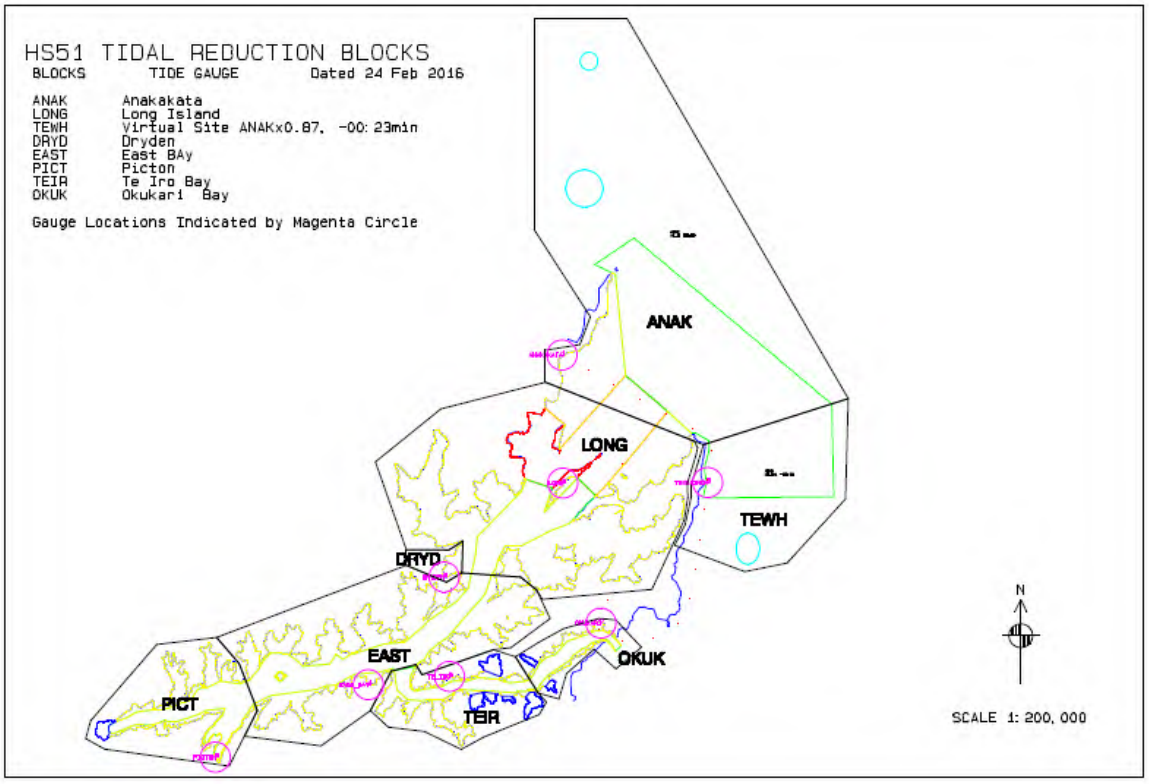

Figure 1-9: HS51 Tidal Reduction Blocks.

1.8.2 MBES Bathymetry

For HS51 the EM2040 MBES system on-board RV *Ikatere* was operated at 300 kHz equidistant spacing CW mode for depths less than 110 m. In water depths of 100–200 m the frequency was lengthened to 200 kHz, and for depths >200 m the operation mode was changed to FM. The opening beam angle in depths <25 m was 130^0. This angle was reduced to 120^0 in depths >25 m, and at depths >60 m the beam angle was reduced further to 110^0. The opening beam angle and vessel speeds in greater depths were progressively reduced to ensure the ping rate achieved LINZ 1 target detection specifications. East of Walker Rock a maximum depth of 385m was recorded whereas the charted depths indicated "no bottom" at 183 m.

1.8.3 EM2040 Bathymetry

The acquisition and processing of bathymetry acquired by the Kongsberg EM2040 multibeam is covered in detail by the Report of Survey.

At the end of this processing routine, the EM2040 bathymetric data consisted of multiple projects generated within CARIS HIPS software. Each project was based on tidal blocks with processed bathymetric surfaces generated with a shoal bias (i.e. shallowest depth soundings are preserved at the cost of the deeper soundings) as per LINZ Hydrographic specifications.

For the generation of bathymetric products for science, a technique known as CUBE (Combined Uncertainty and Bathymetric Estimator) is run within CARIS HIPS software to generate new non-biased bathymetric surfaces. CUBE is an error-model based, direct digital-terrain model generator that

estimates the depth plus a confidence interval directly on each node point of a bathymetric grid. In doing this, the approach provides an automated mechanism to process most of the bathymetric data and, most importantly, the technique produces an estimate of uncertainty associated with each grid node. When the algorithm fails to make a statistically conclusive decision, it will generate multiple hypotheses, attempt to quantify the relative merit of each hypothesis and present them to the operator for a subjective decision. In the interests of efficiency and consistency, the operator needs to interact only with a small subset of data for which there is some ambiguity, rather than going through the very time-consuming process of subjectively examining all data points. The result is an accurate bathymetric surface gridded at a 2 m cell size.

Figure 1-10 shows the workflow for processing the MBES bathymetry data.

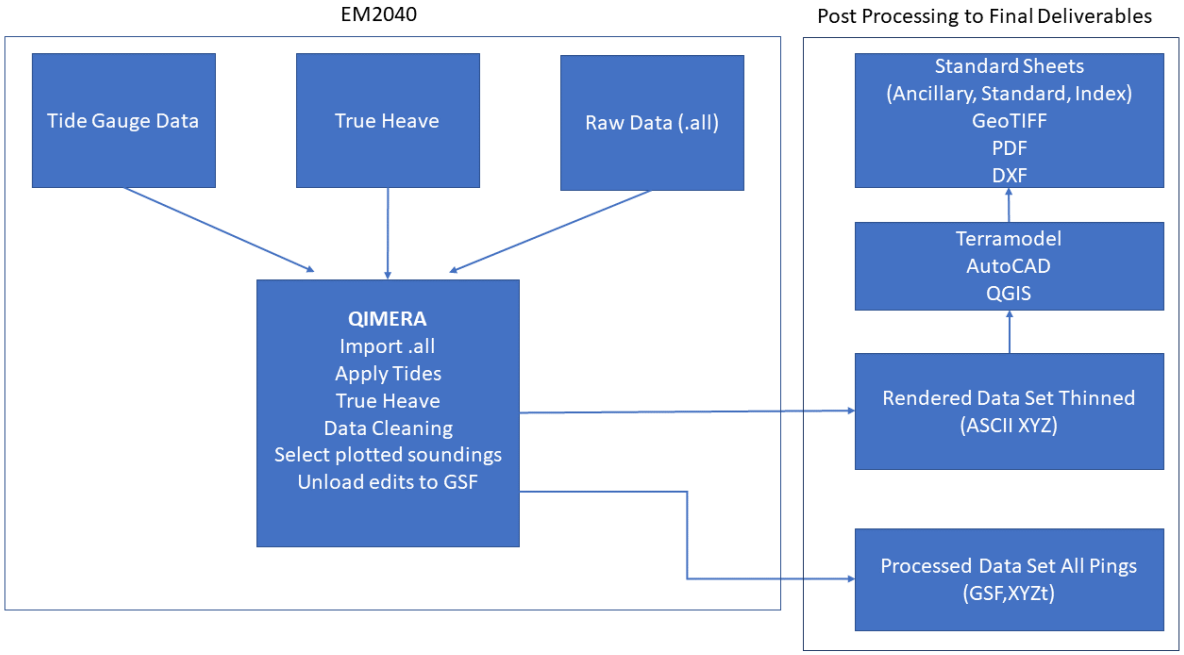

Figure 1-10: MBES bathymetry processing workflow.

1.8.4 Geoswath Bathymetry

A Kongsberg GeoAcoustics GeoSwath Plus bathymetric sonar was used to collected bathymetry along the shallow waters (0-5 m depth) of the coastline.

Once the bathymetry and backscatter (side-scan) data had been acquired ensuring that LINZ 2 specifications had been met, the daily acquisition project was loaded into the Kongsberg's 64-bit GS4 software (supplied by Kongsberg). This daily project contains the survey day files such as SVP's, raw data files, Geodetic parameters and installation parameters. The "feature filter" function was applied to the surveying days soundings, which filters the seafloor sonar returns from the raw data. The

resulting data was then imported into CARIS HIPS software for further bathymetric cleaning and tide application.

Within CARIS HIPS, a CUBE function was applied to the imported soundings to generate a reference surface. This surface was then used to produce a set of cleaned bathymetric soundings, from which an accurate final bathymetric surface grid at a 2 m cell size is generated.

Figure 1-11 shows the workflow for processing the GeoSwath bathymetry data.

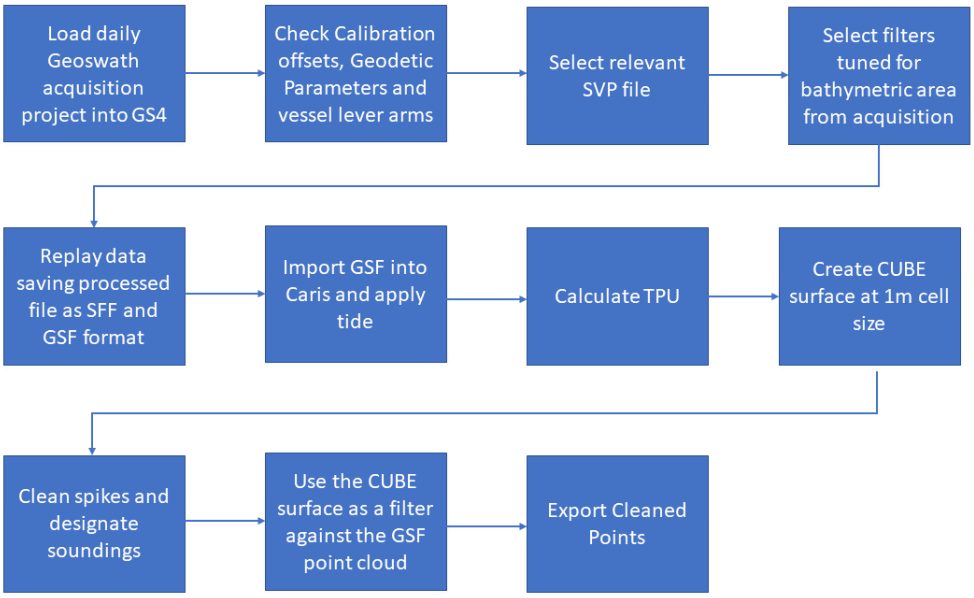

Figure 1-11: Geoswath bathymetry processing workflow.

1.8.5 Satellite-Derived Bathymetry

Satellite-derived bathymetry (SDB) was used early in the survey process to aid in the planning of the multibeam survey, to provide bathymetry to areas likely unable to be covered by multibeam and geoswath, and to use the satellite imagery to perform a basic benthic habitat classification. This SDB processing was undertaken by EOMAP GmbH & Co. KG.

The Queen Charlotte Sound/ Tōtaranui and Tory Channel/Kura Te Au area features a relatively narrow shallow water strip extending from the shoreline, followed by a rapid steepening of the underwater topography. The SDB component was initiated at the beginning of the project and completed during the ship-based campaigns. Aerial imagery was used both to check the positional accuracy of the satellite imagery as well as for the benthic classification.

A detailed explanation of methods employed by EOMAP GmbH & Co. KG. are included in Appendix C.

Satellite imagery

Archived satellite imagery was chosen which fulfilled the requirements to be used for SDB processing. Care was taken to avoid satellite images recorded under unfavorable environmental conditions. In total, five WorldView-2 and one Quickbird satellite images were purchased and analyzed. Table 1-3

summarises the purchased satellite image data license with the unique catalogue ID of DigitalGlobe, date of image recording. The satellite image was accessed as so-called processing level 2 standard product. This processing level is orthorectified by a coarse resolution terrain model.

Table 1-3: List of suggested archived satellite image data which meet the requirements. DigitalGlobe is the satellite image owner. Satellite image data are licensed not sold under the terms and conditions of DigitalGlobe

Sensor	Recording data of satellite image	DigitalGlobe Catalogue ID
WorldView-2	2010-09-30T22:27:54	10300100078C9F00
WorldView-2	2012-10-30T22:30:07	103001001D18D100
WorldView-2	2013-01-05T22:59:47	103001001D4C1D00
WorldView-2	2013-12-24T22:56:55	103001002BC27D00
WorldView-2	2014-10-08T22:39:17	103001003827F900
Quickbird	2007-11-24T22:45:00	1010010007642800

Survey control data and ancillary data

No bathymetric survey data or local ground control points (GCPs) were accessible for this location during the SDB production phase. Following the SDB data processing, acoustic data were provided by NIWA, but these data were used for visual comparison and validation purposes only.

Satellite Derived Bathymetry data

SDB data were successfully created for the Marlborough Sound area down to depth of around 10 m on average (Figure 1-12).

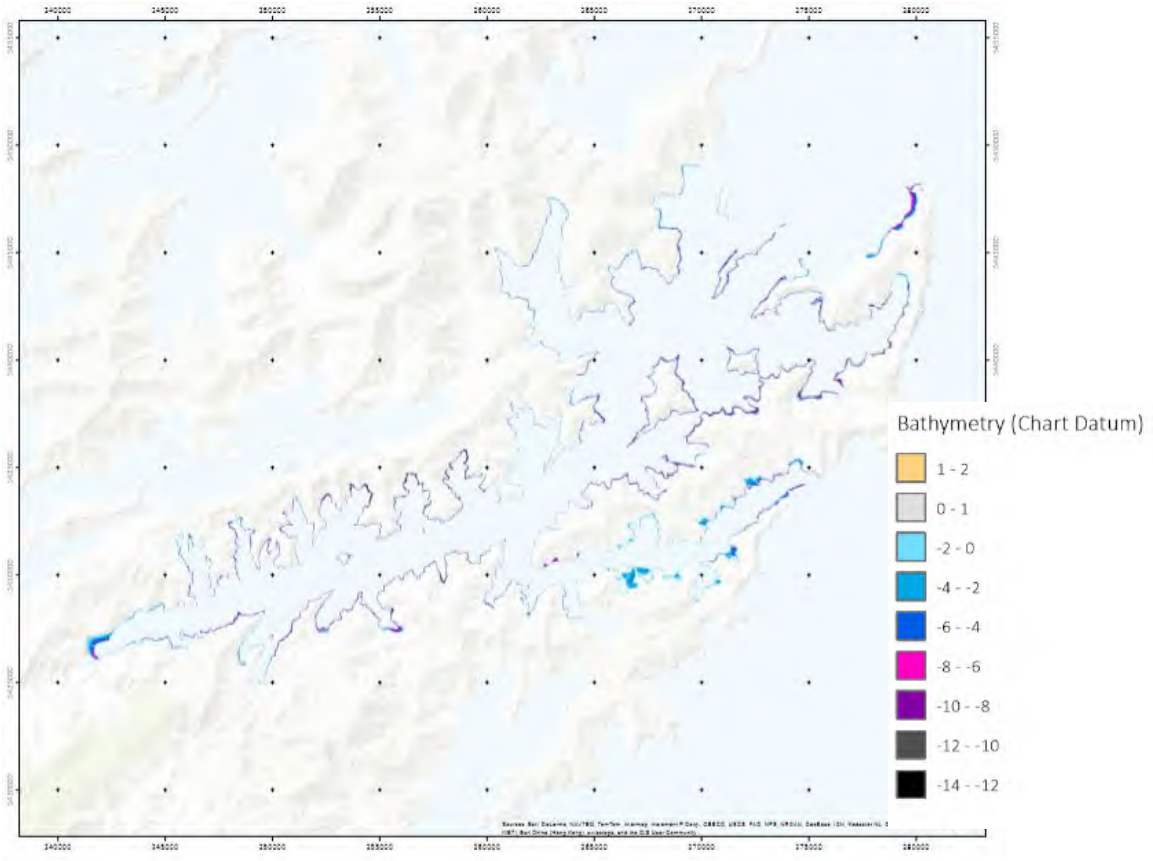

Figure 1-12: Overview map of the SBD bathymetric data.

The mapping of the shallow water bathymetry of Marlborough Sound included common but not significant issues:

- Cloud conditions: Prior to the SDB processing care was taken to identify the most feasible satellite imagery with respect to the HI specifications and EOMAP's expertise. Although the total cloud cover can be considered as very low, little cloud gaps might occur occasionally.
- Dark seafloor: Dark hard bottom limited the depth penetration for this bottom type because little light is reflected off this surface.

1.8.6 Combining Bathymetry Surfaces

Depths acquired from the EM2040 multibeam will always be more accurate than those based acquired by the GeoSwath sonar because of the better accuracies of a beam-forming multibeam versus a phase measuring bathymetric sonar system. However, the geometry of the EM2040 multibeam is such that the shallowest depths that can be systematically and safely measured is 5 m. The GeoSwath sonar can safely acquire depths where the EM2040 cannot, i.e. from 5 m to the waterline.

Similarly, in the shallow water, bathymetry acquired from the GeoSwath will always be more accurate than that interpreted from SBD because the GeoSwath depths are a direct measurement and the SDB is an interpretation from imagery.

Hence, any final bathymetric surface was formed by merging the source surfaces where the depth value for any given cell will be based on the following priority:

1. EM2040 measured depth;
2. GeoSwath measured depth;
3. Satellite-derived bathymetry.

The final combined bathymetric surface were generated using the CARIS Bathy DataBASE software. This software utilises the Combine Surfaces function to stitch together multiple bathymetric surfaces to form one seamless surface. Bathymetric surfaces from the EM2040, GeoSwath and satellite imagery were combined using the rule that for the new combined surface, with any cell the depth from the EM2040 will always be used in preference to a depth from the GeoSwath. And likewise, and depth from the Geoswath will be used in preference to that derived from satellite imagery.

The final combined bathymetric surface was exported to ArcMap as a raster grid for analysis and the generation of attribute and derived products.

1.9 Identification of second-derivatives of bathymetry features

Two second-derivative classes of bathymetry were generated primarily to aid the identification of relationships between kelp and seeps to the benthic terrain. The geomorphometric measurements generated from the BTM tools were used to attempt to automatically identify rocky outcrops which may or may not show a relationship to the occurrence of kelp, and to identify fine-scale depressions (e.g. pockmarks) which may show associations to active seeps.

1.9.1 Rocky outcrops

The identification of rocky outcrops was calculated by a GIS analysis of the combination of positive curvatures (including plan and profile curvatures) coupled with high ruggedness over multiple resolutions of the combined bathymetry grid.

1.9.2 Small depressions

Small depressions are widely distributed in Queen Charlotte Sound and many can be defined as pockmarks (see Section Part 1, 3.4.3).

The hillshade layer of Queen Charlotte Sound/Tōtaranui and Tory Channel/Kura Te Au shows that individual pockmarks appear symmetrical and visually distinct, however their morphologies can be complex (Hovland and Judd, 1988). Such irregularities complicate pockmark delineation based on visual inspection. Further, pockmark fields may comprise thousands of features and manual interpretation becomes impractical and subjective. Consistent and repeatable delineation of pockmarks by automated techniques requires a morphologic definition that includes diagnostic features and distinguishes them from other forms.

Andrews et al. (2010, Figure 3-13) define a pockmark as a roughly circular seafloor depression that consists of three elements: 1) the depth to the lowest point (bottom) of the depression; 2) the depth to the rim; and 3) the diameter of the rim defined here operationally by the intersection of pseudo-“watershed boundary” and the nominally flat seafloor. This rim also marks the locus of greatest

change in slope gradient (profile curvature) at each pockmark. Most pockmarks in Queen Charlotte Sound/Tōtaranui and Tory Channel/Kura Te Au and worldwide are sufficiently described by this definition; however, it does not adequately characterise other morphological classes of pockmarks, which are non-circular and/or have irregular highs and lows throughout the depression.

Several morphological classes have been identified by Hovland et al. (2002), who define a *normal* pockmark to be a circular depression typically measuring 10-700 m in diameter and 1-45 m in depth. Current scour erosion, merging of individual pockmarks, and inward gravity sliding of unstable pockmark flanks may alter the initial circular geometry of the pockmark giving rise to other geometric classes, such as *elongated*, *composite*, *complex* and *eyed* pockmarks (Hovland, 1982, 1983; Hovland & Judd, 1988; Stewart, 1999).

In the case of Queen Charlotte Sound/Tōtaranui and Tory Channel/Kura Te Au, GIS analysis using ArcMap software was employed to identify pockmarks and other fine-scale depressions. The GIS analysis was done by of a combination of identifying negative curvature (including plan and profile curvatures) of the seafloor that are continuous and join onto itself (i.e. define a polygon), coupled with the *Sink*, *Fill*, and *Watershed* functions in ArcGIS. Curvature and sinks identify the location of these small depressions, and the watershed defines the extent, or boundary, of the feature.

Initial results from these analyses also identified large depressions, such as tidal scours, that were overwhelming the identification of the smaller-scale depressions. In fact, at larger scales, the entire Queen Charlotte Sound/Tōtaranui and Tory Channel/Kura Te Au and Cook Strait seafloor are themselves broad-scale depressions. Therefore, an upper limit of 0.08 km^2 was set to ensure that only fine-scale features were identified.

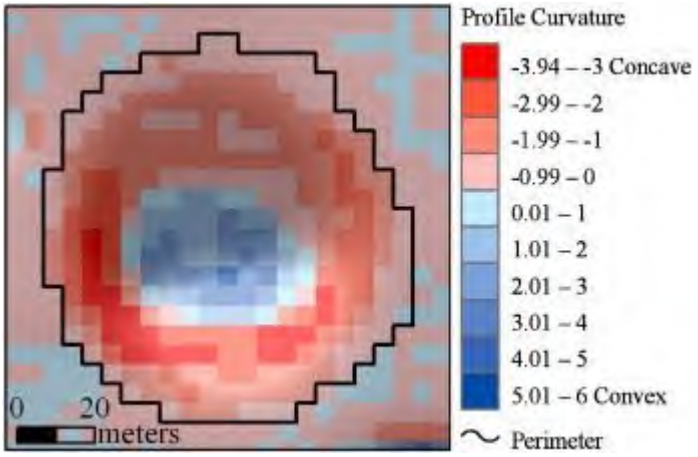

Figure 1-13: Plan view of single pockmark color-coded by profile curvature (the rate of change in slope gradient) draped over hill-shaded bathymetry. Red cells (negative values) are convex and blue (positive values) cells are concave in the direction of greatest slope. Black outline represents to pockmark perimeter derived from the watershed delineation (Andrew et al., 2010).

1.10 Backscatter

1.10.1 EM2040 Backscatter Calibration and Processing

NIWA adopts international best practice for backscatter data acquisition and calibration, as outlined in Lurton and Lamarche (2015). Compulsory check lines were run weekly over a reference surface, using

standardised system settings applied over the duration of the survey. These repeat reference checks were used to compensate the response of the EM2040 system and monitor systems performance. Reciprocal diagonal passes over the reference area were used to compare the absolute difference in backscatter responses of the system over time.

Figure 1-14 shows the workflow for generating beam-pattern compensation curves. The raw EM2040 files (*.all) were imported into CARIS HIPS software for cleaning of bathymetric outliers following the standard CARIS workflow.

NIWA used the standardised and widely established procedure developed by QPS, and implemented in FMGT, to compensate for the variations in the backscatter intensities as a function of the sound-wave transmission angle. FMGT applies a method which compares the actual backscatter response to expected acoustic response curves based on a mathematical model (Jackson and Briggs, 1992). FMGT compensates the backscatter angular response by subtracting the best-fitting theoretical angular profile to the data. The resulting image is improved visually because the contrast is enhanced. This compensated image is also offers the utility of a standardised relative intensity across the survey region.

For this, a Fledermaus GeoCoder Toolbox (FMGT) project was created for each weekly backscatter check operation. A beam-pattern correction file (*.bpt) was generated for each system configuration and setting (frequency/pulse, etc.). The relevant check lines were imported into the FMGT project as data pairs consisting of the *.all files for the backscatter datagrams together with the corresponding processed bathymetric data from CARIS HIPS HDCS (Figure 1-15). The beam pattern-correction files were then used to compensate the measured backscatter data and to generate seafloor backscatter values (Figure 1-16). Beam-pattern correction files contain the difference between the measured backscatter value and a theoretical model value for each angle (0 to 180) from Jackson et al. (1992).

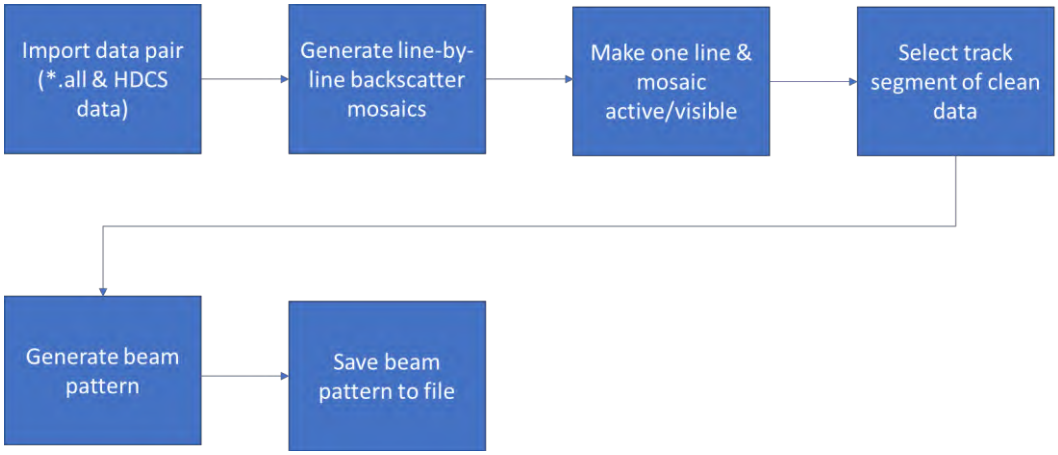

Figure 1-14: Flow diagram for the generation of beam pattern files.

The information contained in the beam-pattern correction files is unique to the acquisition system (transducer, frequency, system setting, vessel etc. New beam-pattern correction files were also generated when any major system components were changed. Check lines were run for each frequency and mode used on this survey. The MBES modes used in this survey were:

- 200 kHz, medium CW pulse;
- 200 kHz, FM pulse; and

- 300 kHz, medium CW pulse.

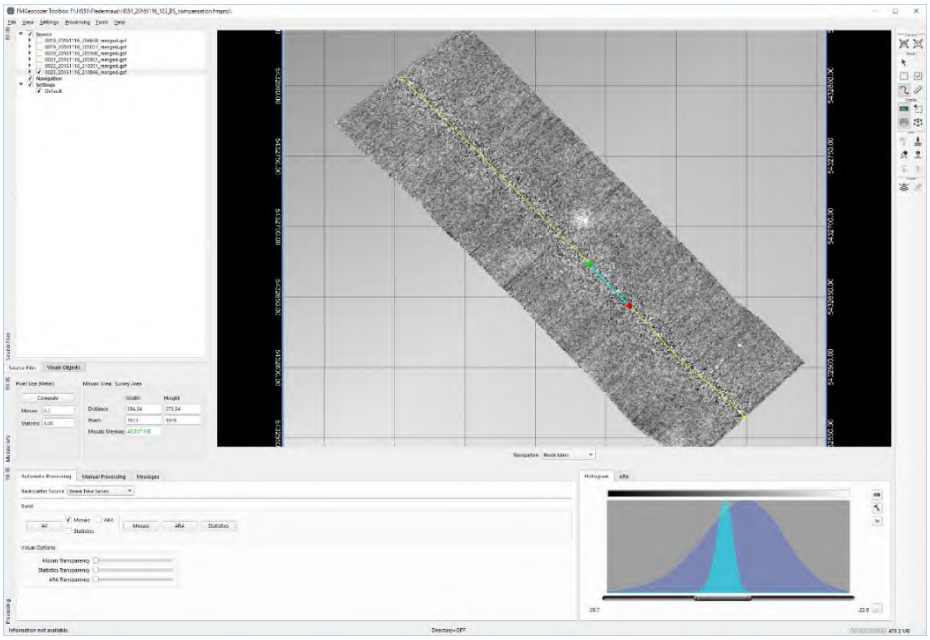

Figure 1-15: FMGT processing panel screenshot. Showing an example of one check line, with a sample of a data section (blue) for generating the beam-pattern correction file (*.bpt).

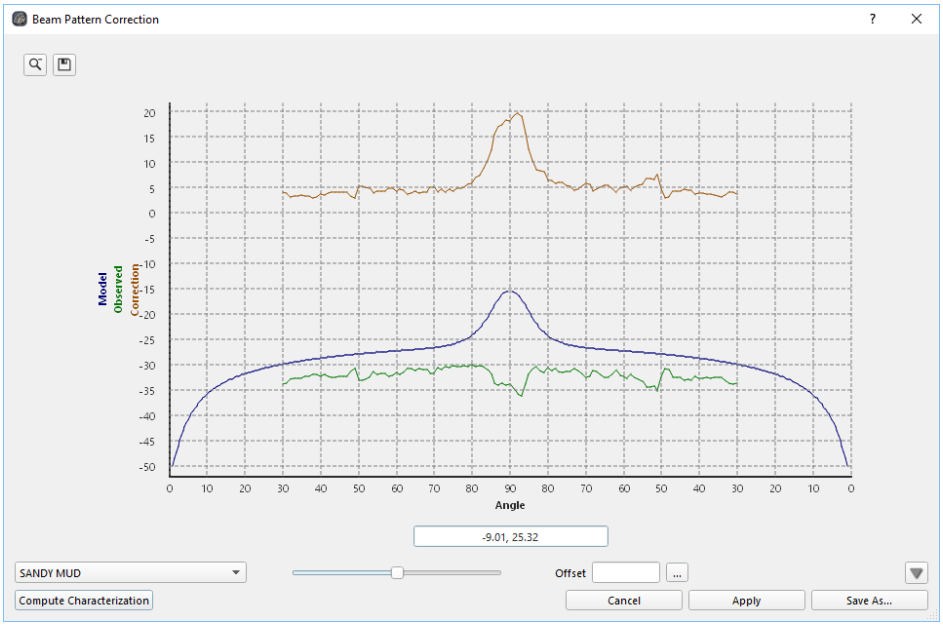

Figure 1-16: Example of the FMGT Beam-Pattern Correction File viewer.

Following the generation of the beam-pattern correction files from all check lines, an average function was applied and new beam pattern curves were generated for each mode and transducer combination (Figure 1-17).

Due to hardware issues with the EM2040 transmit transducer (Tx), four different transducers were used on this survey. As the beam patterns are system specific, each Tx required an individualised calibration setup, even though the receiver transducer (Rx) and the processing unit were unchanged.

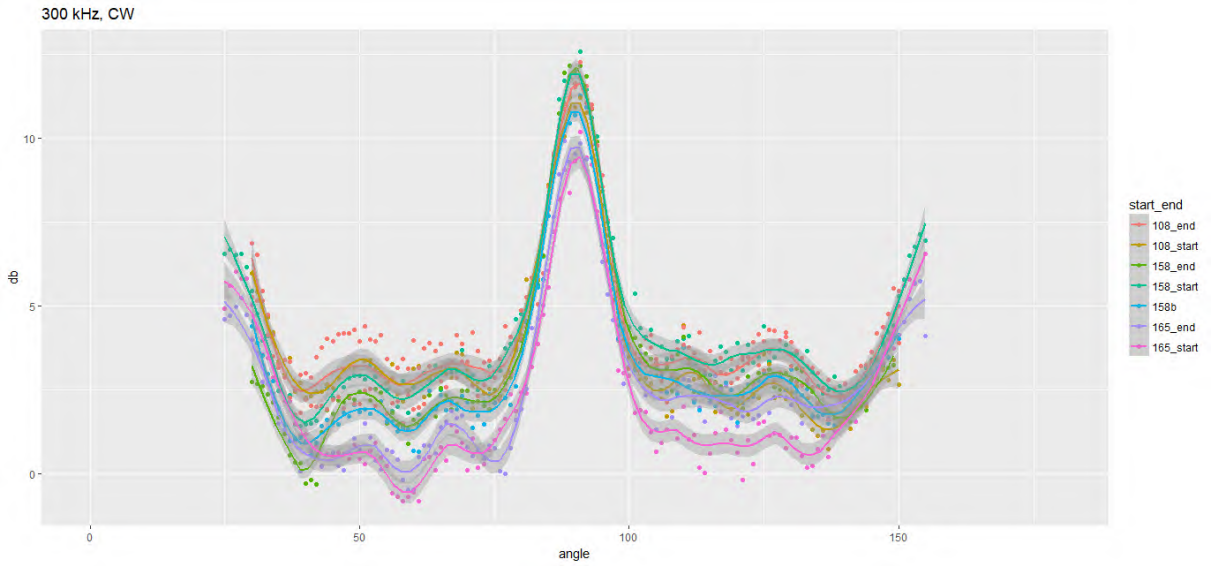

Figure 1-17: EM2040 average beam-pattern corrections processed using in the statistical software *R*. Red dots are actual beam-pattern corrections (observed delta from the model) of all weekly checks (grouped by Tx and when required by start/end of use). The curves are a splined average of all the grouped observations to form an average of the specific groups weekly observations. The 95% confidence interval around the curves is outlined by the grey envelope.

Once the beam-pattern correction files were generated from the reference area, processing of all the survey data was undertaken. FMGT project templates were generated for each hydrographic processing block. These contain the beam-pattern correction files generated for each Tx and mode combination.

FMGT imports the survey data, extracts and compensates the backscatter signal using the beam-pattern correction file included in the template projects. It then calculates the incidence angles and beam foot print using the bathymetry data. Beam flags from the bathymetry data processing were applied at that stage, thus eliminating major error soundings (but not all backscatter artefacts). Consequently, some changes in backscatter dB levels are carried forward within the processed data, and display in the mosaics as apparent sharp boundaries or a step in the dB level (block variability in the grey scale) over otherwise gradual seafloor change. Such limitations are not uncommon for large backscatter mosaics that span a range of water depths and bottom substrates, and were acquired over long survey campaigns.

Once the above procedures of importing and processing line data were complete, the line data were merged into 0.5 m resolution mosaics. These mosaics were then renamed to reflect the processing block, Tx, and mode (frequency/pulse), allowing tracking of the source configuration when exported to a floating point Geotiff format.

1.10.2 Geoswath Backscatter Processing

Backscatter processing was undertaken using Kongsberg's "Geotexture" software. NIWA commissioned a report and workflow from Kongsberg which detailed the recommended work flow and calibration processes specifically focussed on the HS51 data set. This workflow was followed as summarised below to produce a normalised mosaiced data set.

A master beam function was derived from an area which had the following characteristics:

- The seabed is approximately flat;
- The seabed material is approximately uniform (in particular, uniform between port and starboard sides); and
- The seabed is shallow (to provide data at low inclination angles).

Following the derivation of the master beam function a scatter function was then derived from the same area (Figure 1-18).

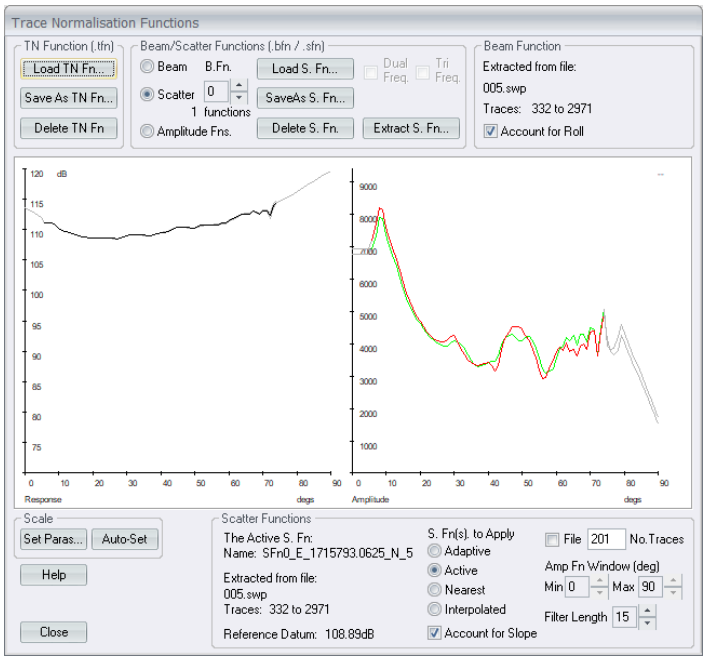

Figure 1-18: Derived Normalisation Curve and Scatter Function.

Comparisons of the master beam functions derived from the weekly calibration lines were used to check the performance of the Geoswath transducers. The Geoswath backscatter was then processed using the work flow as detailed in the manufacturer supplied reference and more specifically the commissioned processing report (Figure 1-19).

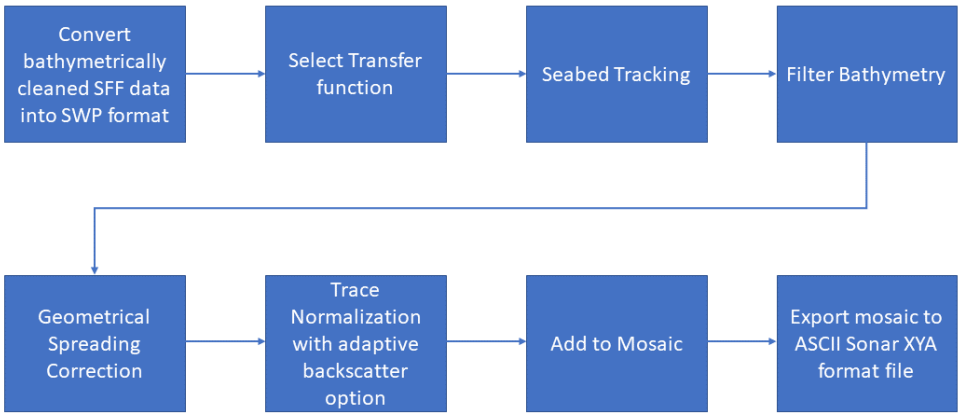

Figure 1-19: Geoswath Backscatter Processing Workflow.

Due to the acoustic response of the seabed, and the subsurface varying with the multibeam operating frequency the Geoswath, data was exported as normalised sidescan imagery and not as calibrated backscatter (Figure 1-20). This approach was also used due to the majority of the area that the Geoswath surveyed being steeply sloping coastal strips with a steep grazing angle.

As the Geoswath backscatter is not calibrated, it cannot be compared quantitatively with the multibeam echosounder backscatter data, i.e. the dB values of the Geoswath data have no correspondence with that of the compensated values of the multibeam echosounder. The 500 kHz Geoswath data when merged with the 300 kHz EM2040 backscatter was grey-scale aligned so that the facies of the Geoswath backscatter were comparable to the EM2040 facies.

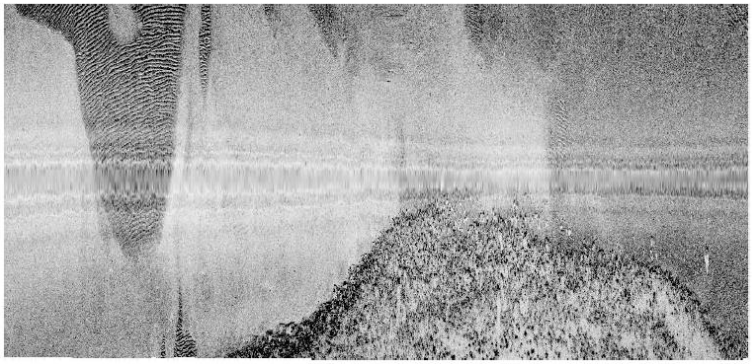

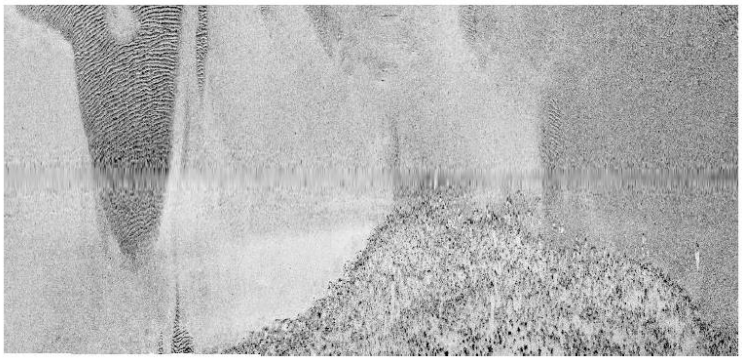

Figure 1-20: Geoswath trace with no normalisatons (top) and trace normalisation (bottom).

1.11 Seafloor classification

1.11.1 Backscatter Seafloor Classification

Following post-processing of the raw seafloor backscatter data, a supervised segmentation/ classification approach was undertaken using the EM2040 backscatter data alone (i.e. no other surrogates). Four classes of coherent backscatter facies representative of seafloor or sediment types were selected. We used ESRI ArcGIS for the supervised segmentation (partitioning) of the backscatter. Training regions were first generated using end member of the backscatter facies. Validation of the classes was undertaken using random-adjusted surficial seafloor samples (collected as a requirement of hydrographic specifications) as a ground truth dataset (Figure 1-21). One hundred and thirty sites of which 124 comprised samples and seafloor images, with six sites being seafloor image collections only. Grainsize was derived for the samples (see Section1.10) with mean grainsize values and dB values at the sample sites used to inform the seafloor backscatter classification.

Samples from Queen Charlotte Sound predominately fall within two textural groups muds to sandy-muds and gravelly-mud to gravel, with a small number of samples represented by the muddy-sand to sand textural classes (Figure 1-22). Grain size is given as Phi=-log 2d, with d the grain diameter in mm. A grainsize value commensurate with gravel was assigned to video image samples comprising rocky reefs, where physical samples could not be obtained. A random selection of 66% (86 samples) was used to define the Backscatter Strength boundaries (in dB) relative to mean grainsize and inform the seafloor classification (Figure 1-23). The remaining 33% (44 samples) were used as a test dataset to validate the classification model (e.g. Diesing and Stephens 2015; Figure 1-24).

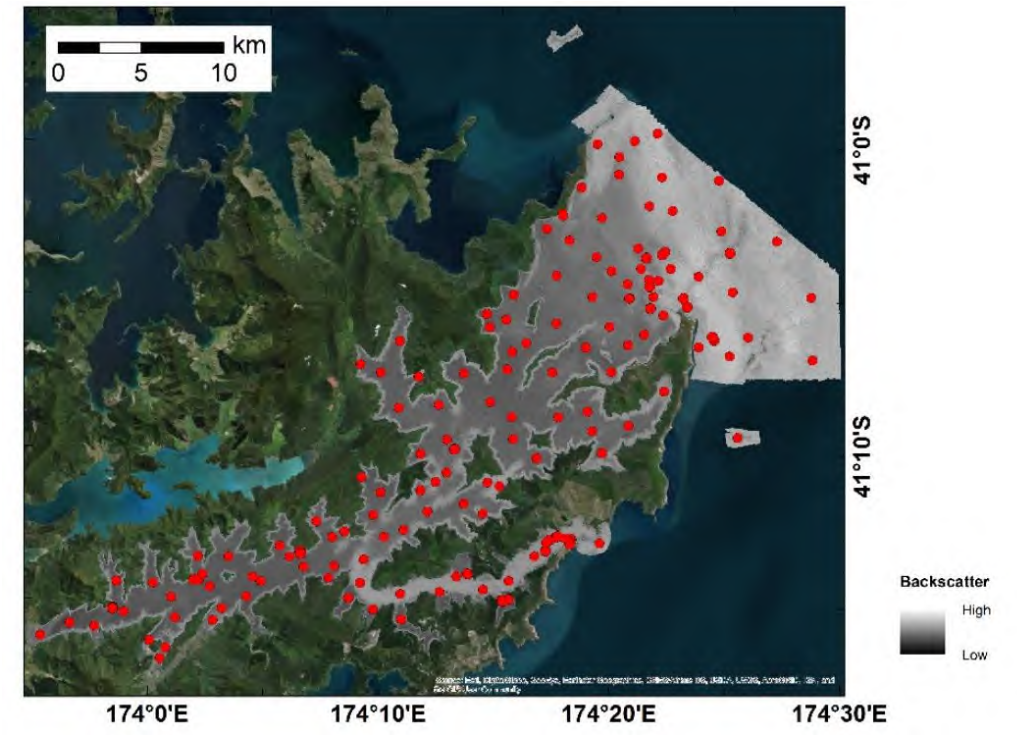

Figure 1-21: Seafloor ground truth sites in relation to backscatter imagery. Sample locations represented by red dots.

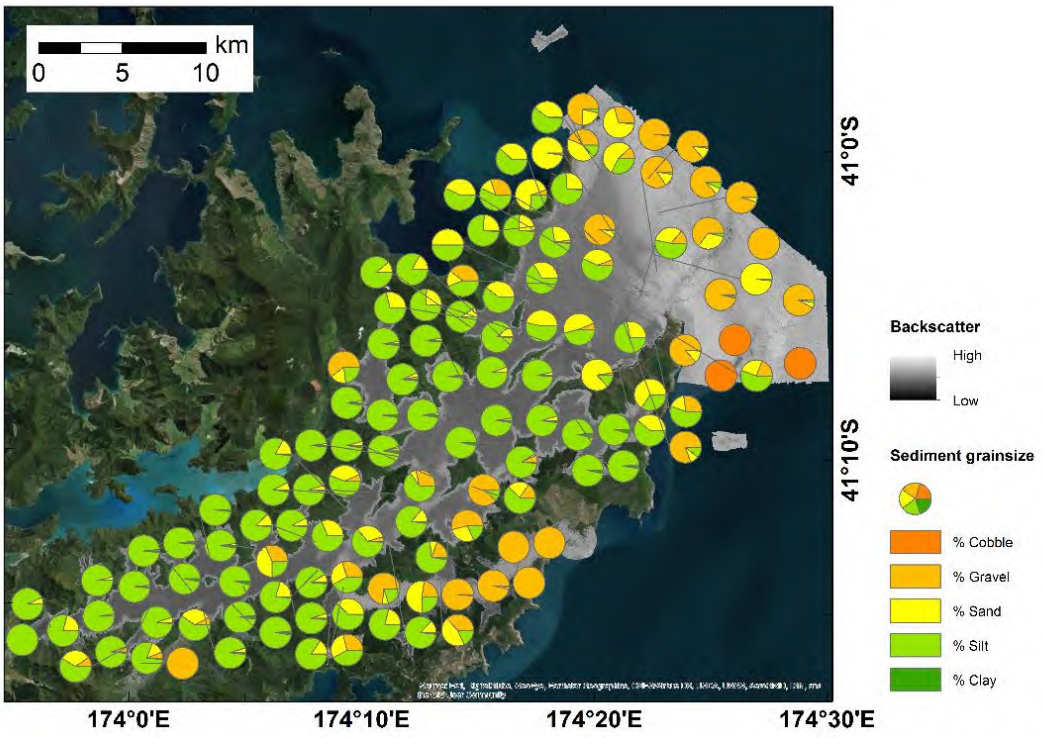

Figure 1-22: Sediment grainsize and seafloor backscatter imagery.

Based on the predominating grainsize classes, and considering the grain-size based subtidal to deep subtidal level five classification scheme (Department of Conservation and Ministry of Fisheries 2011), we selected four backscatter classes from the grain size - backscatter intensity diagram (Figure 1-23):

1. Coarse sand and gravel (cS, Fig. 1-23), defined as Phi<1 resulting in backscatter intensity greater than -14 dB, based on the regression line generated from the 66% groundtruth samples.

4. Medium sand, defined as 1<Phi<2 (mS Fig. 1-23) resulting in backscatter intensity between -14 dB and -18 dB.

5. Fine sand, defined as 2<Phi<4 (fS, Fig. 1-23), resulting in backscatter intensity between -18 dB and -22 dB; and

6. Mud, defined as Phi> 4 (M, Fig. 1-23), resulting in backscatter intensity lower than -22 dB.

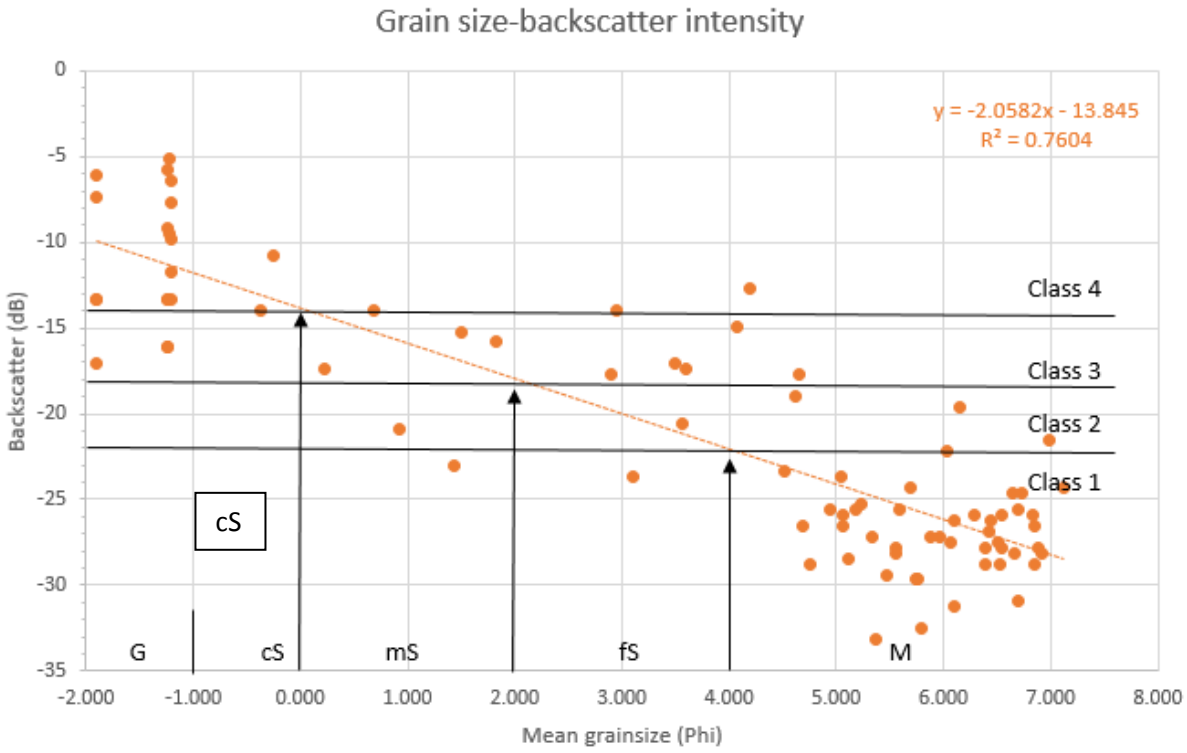

Figure 1-23: Mean grainsize and backscatter dB values for 66% of the groundtruth sites. G: Gravel; Cs: Coarse sand; mS: medium sand; fS: Fine sand; M: Mud.

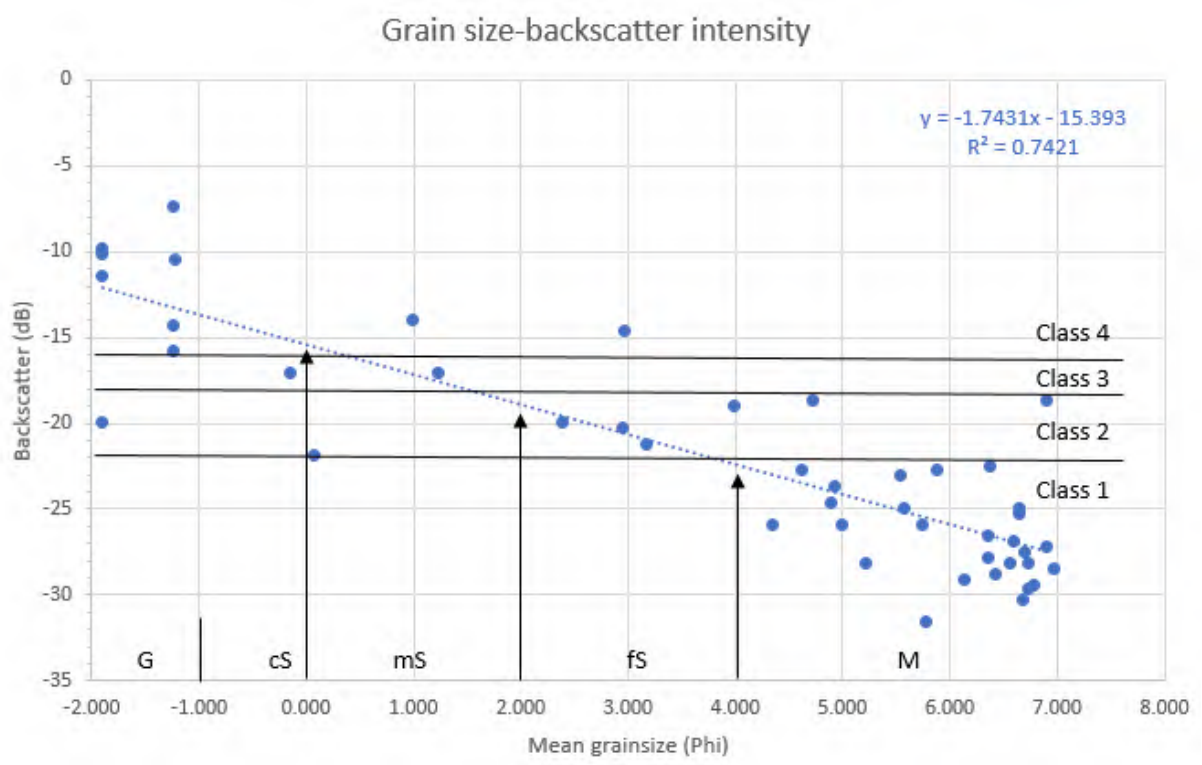

Figure 1-24: Test dataset mean grainsize and backscatter dB values for 33% of the groundtruth sites. G: Gravel; Cs: Coarse sand; mS: medium sand; fS: Fine sand; M: Mud.

The distribution of the combined (training and validation) ground-truth samples within the resultant four-class map is as follows (See Section Part 1, 3.3.1):

- 52% of the samples correspond to Class 1, a homogeneous low reflectivity mud facies (Phi>4; BS>-22 dB)
- 24% of the samples fall into Class 4 a highly heterogeneous (high) reflectivity substrate corresponding to coarse sand gravel (2<Phi<4; -22 dB<BS<-18 dB)
- 13% of the samples fall into Class 3 a homogeneous, medium-to-high reflective substrate corresponding to medium sand (1<Phi<2; -18 dB<BS<-16)
- 10 % of the samples fall into Class 2 a homogeneous, mdeium-to-high reflective class corresponding to fine sand (Phi<1; BS>-16dB).

1.11.2 Satellite-Derived Seafloor Classification

The classification of the seafloor from satellite imagery was undertaken by EOMAP GmbH & Co. KG.

Satellite image data, which were corrected for atmosphere, adjacency and water surface effects were semi-manually classified following an object-based classification approach. This approach considers texture, shape and color of the seafloor and classifies objects with comparable properties. These objects were than classified and manipulated by the analyst. Three seafloor classes were derived for the Marlborough Sound (Figure 1-25):

- Vegetated seafloor - this class is dominated by vegetated seafloor coverage which is either seagrass on soft bottom or algae on hardbottom types;
- Hardbottom - hardbottom types which might partially be covered by algae; and
- Unconsolidated sediment - soft bottom, not or sparsely covered by vegetation.

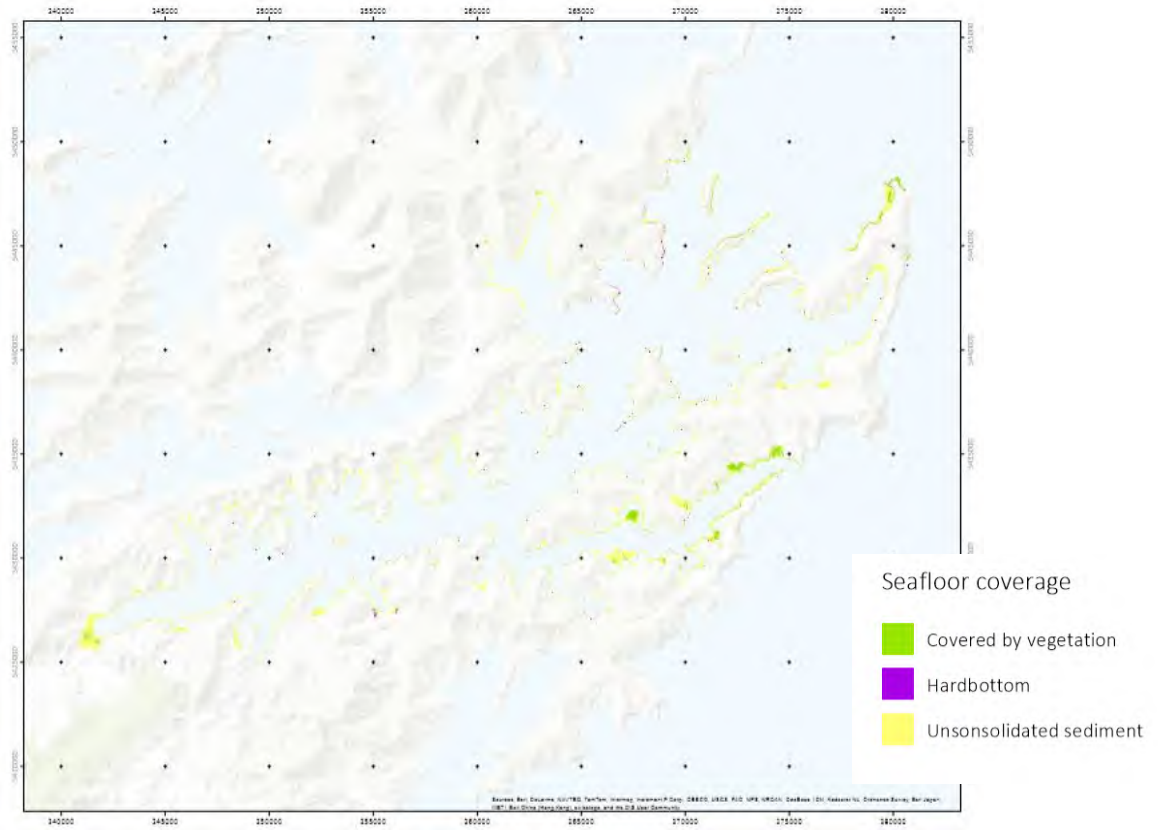

Figure 1-25: Overview map of the seafloor coverage classification.

1.12 Water Column Processing

EM2040 water column data were collected during HS51 on all lines, at the same time as the bathymetry. These data were logged to a separate file (*.wcd) for later examination and processing (Figure 1-26).

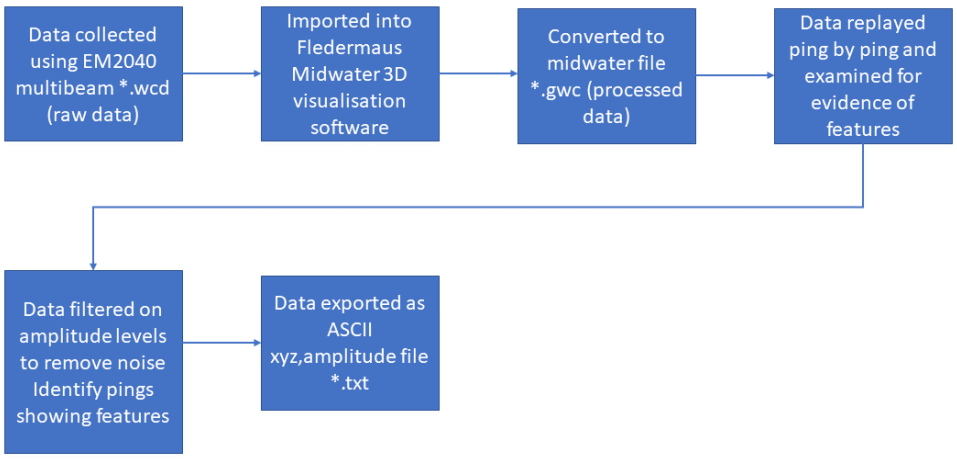

Figure 1-26: Water column processing flow.

The examination of this data involved the viewing of the stacked data for each line, followed by the replaying of the processed data and examining them ping by ping (Figure 1-27). Due to the water depth the multibeam was often acquiring data samples at several samples/second which resulted in the line replay rate slower than the actual acquisition speed. The line replay rate was slowed or paused whenever potential water column features were observed to allow for the examination of every ping in greater detail.

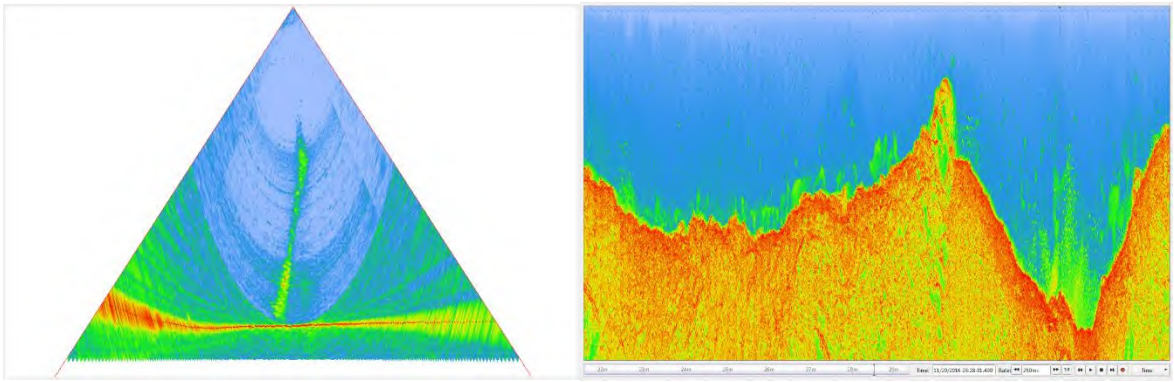

Figure 1-27: Water column data replayed ping by ping (fan) (left) and data displayed in stacked format(right).

Once potential water column features were identified the following workflow was completed:

- Display full multibeam line data in stacked format;
- Select fan of view of feature and filter to relevant beams only;
- Zoom into feature in stacked view;
- Filter data on amplitude level to display feature only;
- Note position and feature classification;
- Take screen grab of representative features or features of interest; and
- Import features into GIS layer.

Features present and able to be identified within this water column dataset include:

- **Wrecks**;
- **Seeps** - measured from center of seep and at connection to seafloor, then classified into the following categories:
    1. Dominant Seep (>2/3 of water column);
    2. Minor Seep (<2/3 water column);
    3. Dominant Diffuse Seep;

4. Minor Diffuse Seep.

- Seeps where further classified by their association with other nearby seeps:
  1. Solitary;
  2. Member of Field of Seeps (>4);
  3. Member of Seepage Field
- **Kelp** - classified into the following categories of:
  1. low (young or nascent);
  2. tall (>1 m);
  3. mixture of the two previous categories.
- **Anthropogenic features** such as lines from moorings, wharfs, marina structures, marine farm structures.

The images below (Figure 1-28) provide an example of a feature that is evident in bathymetry, backscatter and water column data. This example feature is a wreck of a yacht (Feature 192.1 in Report of Survey) detected with least depth of 48 m in the bathymetry (over hull), and least depth of 37.5 m in water column (over mast and rigging).

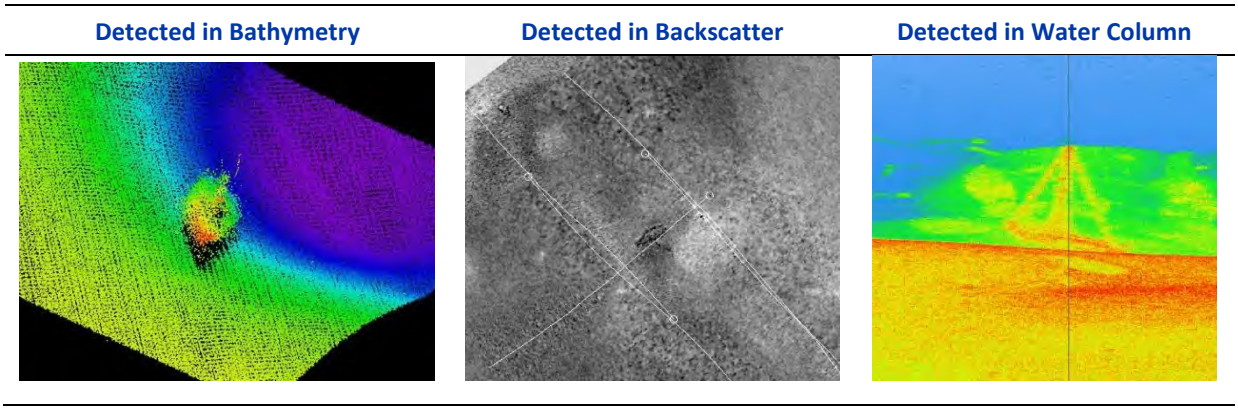

Figure 1-28: Wreck in Bathymetry, Backscatter and Water Column Data.

The survey area also contains numerous mussel lines, caged fish farms, and high density mooring areas. Fledermaus 3D scenes were created for all of the marine farms in the survey area. These scenes allow an observer to visualise the area and structure of the farms. Representaive static images were extracted and are presented in the portfolio. The process for generating the 3D scenes is detailed In Figure 1-29.

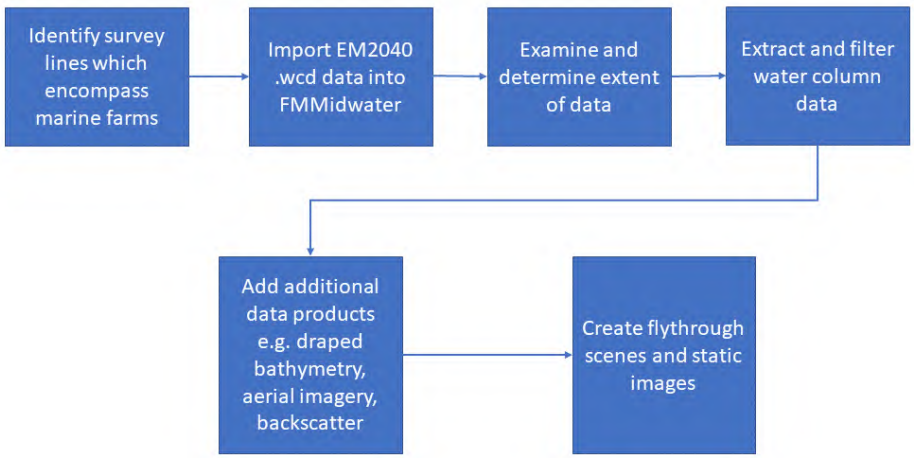

Figure 1-29: Fledermaus 3D scenes workflow.

The Fledermaus scenes are provided in a proprietary file format. To view these scenes, the freely available software program "iView4D" can be used. iView4D is currently available for Windows XP/Vista/W7 platforms, Linux, and Mac OS X. An OpenGL compatible card with good driver support is also required.

iView4D can be downloaded by clicking http://www.qps.nl/display/fledermaus/iview.

1.13 Seabed Sampling

The acquisition of seabed samples for hydrographic and backscatter ground-truthing is a fundamental part of providing information to enable the analysis of the benthic habitat. Samples and video/still images were acquired at designated sites which were determined primarily by the hydrographic criteria, with a few targeted samples on specific acoustic backscatter, geomorphic feature or biogenic habitats.

Seabed samples were collected via Dietz-Lafond and Van Veen Grabs. A Dietz-Lafond grab is a small spring loaded 'snapper' type grab ideal for recovering undisturbed samples from a muddy seafloor (Figure 1-30). It has spring and weight loaded jaws which close around a seafloor sample upon striking the seafloor after being triggered by a mechanical lever. A Van Veen Grab is a bedload sampler, which is a heavier grab ideal for recovering gravels. Prior and during deployment to the seafloor the two buckets are held in open position by the means of a hook. When the grab contacts the seafloor the tension on the hook is released and the hook disengaged. When the grab is hoisted back from the seafloor the buckets dig into the sea bed and close.

Seabed imagery was acquired from either a Deep Blue Splashcam or NIWA's CoastCam. The Deep Blue Splashcam system is a hand deployed camera system with integral lights and 100 m cable. Realtime video data is logged onto a ruggedised laptop.

NIWAs CoastCam system, acquires high resolution video which are stored on an underwater unit and downloaded once the camera system is recovered on deck (Figure 1-31). Low definition video is monitored in realtime via a VDSL modem connection through the winch cable. Coast Cam uses labview

software to remotely control a 12 MegaPixel Canon EOS 540 SLR and a Sony AVC HD hybrid HDD handy Cam.

Figure 1-30: Dietz-Lafond grab used for sediment sampling (left) and sample on collection plate (right).

Seabed samples were obtained from *RV Ikatere* during two campaigns: 5-7 December 2016 and 5-7 May 2017. The samples were photographed, labelled, and given a first level of description upon retrieval on deck. All seabed samples were retained for grain size analysis at NIWA Wellington for use in backscatter classification. Additional high-definition imagery was made available to this survey from NIWA's Coasts and Oceans programme.

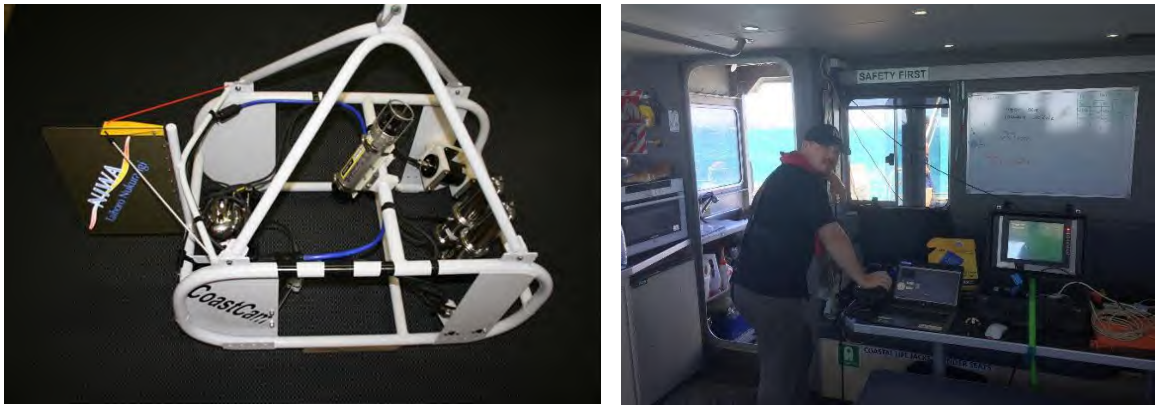

Figure 1-31: NIWA Coastcam video and stills camera system(left), topside control system (right).

For each sample RV *Ikatere* was positioned over the preselected site while the CoastCam system was deployed, ensuring resulting imagery was of undisturbed seafloor. Once the camera was recovered, the grab was deployed using a hydraulic winch.

When the grab reached the seafloor its layback position was recorded from the A-Frame position on the Navipac navigation screen. Following retrieval sediment samples were transferred to a collection plate, a photo taken, sample described for hydrographic (IHO) purposes, and then retained in a 500-ml jar for further processing.

All relevant video and still camera imagery was later analysed producing biological faunal presence data.

1.13.1 Textural classification

Consistent with NIWA laboratory procedures for marine sediments, sampling protocols were adopted to ensure accurate and representative results, and followed standard best practice. The basic methodology adopted a systematic process of: (1) homogenize and representatively sub-sampling; (2) analyse particle size of subsamples (using both laser diffraction and sieve methods where appropriate); and, (3) data export and analysis.

Homogenisation and representative subsampling

After stirring the sample jar, around 10 cm^3 (2-tablespoons) of subsample was removed, homogenised, and then another small subsample ~ 1cm^3 is removed for laser sizing. Samples are sieved at 1600 um prior to going in the sample bath and anything left in the sieve can be noted.

Particle-size analysis

Sediment samples <2000 µm were analysed for particle size using a Beckman Coulter LS 13 320 Dual Wavelength Laser Particle Sizer. The basis of the method is well established and the instrument has been a popular choice in commercial and research applications, particularly for sandy sediments (e.g. McCave and Syvitski, 1991; McCave et al., 2006). A laser light source is used to illuminate the suspended particles passing through a glass chamber. The light scattered by the particles is detected by silicon photo-detectors. The intensity of light on each detector, measured as a function of angle, is then subjected to mathematical analysis using a complex inversion matrix algorithm. The result is a particle size distribution covering a size range from 0.4–2000 µm, displayed as volume percent across 92 discrete size classes. For sandy or muddy samples this method offers several advantages over traditional sieve stacks, including much improved efficiency and accuracy; resolution and repeatability.

Operational protocols followed well established laboratory procedures for heterogeneous marine sediments, with the exception of dispersal considerations. To achieve appropriate obscuration (a function of turbidity) approximately 0.5–1 cm^3 of sediment was initially dispersed in a 50 ml container with weak washing solution (4 g of $NaHCO_3$ and 1 g Na_2CO_3 dissolved in 20 L of ultra-pure water), sonicated in a bath for around 10 seconds, and then flushed through a 1.6 mm sieve into the laser-sizer's sample bath containing approximately 1 L of 1 µm filtered-tap water. Pre-sieving is required because gravel-sized particles can block and damage the laser sizer plumbing and optical cell. Any visual estimates of the quantity and nature of the gravel components left on the sieve are recorded.

The gravel component was estimated from the remaining sub-sample and passed through the 1.6 mm sieve, then the components dried and weighed to estimate the gravel content.

Data export and analysis

Raw results from the laser-sizer were checked after each analysis to ensure correct instrument operation, and exported into Excel spreadsheets for data manipulation and presentation. Any gravel fraction was added and normalised into the percentage size-class data. Granulometric analyses were achieved in Excel using GRADISTAT version 8.0 (Blott, 2010), which calculates the standard granulometric statistics, textural descriptions and size fraction percentages.

Sediment textural descriptions follow the well-established guidelines of Udden (1914) and Wentworth (1922), but to also align with hydrographic definitions “gravel” refers to all material > 2mm. Where appropriate, an estimated maximum clast size or composition (e.g. shell versus rock) was recorded to aid bottom-substrate descriptions. As a nomenclature rule, size-class components needed to be >5% by volume to be included as a textural modifier if appropriate, e.g. slightly sandy shelly mud.

1.14 Application of Benthic Terrain Modeler

Benthic Terrain Modeler (BTM) is a collection of ArcGIS-based tools developed for analysing and classifying the benthic environment based on final combined bathymetric surface (e.g. Erdey-Heydorn, 2008; Lundblad et al. 2006). These tools include the creation of standardised bathymetric position index (BPI) grids, aspect, slope, rugosity, and other geomorphometric measurements from an input bathymetric data set. These BTM tools where applied to multiple resolutions of the combined bathymetric surface (2 m, 10 m, 30 m, and 50 m cell size) to provide assessment of, and identify trends on the benthic terrain at a variety of scales, as well as to analyse fine- and broad-scale features.

Outputs from the BTM include:

- **Bathymetric Position Index (BPI) Grids**. BPI is principally a measure of where a referenced location is relative to the locations surrounding it. Hence positive window values indicate features that are higher than the surrounding area e.g. ridges and negative window values designate features that are lower than the surrounding area e.g. depressions or scour. Window values near zero are either flat areas or areas of constant slope. The creation of BPI data sets at two different scales is central to the methods behind the benthic terrain classification process. BPI is a derivative of the input bathymetric data set, and is used to define the location of specific features and regions relative to other features and regions within the same data set (Figure 1-32).
  - *Broad-Scale BPI* is a broad-scale BPI data set that allows you to identify larger regions within the benthic landscape.
  - *Fine-Scale BPI* is a fine-scale BPI data set that allows you to identify smaller features within the benthic landscape.

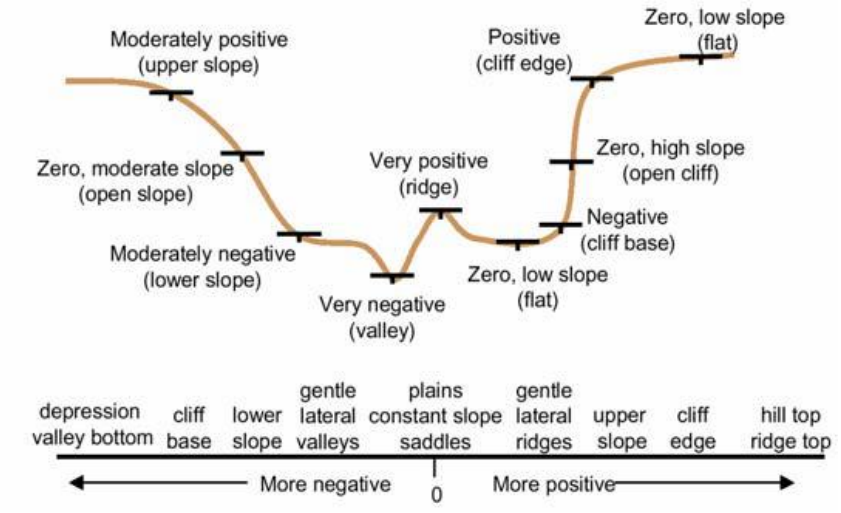

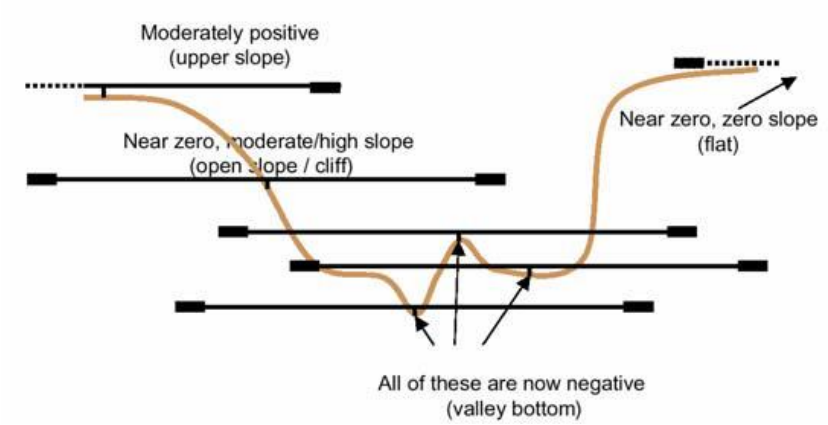

Figure 1-32: Fine-scale BPI (top) where subtle topographic features show up. Broad-scale (bottom) BPI results in broad scale topographic features (from Weiss, 2001).

The standardized BPI data sets are classified to identify various benthic zones and/or structures:

- **Depth Statistics** are depth summary statistics over a set neighbourhood size, where a neighbourhood is defined as the neighbouring cells around every cell in an input raster. The four neighbourhood sizes used in this project are: 3 x 3 cell; 5 x 5 cell; 7 x 7 cell; and 15 x 15 cell neighbourhoods. These statistics can be useful predictors in understanding the benthic zones in analyses tasks like habitat classification. The depth statistics calculated are:
  - **Range of depth** shows the difference between the minimum and maximum depths within the neighbourhood.
  - **Standard deviation of depth** shows the standard deviation of the depth values within the neighbourhood.
- **Slope** identifies the slope (gradient, or rate of maximum change in depth) from each cell of a raster surface.
  - **Standard deviation of slope** shows the standard deviation of the slope values within the neighbourhood.
  - **Curvature** is a 'slope of slope' raster. A positive curvature indicates the surface is upwardly convex at that cell. A negative curvature indicates the surface is upwardly concave at that cell. A value of 0 indicates the surface is flat.
- **Aspect** identifies the downslope direction of the maximum rate of change in value from each cell to its neighbours. Aspect can also be thought of as the slope direction.
- **Terrain Ruggedness (VRM – Vector Ruggedness Measure)**, or rugosity, is the variation in three-dimensional orientation of grid cells within a neighbourhood, i.e. the ratio between the surface area and the planar area for each cell (Figure 1-33). This method effectively captures variability in slope and aspect into a single measure. Ruggedness values in the output raster can range from 0 (no terrain variation) to 1 (complete terrain variation). Typical values for natural terrains range between 0 and about 0.4.

1.14.1 Benthic Terrain Classification

Benthic terrain classification is a user-defined (dictionary) structures layer based on BPI's, slope, standard deviation breaks, and depth. The benthic zones in the output layer include crests, depressions, flats, and slopes. The benthic structures in the output layer consist of:

- flat plains;
- broad slopes;
- steep slopes;
- broad platforms or depressions;
- lateral mid-slope platforms or depressions;
- scarps (or cliffs);
- depressions;
- crevices, narrow gullies over elevated terrain;
- narrow slopes;
- rock outcrop highs,
- narrow ridges; and
- local depressions, current scours.

The following are also finer-scale benthic structures that occur in or on larger scale benthic structures:

- local ridges, boulders, pinnacles in depressions (i.e. smaller scale ridges on a larger scale depression);
- local ridges, boulders, pinnacles on broad flats (i.e. smaller scale ridges on a larger scale broad flats);
- local ridges, boulders, pinnacles on slopes (i.e. smaller scale ridges on a larger scale slopes).

2 Glossary of abbreviations and terms

DEM	Digital Elevation Model
DML	Discovery Marine Limited
GDP	Geodetic Data Pack
Geoswath	Interferometric multibeam: side scan (backscatter)and bathymetry
GNSS	Global Navigation Survey System
HS51	LINZ Project HYD-2016/17-01 (HS51) Hydrographic Survey of Queen Charlotte Sound / Tōtaranui and Tory Channel / Kura Te Au
IMU	Inertial Measurement Unit
LD	Least Depth
LINZ	Land Information New Zealand
MBES	Multibeam Echo Sounder
MDC	Marlborough District Council
MRU	Motion Reference Unit
NIWA	National Institute of Water and Atmospheric Research Ltd
NMEA	National Marine Electronics Association
NZGD2000	New Zealand Geodetic Datum 2000
NZTM	New Zealand Transverse Mercator Projection
POSMV	Position and Orientation System for Marine Vessels
QADP	Quality Assurance Data Pack
ROS	Report of Survey
RV	Research Vessel
SBES	Single Beam Echo Sounder
SIC	Surveyor In Charge
SIS	Seafloor Information System
SSS	Side-Scan Sonar
SV	Sound Velocity
SVP	Sound Velocity Profile
TDP	Tidal Data Pack
WADGNSS	Wide Area Differential Global Navigation Satellite System
WGS-84	World Geodetic System 1984

3 Bibliography

Anderton, P.W. (1981) Structure and evolution of the south Wanganui Basin, New Zealand. New Zealand Journal of Geology and Geophysics, 24(1): 39-63.

Andrews, B. D., Brothers, L. L., & Barnhardt, W. A. (2010). Automated feature extraction and spatial organization of seafloor pockmarks, Belfast Bay, Maine, USA. Geomorphology, 124(1-2): 55-64.

Barnes, P.M., Audru, J.-C. (1999) Recognition of active strike-slip faulting from high-resolution marine seismic reflection profiles: Eastern Marlborough fault system, New Zealand. Geological Society of America Bulletin, 111(4): 538-559.

Begg, J.G., Johnston, M.R. (2000) Geology of the Wellington area. Institute of Geological & Nuclear Sciences, 1:250 000 geological map 10: 64p.

Broekhuizen, N., Hadfield, M. (2016) Additional salmon farms in Tory Channel: An assessment of effects on water-quality using a biophysical model. NIWA Client report prepared for the Ministry for Primary Industries. NIWA Client Report HAM2015-039.

Brothers, L.L., Kelley, J.T., Belknap, D.F., Barnhardt, W.A. and Koons, P.O. (2011) Pockmarks: self-scouring seep features? Proceedings of the 7th International Conference on Gas Hydrates. Warehouse, U.P., Edinburgh, Scotland, July 17-21 2011.

Carter, L. (1976) Seston transport and deposition in Pelorus Sound, South Island, New Zealand. New Zealand Journal of Marine and Freshwater Research, 10(2): 263-282.

Carter, L. (1992) Acoustical characterisation of seafloor sediments and its relationship to active sedimentary processes in Cook Strait, New Zealand New Zealand Journal of Geology and Geophysics, 35: 289-300.

Carter, L. and Lewis, K.B. (1995) Variability of the modern sand cover on a tide and storm driven inner shelf, south Wellington, New Zealand New Zealand Journal of Geology and Geophysics, 38: 451-470.

Cartwright, J., Huuse, M., and Aplin, A. (2007) Seal bypass systems. American Association of Petroleum Geologists Bulletin, 91: 1141-1166.

Colbo, K., Ross, T., Brown, C., Weber, T., 2014. A review of oceanographic applications of water column data from multibeam echosounders, Estuarine, Coastal and Shelf Science, 145: 41-56

Cotton, C.A. (1974) Bold coasts - annotated reprints of selected papers on coastal geomorphology, 1916-1969 by the late Sir Charles Cotton. A.H and A.W. Reed, Wellington, New Zealand.

Craw, D., Anderson, L., Rieser, U., Waters, J. (2007) Drainage reorientation in Marlborough Sounds, New Zealand, during the last interglacial. New Zealand Journal of Geology and Geophysics, 50(1): 13-20.

Craw, D., Waters, J. (2007) Geological and biological evidence for regional drainage reversal during lateral tectonic transport, Marlborough, New Zealand. Journal of the Geological Society, 164(4): 785-793.

Davidson, R., Duffy, C., Gaze, P., Baxter, A., DuFresne, S., Courtney, S. and Hamill, P. (2011) Significant Marine Sites Inventory Report 2011.

https://www.marlborough.govt.nz/environment/coastal/coastal-ecosystems/significant-marine-sites-inventory-report-2011

Davey, N., Neil, H., HS51 Survey team (2017) Marine Mammal Report. NIWA Client Report 2017208WN.

Department of Conservation and Ministry of Fisheries (2011). Coastal marine habitats and marine protected areas in the New Zealand Territorial Sea: a gap analysis. Appendix 1 Habitat Classification Scheme.

Diesing, M., Stephens, D., 2015. A multi-model ensemble approach to seabed mapping. Journal of Sea Research 100: 62-69.

Erdey-Heydorn, M.D. (2008) An ArcGIS Seabed Characterization Toolbox Developed for Investigating Benthic Habitats Marine Geodesy, 31(4): 318-358.

Gibbs, M.M., James, M.R., Pickmere, S.E., Woods, P.H., Shakespeare, B.S., Hickman, R.W., Illingworth, J. (1991) Hydrodynamic and water column properties at six stations associated with mussel farming in Pelorus Sound, 1984–85. New Zealand Journal of Marine and Freshwater Research, 25(3): 239-254.

Harris, T.F.W. (1990) Greater Cook Strait: Form and Flow. DSIR Marine and Freshwater, Wellington, New Zealand: 212p.

Hadfield, M., Broekhuizen, N., Plew, D. (2014). A biophysical model for the Marlborough Sounds. Part 1: Queen Charlotte Sound and Tory Channel. NIWA Client Report CHC2014116

Hayward, B.W., Grenfell, H.R., Sabaa, A.T., Kay, J., Daymond-King, R., Cochran, U. (2010) Holocene subsidence at the transition between strike-slip and subduction on the Pacific-Australian plate boundary, Marlborough Sounds, New Zealand. Quaternary Science Reviews, 29(5-6): 648-661.

Heath, R.A. (1974) Physical oceanographic observations in Marlborough Sounds. New Zealand Journal of Marine and Freshwater Research, 8(4): 691-708.

Hovland, M. (1982) Pockmarks and the recent geology of the central section of the Norwegian Trench. Marine Geology 47: 283-301.

Hovland, M. (1983) Elongated depressions associated with pockmarks in the western slope of the Norwegian Trench. Marine Geology 51:35-46.

Hovland, M., Heggland, R., de Vries, M. H., and Tjelta, T. I. (2010) Unit-pockmarks and their potential significance for the prediction of fluid flow. Journal of Marine and Petroleum Geology 27: 1190-1199.

Hovland, M. & Judd, A. G. (1988) Seabed Pockmarks and Seepages Impact on Geology, Biology and the Marine environment. Graham & Trotman, London, 293pp.

Ingram, C.W.N. (1984). New Zealand Shipwrecks 1795 – 1982. A.H. and A.W. Reed, New Zealand.

Jackson, D.R. and Briggs, K.B. (1992) High-frequency bottom backscattering: Roughness versus sediment volume scattering. Journal of the Acoustical Society of America, 92(2): 962-977.

Klaucke, I., Sarkar, S., Bialas, J., Berndt, C., Dannowski, A., Dumke, I., Hillman, J., Koch, S., Nodder, S., Papenberg, C., von Deimling, J. (2018). Giant depressions on the Chatham Rise offshore New Zealand – Morphology, structure and possible relation to fluid expulsion and bottom currents. Marine Geology 399: 158–169.

Kurland, J. and Woodby, D. (2008) What Is Marine Habitat Mapping and Why Do Managers Need It? In: Reynolds, J.R., and Greene, H.G. (Eds). Marine Habitat Mapping Technology for Alaska, Alaska Sea Grant College Program, University of Alaska Fairbanks

Lamarche, G., Proust, J.N., Nodder, S.D. (2005) Long-term slip rates and fault interactions under low contractional strain, Wanganui Basin, New Zealand. Tectonics, 24(4).

Lamarche, G., Lurton, X., Verdier, A.-L. and Augustin, J.-M. (2011) Quantitative characterization of seafloor substrate and bedforms using advanced processing of multibeam backscatter. Application to the Cook Strait, New Zealand, Continental Shelf Research, 31(2 SUPPL): S93-S109.

Lamarche, G. and Lurton, X. (2018) Introduction to the Special Issue "Seafloor backscatter data from swath mapping echosounders: From technological development to novel applications", in Lamarche, G., and Lurton, X. (Eds) Seafloor backscatter data from swath mapping echosounders: From technological development to novel applications Marine Geophysical Research, 39(1-2): 1-4.

Lauder, G.A. (1987) Coastal landforms and sediments of the Marlborough Sounds. PhD thesis submitted in fulfilment of the Degree of Doctor of Philosophy. Department of Geography. University of Canterbury, Christchurch, New Zealand: 327p.

Lauder, W.R. (1970) The ancient drainage of the Marlborough Sounds. New Zealand Journal of Geology and Geophysics, 13(3): 747-749.

Lewis, K.B., Carter, L., Davey, F.J. (1994) The opening of Cook Strait: interglacial tidal scour and aligning basins at a subduction to transform plate edge. Marine Geology, 116(3-4): 293-312.

Lewis, K.B., Mitchell, J.S. (1980) Cook Strait sediments. New Zealand Oceanographic Institute (now NIWA) Chart, Coastal series, 1:200 000.

Litchfield, N.J., Van Dissen, R., Sutherland, R., Barnes, P.M., Cox, S.C., Norris, R., Beavan, R.J., Langridge, R., Villamor, P., Berryman, K., Stirling, M., Nicol, A., Nodder, S., Lamarche, G., Barrell, D.J.A., Pettinga, J.R., Little, T., Pondard, N., Mountjoy, J.J., Clark, K. (2014) A model of active faulting in New Zealand. New Zealand Journal of Geology and Geophysics, 57(1): 32-56.

Lundblad, E.R., Wright, D.J., Miller, J., Larkin, E.M., Rinehart, R., Naar, D.F., Donahue, B.T., Anderson, S.M. and Battista, T. (2006) A Benthic Terrain Classification Scheme for American Samoa Marine Geodesy, 29(2): 89 - 111.

Lurton, X. and Lamarche, G. (eds) (2015) Backscatter measurements by seafloor-mapping sonars. Guidelines and Recommendations. Geohab Report, 200p., http://geohab.org/wp-content/uploads/2013/02/BWSG-REPORT-MAY2015.pdf.

McCave, I.N. and Syvitski, J.P.M. (1991) Principles and methods of geological particle size analysis. In: Principles, Methods and Application of Particle Size Analysis (Ed. J.P.M. Syvitski), pp. 3–21. Cambridge University Press, New York.

McCave, I.N., Hall, I.R. and Bianchi, G.G. (2006) Laser vs. settling velocity differences in silt grainsize measurements: estimation of palaeocurrent vigour. Sedimentology 53: 919–928.

Mitchell, J.S. (1996) Cook Strait bathymetry, 3rd edition. New Zealand Oceanographic Institute (now NIWA) Chart, Coastal series, 1:200 000.

Mortimer, N. (1993) Metamorphic zones, terranes, and Cenozoic faults in the Marlborough Schist, New Zealand. New Zealand Journal of Geology and Geophysics, 36(3): 357-368.

Mortimer, N., Wopereis, P. (1997) Change in direction of the Pelorus River, Marlborough, New Zealand: evidence from composition of Quaternary gravels. New Zealand Journal of Geology and Geophysics, 40(3): 307-313.

Morrisey D, Cameron M, Newcombe E 2018. Effects of moorings on different types of marine habitat. Marlborough District Council. Cawthron Report No. 3098. 41 p. plus appendix.

Neil, H.L., Pallentin, A., Mitchell, J., Kane, T. 2015. Multibeam echo-sounder mapping to identify seafloor habitats northwest of D'Urville Island. NIWA Client Report WLG2015-38.

Neil, H.L., Pallentin, A. and Mitchell, J. (2015a) Northwest D'Urville seafloor habitat maps: A2 map folio series. NIWA Client Report WLG2015-40.

Neil, H.L.; Mackay, K.A.; Mitchell, J.; Pallentin, A.; (2015b). Multibeam echo-sounder mapping to identify seafloor habitats Hikurangi Marine Reserve. NIWA Client Report WLG2015-55.

Nicol, A. (2011) Landscape history of the Marlborough Sounds, New Zealand. New Zealand Journal of Geology and Geophysics, 54(2): 195-208.

Pilcher, R., Argent J., (2007) Mega-pockmarks and linear pockmark trains on the West African continental margin. Marine Geology, 244(1–4): 15-32

Plew, D.R., Stevens, C.L. (2013) Numerical modelling of the effect of turbines on currents in a tidal channel–Tory Channel, New Zealand. Renewable Energy, 57: 269-282.

Proctor, R., Carter, L. (1989) Tidal and sedimentary response to the late Quaternary closure and opening of Cook Strait, New Zealand: results from numerical modeling. Paleoceanography, 4(2): 167-180.

Proctor, R., Hadfield, M. (1998) Numerical investigation into the effect of freshwater inputs on the circulation in Pelorus Sound, New Zealand. New Zealand Journal of Marine and Freshwater Research, 32(3): 467-482.

Singh, L.J. (2001) Late Quarternary Sea Level and Tectonic History of Marlborough Sounds: A Thesis Submitted to the Victoria University of Wellington in Fulfilment of the Requirements for the Degree of Doctor of Philosophy in Geology. Department of Geology. Victoria University of Wellington, Wellington, New Zealand: 214p.

Stern, T.A., Quinlan, G.M., Holt, W.E. (1993) Crustal dynamics associated with the formation of Wanganui Basin, New Zealand. Elsevier, New York.

Stewart, S. A. (1999) Seismic Interpretation of circular geological structures. Petroleum Geoscience 5: 273-285

Stevens, C. (2014) Residual flows in Cook Strait, a large tidally dominated strait. Journal of Physical Oceanography, 44(6): 1654-1670.

Stevens, G.R. (1974, 1990 reprint) Rugged Landscape: the geology of central New Zealand, including Wellington, Wairarapa, Manawatu, and the Marlborough Sounds. DSIR Publishing, Wellington, New Zealand.

Sutton, P.J.H., Hadfield, M.G. (1997) Aspects of the hydrodynamics of Beatrix Bay and Pelorus Sound, New Zealand. New Zealand Journal of Marine and Freshwater Research, 31(2): 271-279.

Te Punga, M.T. (1953) A late Pleistocene land bridge across Cook Strait, New Zealand. NZ Journal of Science and Technology, 35: 161-192.

Townsend M, Thrush S, Carbines M. 2011. Simplifying the complex: an ecosystem principles approach to goods and services management in marine coastal systems. Marine Ecology Progress Series 434: 291-301.

Udden, J.A. (1914) Mechanical composition of clastic sediments. Bulletin of the Geological Society of America 25: 655-744.

Vennell, R., 1994: Acoustic Doppler current profiler measurements of tidal phase and amplitude in Cook Strait, New Zealand. Continental Shelf Research 14: 353–364.

Wallace, L.M., Reyners, M., Cochran, U., Bannister, S., Barnes, P.M., Berryman, K., Downes, G., Eberhart-Phillips, D., Fagereng, A., Ellis, S. (2009) Characterizing the seismogenic zone of a major plate boundary subduction thrust: Hikurangi Margin, New Zealand. Geochemistry, Geophysics, Geosystems, 10(10).

Walters, R.A., Gillibrand, P.A., Bell, R.G., Lane, E.M. (2010) A study of tides and currents in Cook Strait, New Zealand. Ocean dynamics, 60(6): 1559-1580.

Weiss, A. D. (2001) Topographic Positions and Landforms Analysis (Conference Poster). ESRI International User Conference. San Diego, CA, July 9-13.

Wentworth, C.K. (1922) A scale of grade and class terms for clastic sediments. Journal of Geology 30: 377-392.

Wright, D.J., Pendleton, M., Boulware, J., Walbridge, S., Gerlt, B., Eslinger, D., Sampson, D. and Huntley, E. (2012) ArcGIS Benthic Terrain Modeler (BTM), v. 3.0, Environmental Systems Research Institute, NOAA Coastal Services Center, Massachusetts Office of Coastal Zone Management.

Zeldis, J.R., Howard-Williams, C., Carter, C.M., Schiel, D.R. (2008) ENSO and riverine control of nutrient loading, phytoplankton biomass and mussel aquaculture yield in Pelorus Sound, New Zealand. Marine Ecology Progress Series, 371: 131-142.

HS 51 Hydrographic and Science Report & Document Package

Acoustic Imaging Ltd, 2016. *Ikatere* and *Rukuwai* II – Hydrographic Survey Vessels, Vertical Squat Determination.

Aurecon, 2010. Report for RV *Ikatere* Squat Survey.

DML / NIWA, 2017. Mobilisation Report v2. NIWA Client Report 2016149WN.

DML / NIWA, 2017a. Report of Survey – Area A. NIWA Client Report 2017014WN.

DML / NIWA, 2017b. Report of Survey – Area A1 / A2 v2. NIWA Client Report 2017121WN.

DML / NIWA, 2017c. Tidal Data Pack – Area A1 / A2 v2. NIWA Client Report 2017120WN.

DML / NIWA, 2017d. Geodetic Data Pack – HS51. NIWA Client Report 2017123WN.

DML / NIWA, 2017e. Quality Assurance Data Pack – Area A1 / A2. NIWA Client Report 2017128WN.

DML / NIWA, 2017f. Tidal Data Pack – HS51. NIWA Client Report 2017305WN.

DML / NIWA, 2017g. Report of Survey – HS51. NIWA Client Report 2017408WN.

DML / NIWA, 2017h. Quality Assurance Data Pack – HS51. NIWA Client Report 2017409WN.

Land Information New Zealand (LINZ), 2016. Request for Proposals (RFP): Hydrographic Surveying Services, HS51-53.

Land Information New Zealand (LINZ), 2016a. Hydrographic Survey Specification – Queen Charlotte Sound/Tōtaranui and Tory Channel/Kura Te Au V1, Project Number HYD-2016/17-01 (HS51).

Land Information New Zealand (LINZ), 2016b. Contract for Services, Number 200873 (HS51 Hydrographic Surveys).

Marlborough 0.4m Rural Aerial Photos (2011 - 2012), imagery (Photographic Survey SN13373) sourced from Marlborough District Council under CC-BY.

National Hydrographer, New Zealand Hydrographic Authority (LINZ), 2016c. Contract Specifications for Hydrographic Surveys v1.3, 7 June 2016.

New Zealand Hydrographic Authority (NZHA) - Land Information New Zealand (LINZ), 2011: Chart NZ615, Marlborough Sounds, New Edition March 2011.

New Zealand Hydrographic Authority (NZHA) - Land Information New Zealand (LINZ), 2011: Chart NZ6153, Queen Charlotte Sound, New Edition March 2011.

NIWA, 2016. Response to Request for Proposals (RFP): Hydrographic Surveying Services, HS51-53.

NIWA / Davey, N., Neil, H., HS51 Survey team (2017) Marine Mammal Report. NIWA Client Report 2017208WN.

NIWA / DML (2017). East Bay Seafloor Habitat Maps A2 Folio. NIWA Client Report 2017353WN.

NIWA / Neil H.L., Mackay K., Wilcox S., Kane T., Lamarche G., Wallen B., Orpin A., Steinmetz T., Pallentin A. 2018. What lies beneath? Guide to Survey Results and Graphical Portfolio, Queen Charlotte Sound/Tōtaranui and Tory Channel/Kura Te Au (HS51) Survey. NIWA Client Report 2018085WN.

NIWA / Mackay K., Wilcox S., Neil H.L., Kane T., Steinmetz T. 2018. Queen Charlotte Sound/Tōtaranui and Tory Channel/Kura Te Au (HS51) Survey. Habitat Maps: A2 Folio Series. NIWA Client Report 2018084WN.

Appendix A Associated Documents and Data

For completeness Table 1-4 lists documents and data delivered here, and all associated documents and data delivered prior to this guide.

Table A-1: Data and reports delivered for HS51.

Document / Data Name	Quantity	Digital Data File Name
Delivered here		
What lies beneath? Guide to Survey Results and Graphical Portfolio, Queen Charlotte Sound/Tōtaranui and Tory Channel/Kura Te Au (HS51) Survey. NIWA Client Report 2018085WN.	1	What lies beneath? Guide to Survey Results and Graphical Portfolio, plus accompanying data (this document).
Portfolio Map Series Queen Charlotte Sound/Tōtaranui and Tory Channel/Kura Te Au (HS51) Survey. NIWA Client Report 2018084WN.	2 sets of 13 portfolios, plus 13 PDF	Queen Charlotte Sound/Tōtaranui and Tory Channel/Kura Te Au (HS51) Survey. Habitat Maps: A2 Folio Series. Inner Queen Charlotte Sound/Tōtaranui (HS51) Survey. Habitat Maps: A2 Folio Series. Middle Queen Charlotte Sound/Tōtaranui (HS51) Survey. Habitat Maps: A2 Folio Series. Outer Queen Charlotte Sound/Tōtaranui (HS51) Surve.y Habitat Maps: A2 Folio Series. Tory Channel/Kura Te Au (HS51) Survey. Habitat Maps: A2 Folio Series. Outlying Areas Queen Charlotte Sound/Tōtaranui and Tory Channel/Kura Te Au (HS51) Survey. Habitat Maps: A2 Folio Series. Marine Farms Queen Charlotte Sound/Tōtaranui and Tory Channel/Kura Te Au (HS51) Survey. Habitat Maps: A2 Folio Series.
Queen Charlotte Sound/Tōtaranui and Tory Channel/Kura Te Au NIWA Chart, Miscellaneous Series.	3000 - 500 of each Chart	Queen Charlotte Sound/Tōtaranui and Tory Channel/Kura Te Au. NIWA Chart, Miscellaneous Series 101. Neil H.L., Mackay K., Mackay E.J., Wilcox S., Smith R. 2018 Queen Charlotte Sound/Tōtaranui, Grove Arm – Dieffenbach Point. NIWA Chart, Miscellaneous Series 102. Neil H.L., Mackay K., Mackay E.J., Wilcox S., Smith R. 2018 Queen Charlotte Sound/Tōtaranui, Bay of Many Coves – Cape Koamaru. NIWA Chart, Miscellaneous Series 103. Neil H.L., Mackay K., Mackay E.J., Wilcox S., Smith R. 2018 Queen Charlotte Sound/Tōtaranui, Resolution Bay – Cook Strait. NIWA Chart, Miscellaneous Series 104. Neil H.L., Mackay K., Mackay E.J., Wilcox S., Smith R. 2018 Tory Channel/Kura Te Au. NIWA Chart, Miscellaneous Series 105. Neil H.L., Mackay K., Mackay E.J., Wilcox S., Smith R. 2018 Picton Harbour and Waikawa Bay. NIWA Chart, Miscellaneous Series 106. Neil H.L., Mackay K., Mackay E.J., Wilcox S., Smith R. 2018
ESRI fgdb and mxd	1 mxd, 9 fgdb	Mxd and file geodatabases, including all accompanying tabulated data

Document / Data Name	Quantity	Digital Data File Name
3D visualisations	208	3D visualisations of marine farm structures (Fledermaus scenes, i4View), 128 3D visualisations of wreck structures (Fledermaus scenes, i4View), 24 3D visualisations of seep features (Fledermaus scenes, i4View), 36 3D visualisations of kelp (Fledermaus scenes, i4View), 20
Seafloor Video	163	Video files of the sediment sampling sites (.mp4)
MBES Raw data	1,179,152 files	EM2040.all EM2040.wcd Sound Velocity POSMV Navipac Navigation Daily Logsheets
Geoswath Raw Data	36,360 files	Raw Data Daily Logsheets
Geoswath Backscatter Processed	108 files	DB Value Mosaiced Geographic data Geotiff Mosaiced Geographic data
HS51 Hydrographic deliverables	1,826 files	Thick GSF Thick XYZDT Reports Miscellaneous Survey files
Redelivered information and data		For completeness, and ease of future use, some previous reports and processed data have been included in this digital delivery. These are indicated by **bold** in the following list
Previous delivery		
Marine Mammal Observations Report ver 1	1	**HS51 Marine Mammal Observations report** and accompanying data. OBIS at https://nzobisipt.niwa.co.nz/resource?r=hs51marinemammalobs&v=1.0, GBIF at https://doi.org/10.15468/s7ctpf. doi:10.15468/s7ctpf.
East Bay Seafloor Habitat Maps ver 1	2	East Bay Seafloor Habitat Maps A2 folio series (2) and 3D visualisations of marine farm structures (Fledermaus scenes, i4View, ESRI fgdb and mxd).
Standard Sheets	11	HS51_STD_1-8 (1:30,000) version 1 dated 8 December 2017 HS51_STD_9,11 (1:10,000) version 1 dated 8 December 2017 HS51_STD_10 (1:3,000) version 1 dated 8 December 2017
Ancillary Sheets	11	HS51_STD_1-8 (1:30,000) version 1 dated 8 December 2017 HS51_STD_9,11 (1:10,000) version 1 dated 8 December 2017 HS51_STD_10 (1:3,000) version 1 dated 8 December 2017
Index Sheets	1	HS51-INDEX (1:150,000) version 1 dated 8 December 2017
QA Checks of Sheets	23	Sheet_QA_HS51_STD_1-11 Sheet_QA_HS51_ANC_1-11 Sheet_QA_HS51_INDEX

Document / Data Name	Quantity	Digital Data File Name
GeoTIFF Sheets	23	TIFF files of above sheets and TFW files for each
PDF Sheets	23	Digital files of above
MBES Survey Limit (DXF)	1	Digital files
Coastline (DXF)	1	Digitised Coastline for 1:30,000 Sheets
Contours (DXF)	6	Contours_30k & Contours_30k_Zero Contours_10k & Contours_10k_Zero Contours_3k & Contours_3k_Zero
Raw Logged MBES/Backscatter/Water Column/SVP	1,179,437 files in two drives	**Logged data, RAW SIS format .all files, POSMV and SVP data,** Drive A, 624,558 files, 7.19 TB *Ikatere* Projects 102-203 Drive B, 555,067 files, 5.83 TB *Ikatere* Projects 203-286
Raw SBES HydroPro Data	964 files	Drive B, SBES Directory 23.1Gb
Geoswath Sonar Mosaic and Imagery Files	2 folders, 310 Files	Sonar Mosaics, imagery and tfw files 4.53 Gb
Thick GSF **MBES and SBES Data Processed**	14,084 files	**Thick GSF, 873 GB**
Thick GSF Cross Line files	206 files	Thick GSF, 33 GB, one file corrupted
Thick ASCII XYZT	7042 files	**ASCII XYZT soundings, 787 Gb**
Thin ASCII XYZ Sounding Data	5 files Un-truncated, 5 files Truncated	Un-truncated ASCII XYZ; 1.66 Mb Truncated ASCII XYZ (plotted); 1.62Mb
Report of Survey ver 1	1	**HS51 Queen Charlotte Sound/Tōtaranui and Tory Channel/Kura Te Au Report of Survey** and accompanying data
Photographs	Digital Folder	Drive C
Tidal Data Pack ver 1.1	1	**HS51 Tidal Data Pack** and accompanying digital data
Geodetic Data Pack ver 1	1	**HS51 Geodetic Data Pack** and accompanying digital data
Quality Assurance Data Pack ver 1	1	**HS51 QADP** and accompanying digital data
Daily Narrative	1	Included with QADP

Appendix B Seabed Sediment Images

This set of images was initially supplied for hydrographic purposes with the Report of Survey. For ease of use we are appending the images here. Video, from which the stills are extracted, is supplied within the digital delivery.

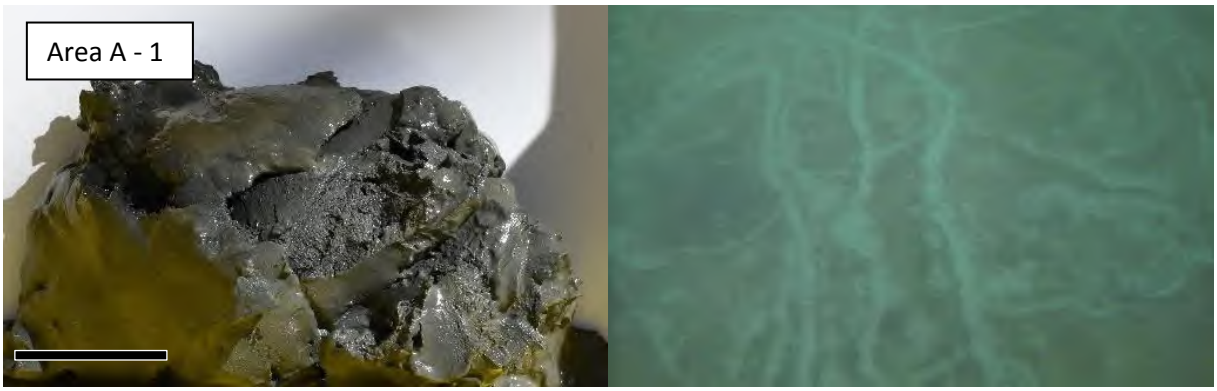

Site A1 physical sample (left), scale = 5 cm; and seafloor image (right).

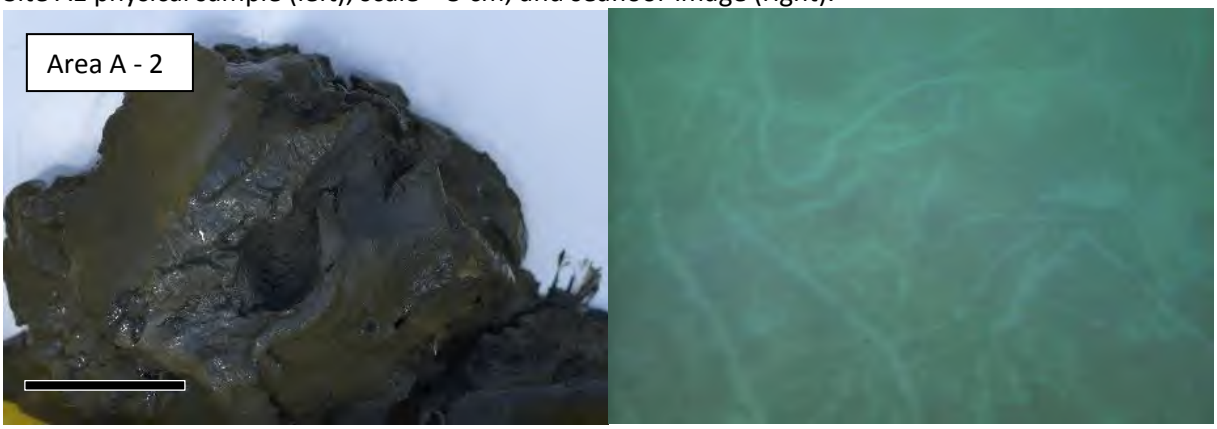

Site A2 physical sample (left), scale = 5 cm; and seafloor image (right).

Site A3 physical sample (left), scale = 5 cm; and seafloor image (right)

Figure B-1: Area A Sediment Sampling Site Images.

Site A4 physical sample (left), scale = 5 cm; and seafloor image (right).

Site A5 physical sample (left), scale = 5 cm; and seafloor image (right).

Site A6 physical sample (left), scale = 5 cm; and seafloor image (right).

Figure B-1 (cont): Sediment Sampling Site Images.

Site A7 physical sample (left), scale = 5 cm; and seafloor image (right).

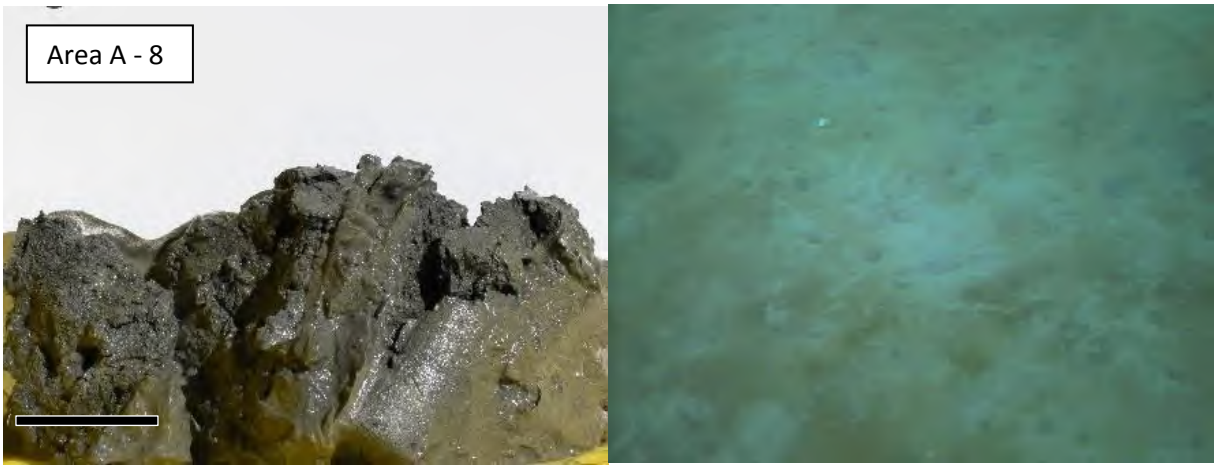

Site A8 physical sample (left), scale = 5 cm; and seafloor image (right).

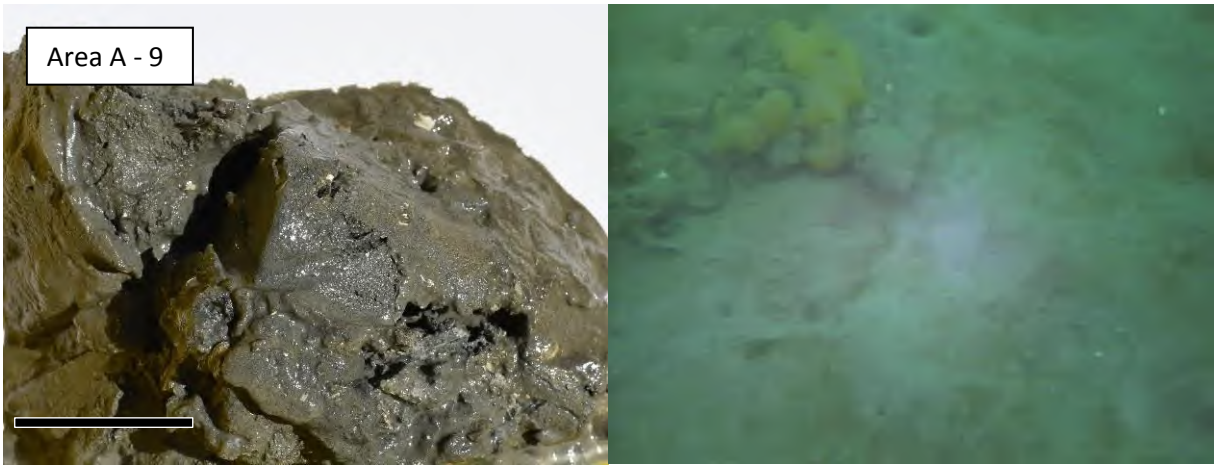

Site A9 physical sample (left), scale = 5 cm; and seafloor image (right).

Figure B-1 (cont): Sediment Sampling Site Images.

Site A10 physical sample (left), scale = 5 cm; and seafloor image (right).

Site A10a physical sample (left), scale = 5 cm; and seafloor image (right).

Site A11 physical sample (left), scale = 5 cm; and seafloor image (right).

Figure B-1 (cont): Sediment Sampling Site Images.

Site A12 physical sample (left), scale = 5 cm; and seafloor image (right).

Site A13 physical sample (left), scale = 5 cm; and seafloor image (right).

Figure B-1(cont): Sediment Sampling Site Images.

Site B1 physical sample (left), scale = 5 cm; and seafloor image (right), scale = 20 cm.

Site B2 physical sample (left), scale = 5 cm; and seafloor image (right), scale = 20 cm.

Site B3 physical sample (left), scale = 5 cm; and seafloor image (right), scale = 20 cm.

Figure B-2: Area B Sediment Sampling Site Images.

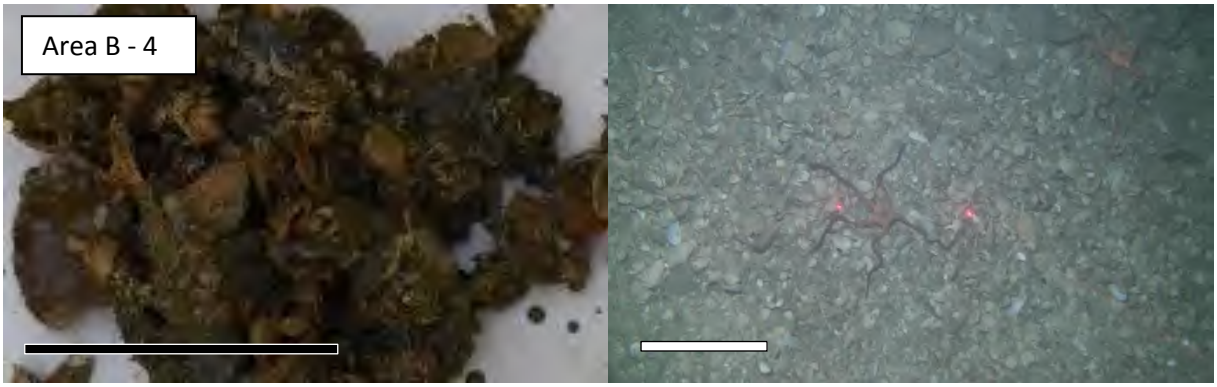

Site B4 physical sample (left), scale = 5 cm; and seafloor image (right), scale = 20 cm.

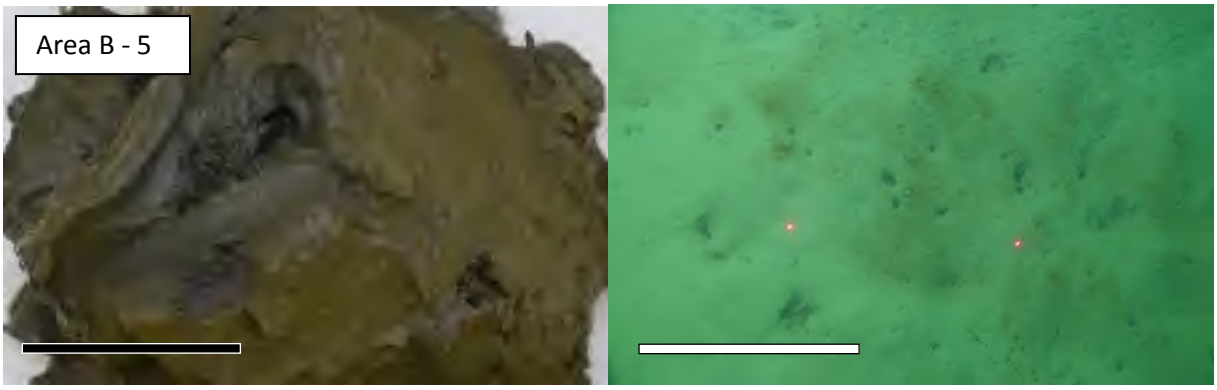

Site B5 physical sample (left), scale = 5 cm; and seafloor image (right), scale = 20 cm.

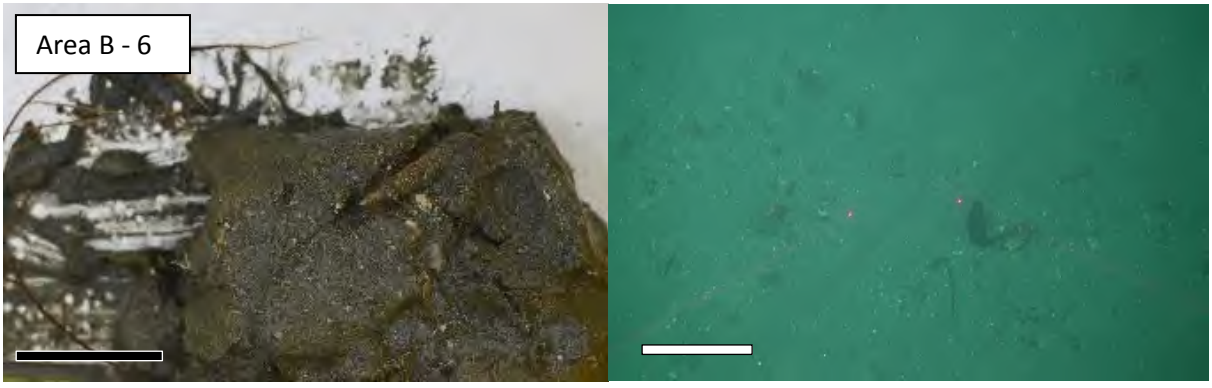

Site B6 physical sample (left), scale = 5 cm; and seafloor image (right), scale = 20 cm.

Figure B-2 (cont): Area B Sediment Sampling Site Images.

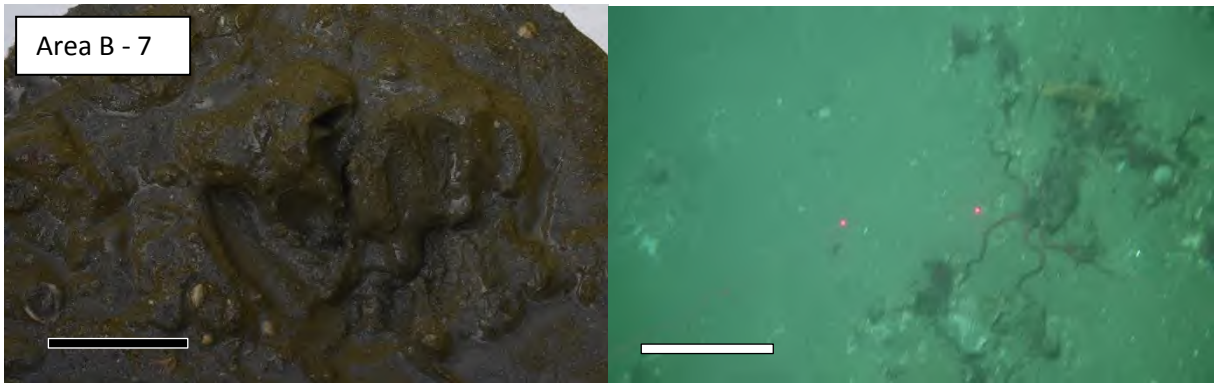

Site B7 physical sample (left), scale = 5 cm; and seafloor image (right), scale = 20 cm.

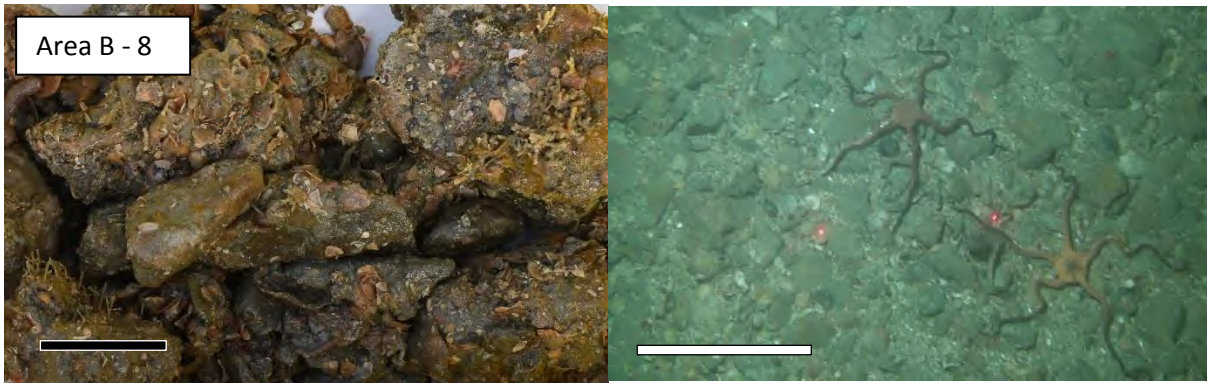

Site B8 physical sample (left), scale = 5 cm; and seafloor image (right), scale = 20 cm.

Site B9 physical sample (left), scale = 5 cm; and seafloor image (right), scale = 20 cm.

Figure B-2 (cont): Area B Sediment Sampling Site Images.

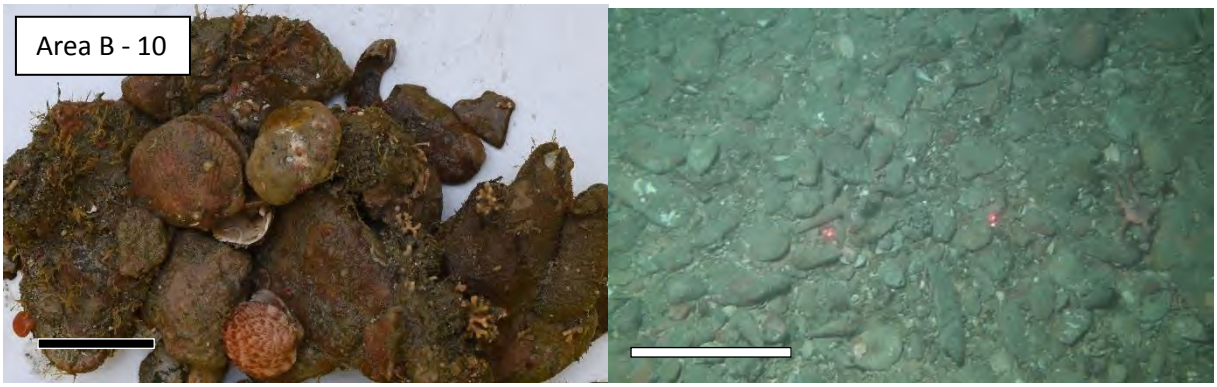

Site B10 physical sample (left), scale = 5 cm; and seafloor image (right), scale = 20 cm.

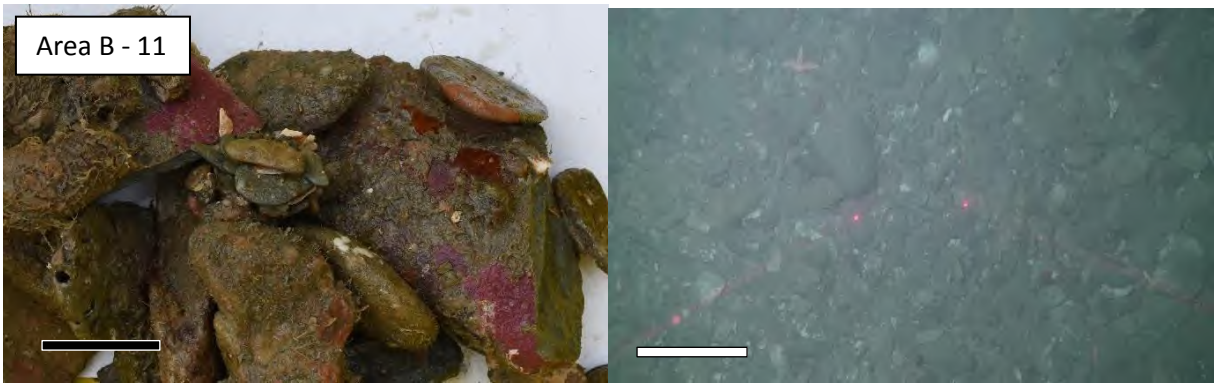

Site B11 physical sample (left), scale = 5 cm; and seafloor image (right), scale = 20 cm.

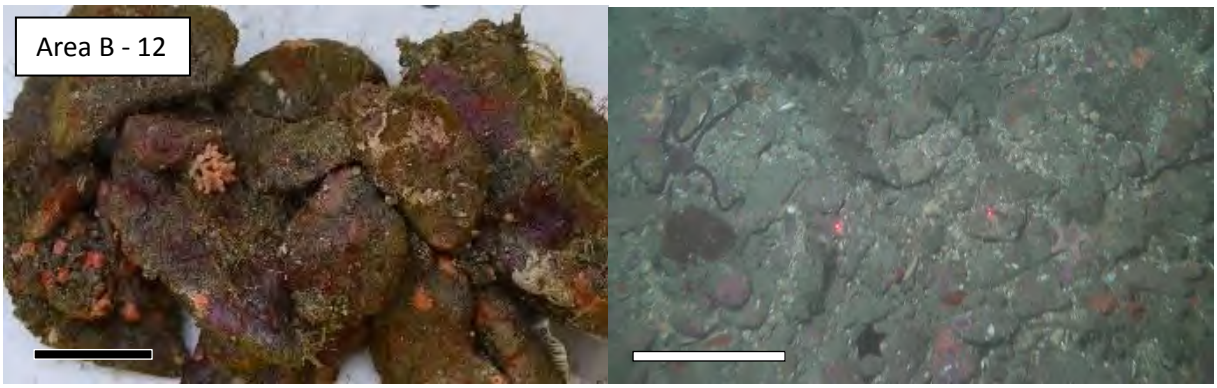

Site B12 physical sample (left), scale = 5 cm; and seafloor image (right), scale = 20 cm.

Figure B-2 (cont): Area B Sediment Sampling Site Images.

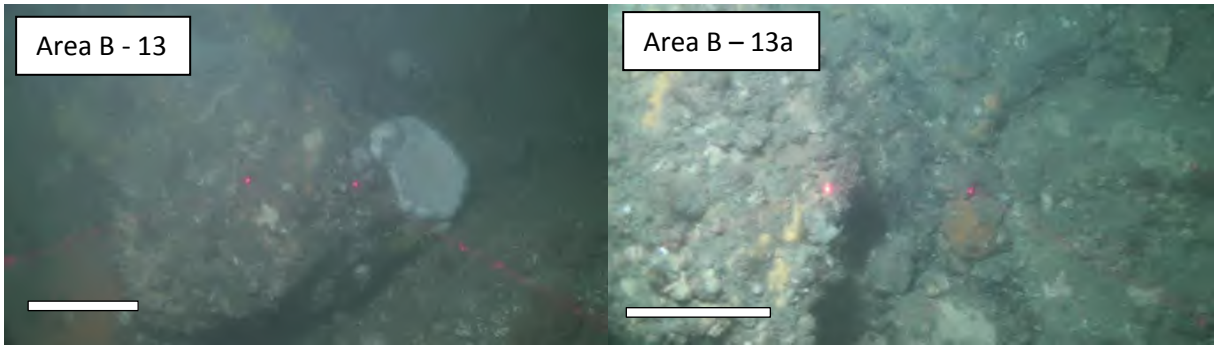

Site B13 seafloor images (scale = 20 cm).

Figure B-2 (cont): Area B Sediment Sampling Site Images.

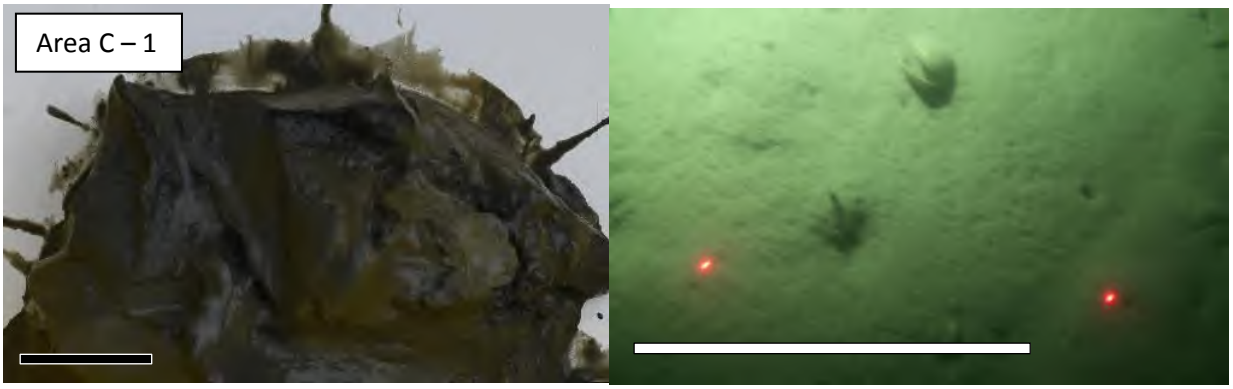

Site C1 physical sample (left), scale = 5 cm; and seafloor image (right), scale = 20 cm.

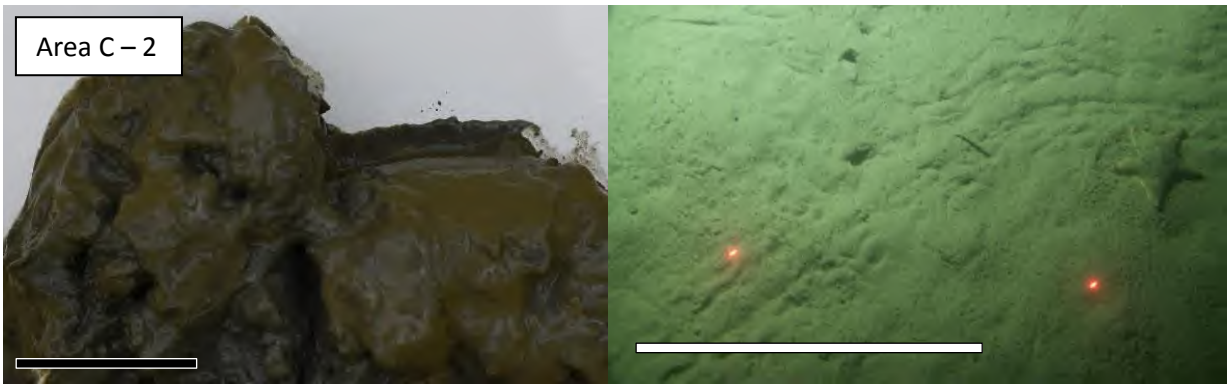

Site C2 physical sample (left), scale = 5 cm; and seafloor image (right), scale = 20 cm.

Site C3 physical sample (left), scale = 5 cm; and seafloor image (right).

Figure B-3: Area C Sediment Sampling Site Images.

Site C4 physical sample (left), scale = 5 cm; and seafloor image (right).

Site C5 physical sample (left), scale = 5 cm; and seafloor image (right).

Site C6 physical sample (left), scale = 5 cm; and seafloor image (right), scale = 20 cm.

Figure B-3 (cont): Area C Sediment Sampling Site Images.

Site C7 physical sample (left), scale = 5 cm; and seafloor image (right), scale = 20 cm.

Site C8 physical sample (left), scale = 5 cm; and seafloor image (right), scale = 20 cm.

Site C9 physical sample (left), scale = 5 cm; and seafloor image (right).

Figure B-3 (cont): Area C Sediment Sampling Site Images.

Site C10 physical sample (left), scale = 5 cm; and seafloor image (right), scale = 20 cm.

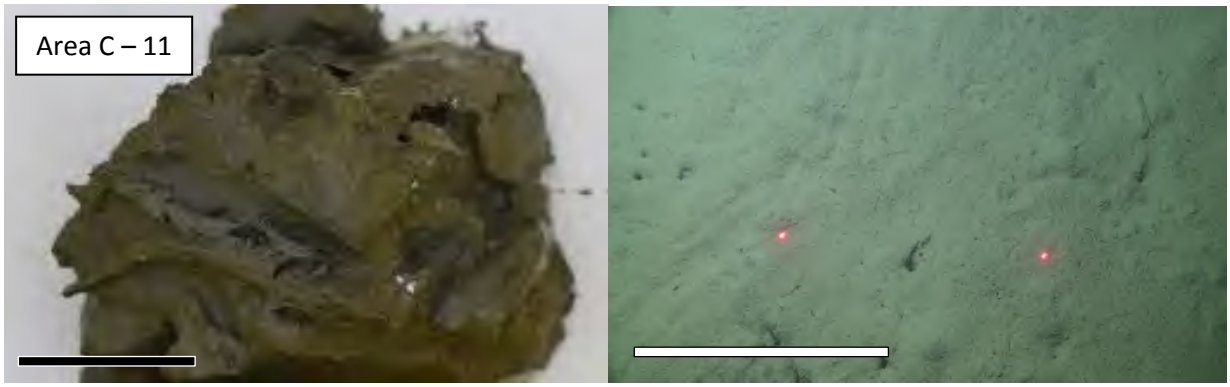

Site C11 physical sample (left), scale = 5 cm; and seafloor image (right), scale = 20 cm.

Site C12 physical sample (left), scale = 5 cm; and seafloor image (right).

Figure B-3 (cont): Area C Sediment Sampling Site Images.

Site C13 physical sample (left), scale = 5 cm; and seafloor image (right), scale = 20 cm.

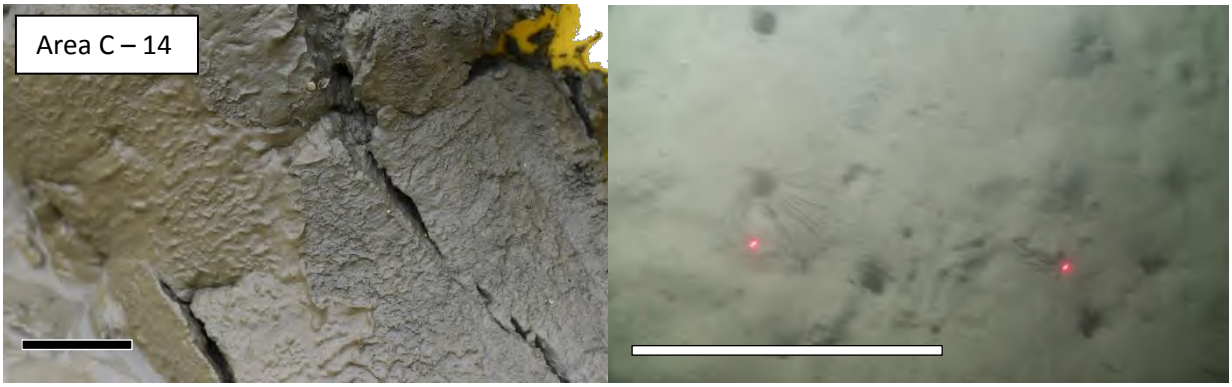

Site C14 physical sample (left), scale = 5 cm; and seafloor image (right), scale = 20 cm.

Site C15 physical sample (left), scale = 5 cm; and seafloor image (right).

Figure B-3 (cont): Area C Sediment Sampling Site Images.

Site C16 physical sample (left), scale = 5 cm; and seafloor image (right).

Site C17 physical sample (left), scale = 5 cm; and seafloor image (right).

Site C18 physical sample (left), scale = 5 cm; and seafloor image (right).

Figure B-3 (cont): Area C Sediment Sampling Site Images.

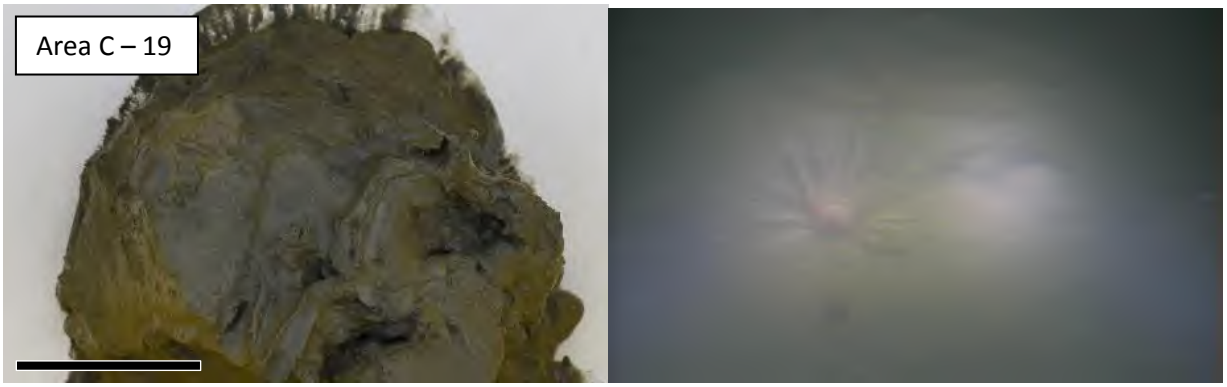

Site C19 physical sample (left), scale = 5 cm; and seafloor image (right).

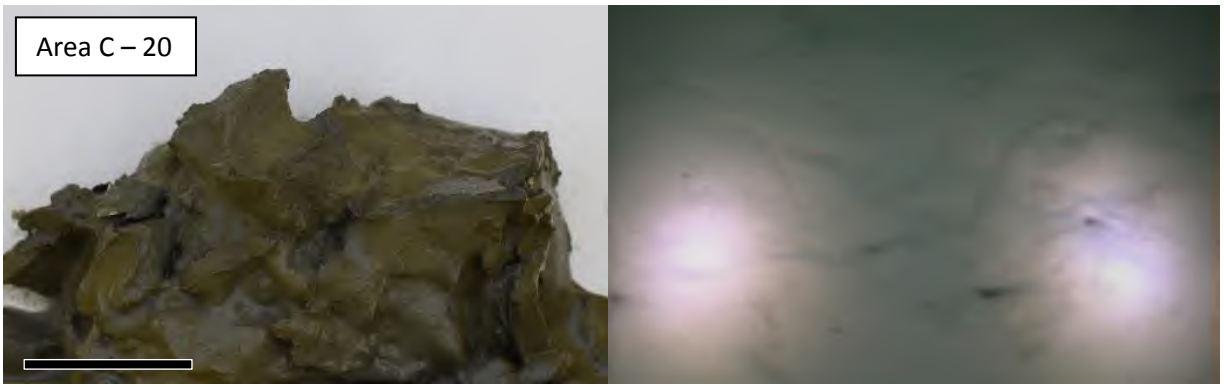

Site C20 physical sample (left), scale = 5 cm; and seafloor image (right).

Site C21 physical sample (left), scale = 5 cm; and seafloor image (right).

Figure B-3 (cont): Area C Sediment Sampling Site Images.

Site C22 physical sample (left), scale = 5 cm; and seafloor image (right).

Site C23 physical sample (left), scale = 5 cm; and seafloor image (right).

Site C24 physical sample (left), scale = 5 cm; and seafloor image (right).

Figure B-3 (cont): Area C Sediment Sampling Site Images.

Site C25 physical sample (left), scale = 5 cm; and seafloor image (right).

Site C26 physical sample (left), scale = 5 cm; and seafloor image (right).

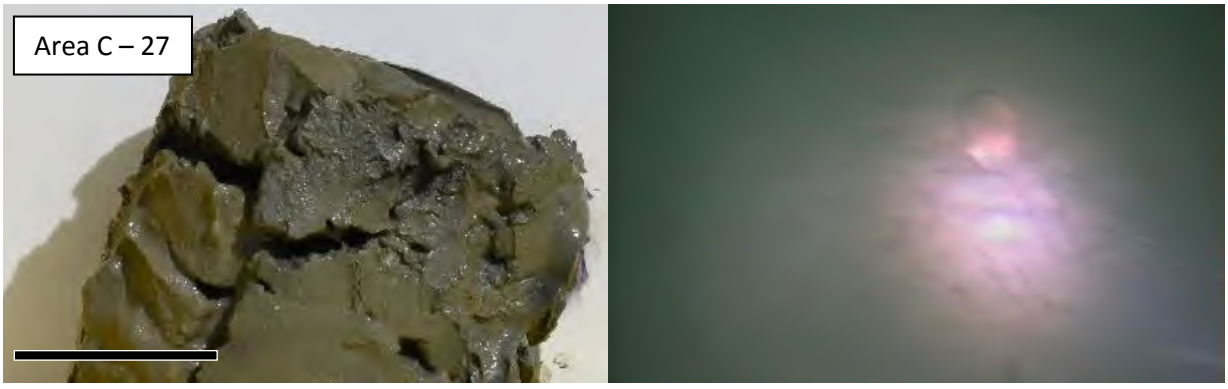

Site C27 physical sample (left), scale = 5 cm; and seafloor image (right).

Figure B-3 (cont): Area C Sediment Sampling Site Images.

Site C28 physical sample (left), scale = 5 cm; and seafloor image (right).

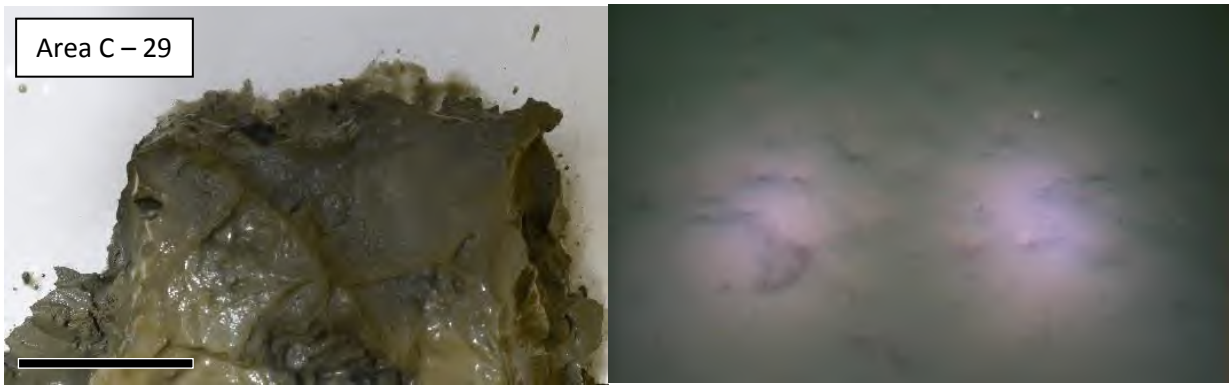

Site C29 physical sample (left), scale = 5 cm; and seafloor image (right).

Site C30 physical sample (left), scale = 5 cm; and seafloor image (right).

Figure B-3 (cont): Area C Sediment Sampling Site Images.

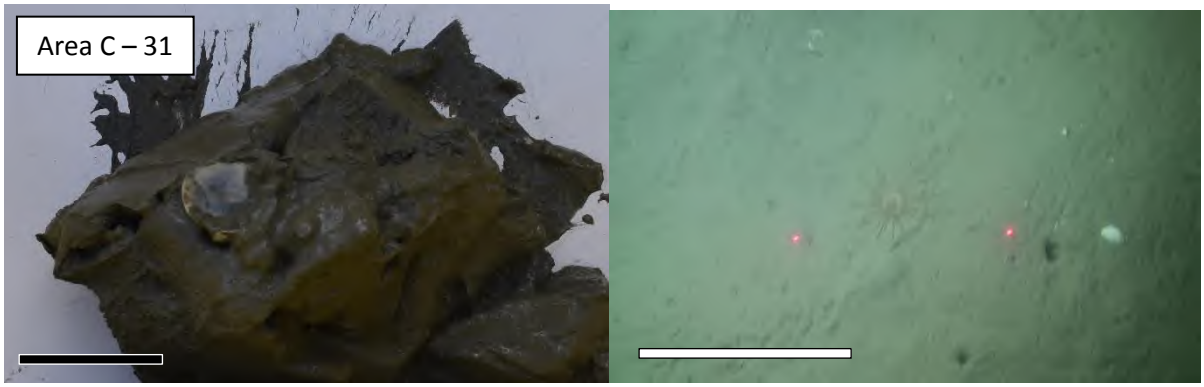

Site C31 physical sample (left), scale = 5 cm; and seafloor image (right), scale = 20 cm.

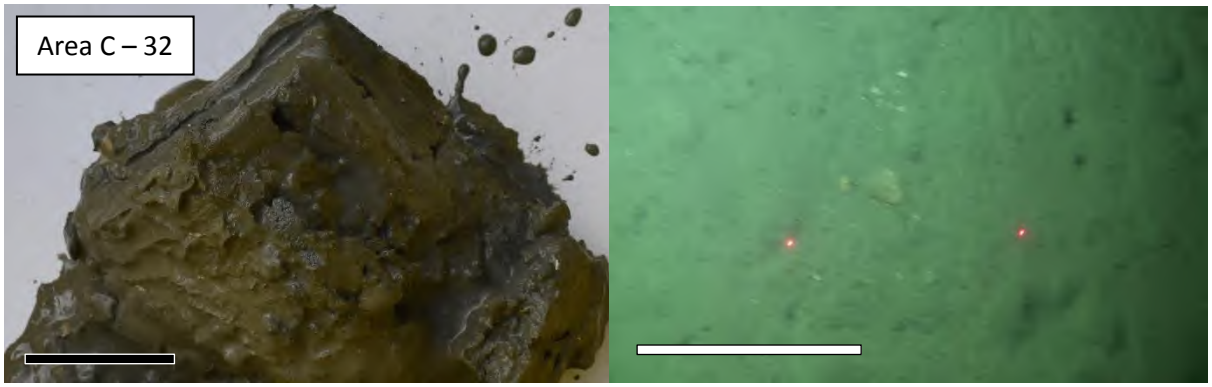

Site C32 physical sample (left), scale = 5 cm; and seafloor image (right), scale = 20 cm.

Site C33 physical sample (left), scale = 5 cm; and seafloor image (right).

Figure B-3 (cont): Area C Sediment Sampling Site Images.

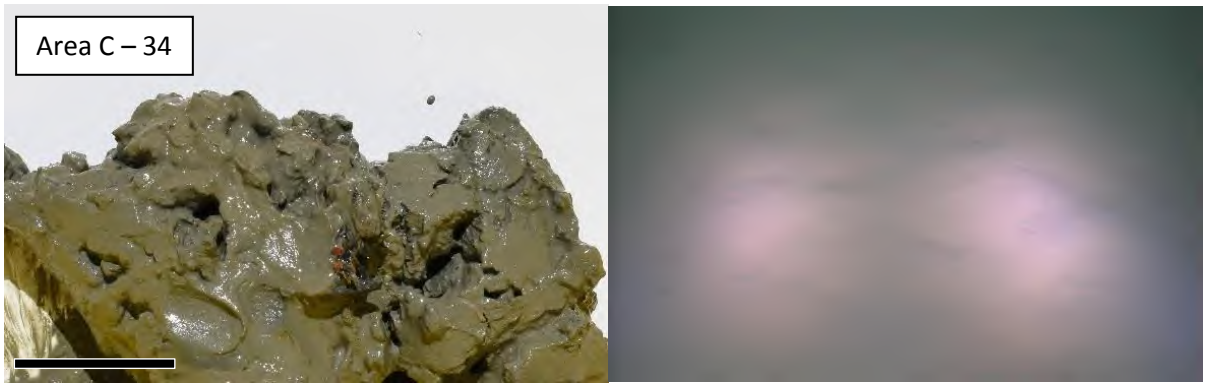

Site C34 physical sample (left), scale = 5 cm; and seafloor image (right).

Site C35 physical sample (left), scale = 5 cm; and seafloor image (right).

Site C36 physical sample (left), scale = 5 cm; and seafloor image (right).

Figure B-3 (cont): Area C Sediment Sampling Site Images.

Site C37 physical sample (left), scale = 5 cm; and seafloor image (right).

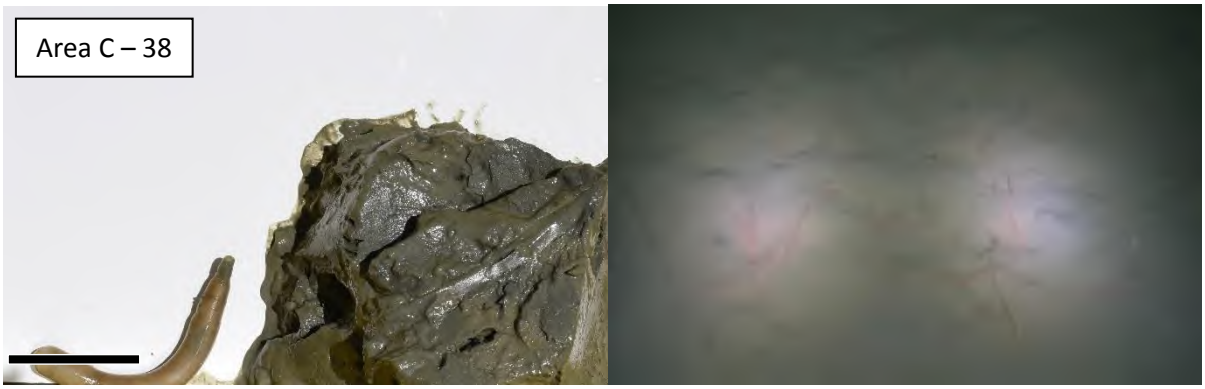

Site C38 physical sample (left), scale = 5 cm; and seafloor image (right).

Site C39 physical sample (left), scale = 5 cm; and seafloor image (right), scale = 20 cm.

Figure B-3 (cont): Area C Sediment Sampling Site Images.

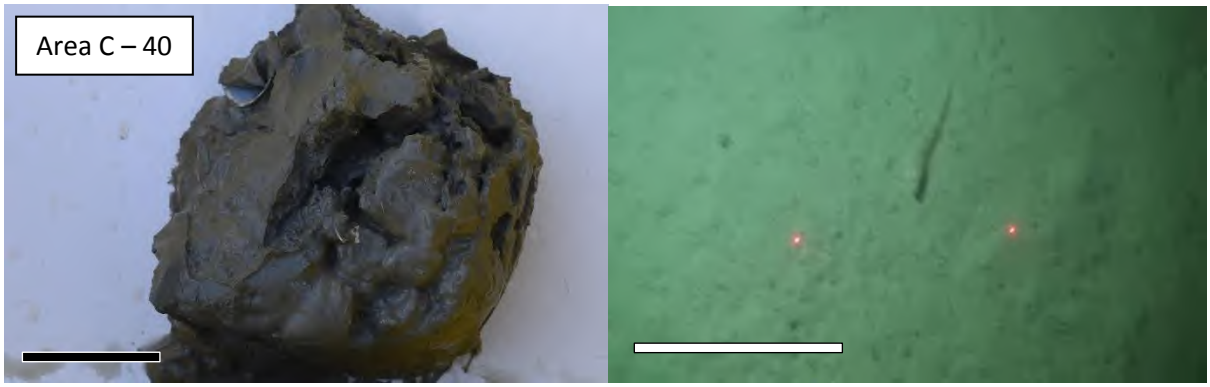

Site C40 physical sample (left), scale = 5 cm; and seafloor image (right), scale = 20 cm.

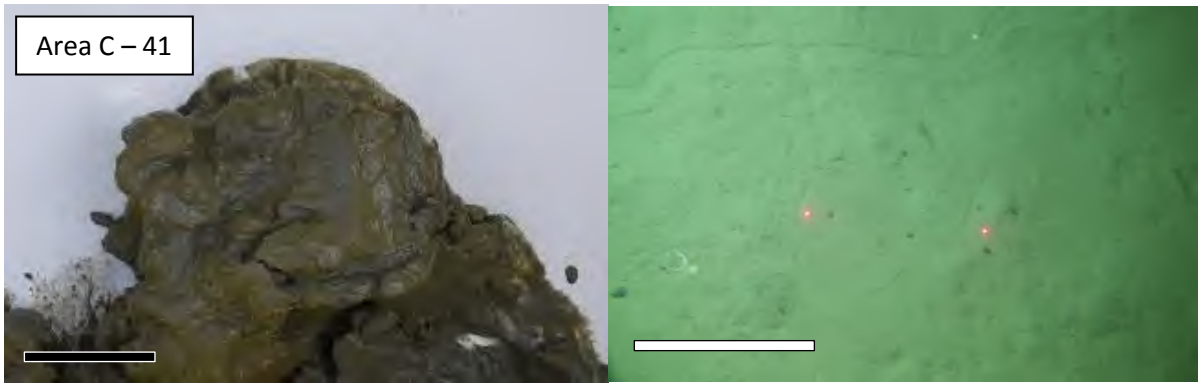

Site C41 physical sample (left), scale = 5 cm; and seafloor image (right), scale = 20 cm.

Site C42 physical sample (left), scale = 5 cm; and seafloor image (right), scale = 20 cm.

Figure B-3 (cont): Area C Sediment Sampling Site Images.

Site C43 physical sample (left), scale = 5 cm; and seafloor image (right).

Site C44 physical sample (left), scale = 5 cm; and seafloor image (right).

Site C45 physical sample (left), scale = 5 cm; and seafloor image (right), scale = 20 cm.

Figure B-3 (cont): Area C Sediment Sampling Site Images.

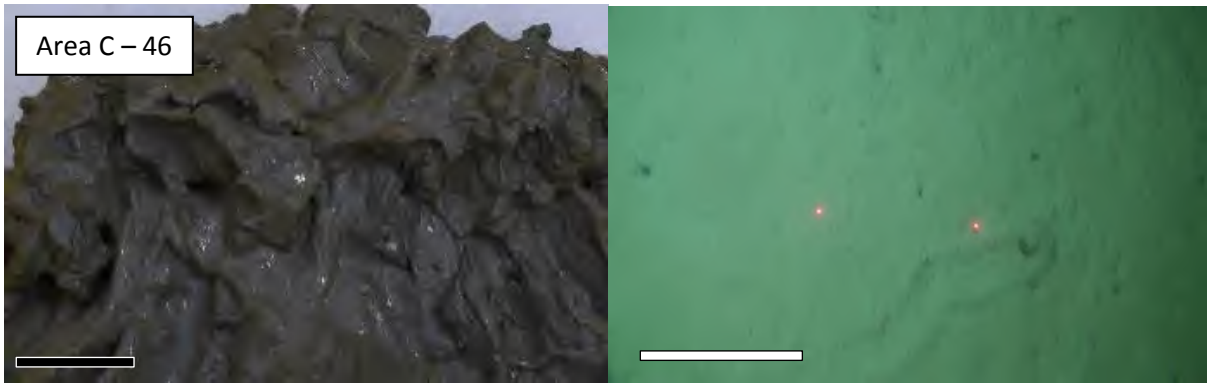

Site C46 physical sample (left), scale = 5 cm; and seafloor image (right), scale = 20 cm.

Site C47 physical sample (left), scale = 5 cm; and seafloor image (right), scale = 20 cm.

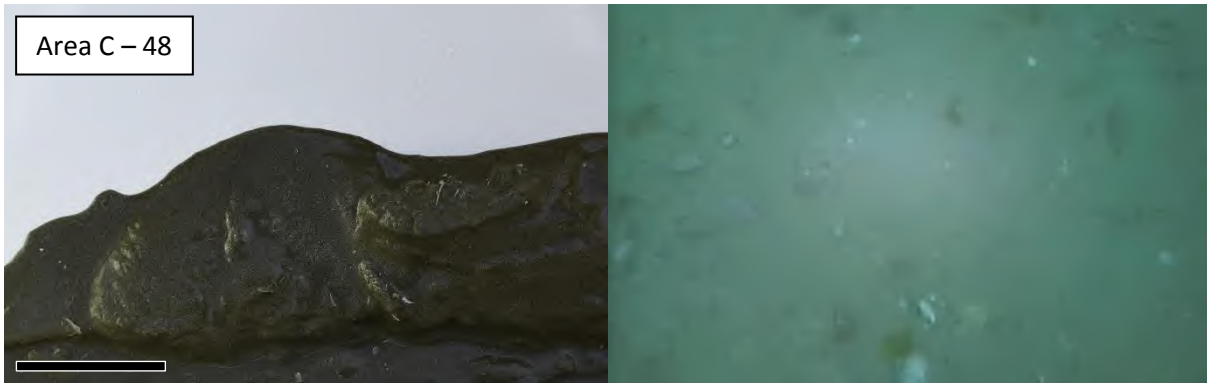

Site C48 physical sample (left), scale = 5 cm; and seafloor image (right).

Figure B-3 (cont): Area C Sediment Sampling Site Images.

Site C49 physical sample (left), scale = 5 cm; and seafloor image (right).

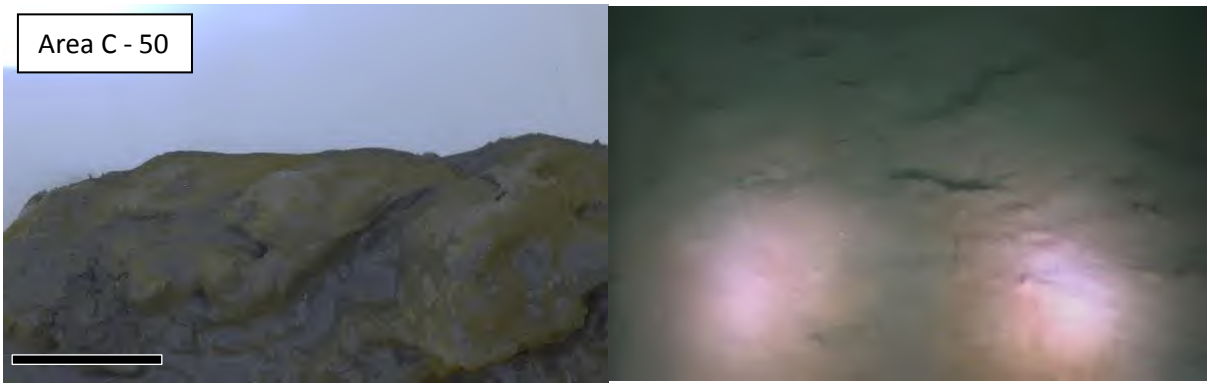

Site C50 physical sample (left), scale = 5 cm; and seafloor image (right).

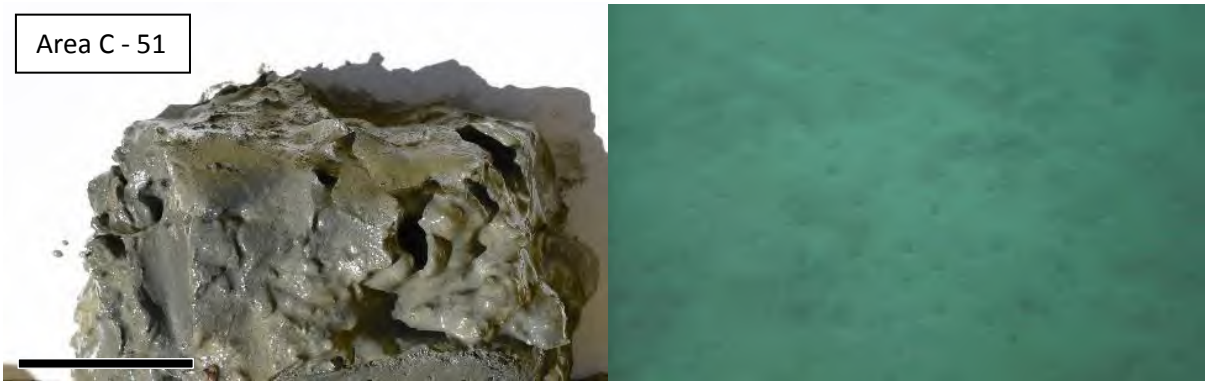

Site C51 physical sample (left), scale = 5 cm; and seafloor image (right).

Figure B-3 (cont): Area C Sediment Sampling Site Images.

Site C52 physical sample (left), scale = 5 cm; and seafloor image (right).

Site C53 physical sample (left), scale = 5 cm; and seafloor image (right).

Site C54 physical sample (left), scale = 5 cm; and seafloor image (right).

Figure B-3 (cont): Area C Sediment Sampling Site Images.

Site C55 physical sample (left), scale = 5 cm; and seafloor image (right).

Site C56 physical sample (left), scale = 5 cm; and seafloor image (right).

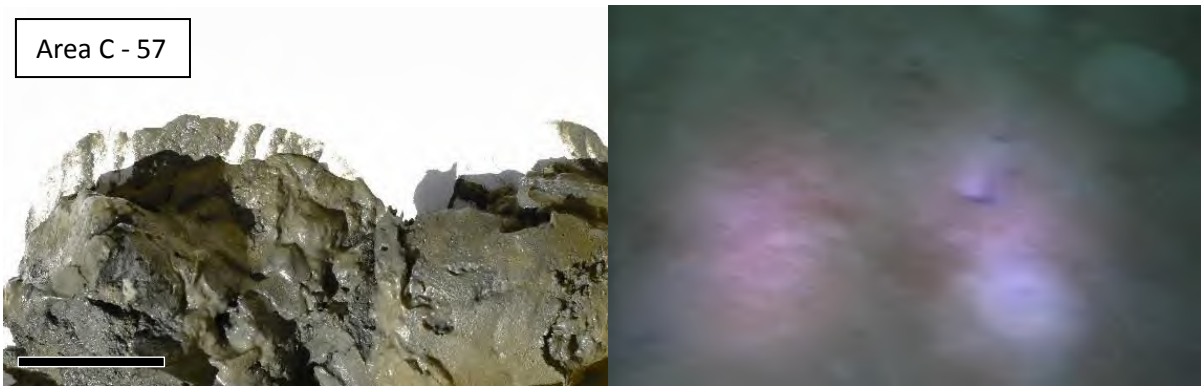

Site C57 physical sample (left), scale = 5 cm; and seafloor image (right).

Figure B-3 (cont): Area C Sediment Sampling Site Images.

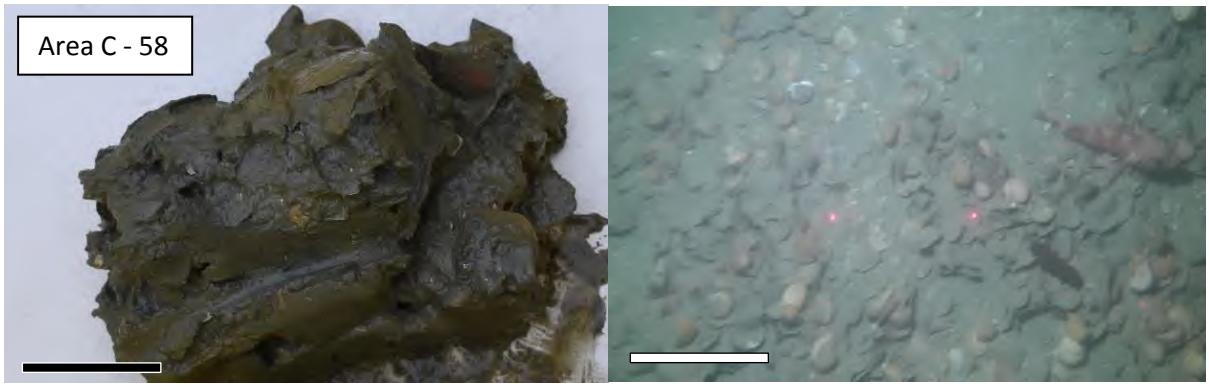

Site C58 physical sample (left), scale = 5 cm; and seafloor image (right), scale = 20 cm.

Site C59 physical sample (left), scale = 5 cm; and seafloor image (right), scale = 20 cm.

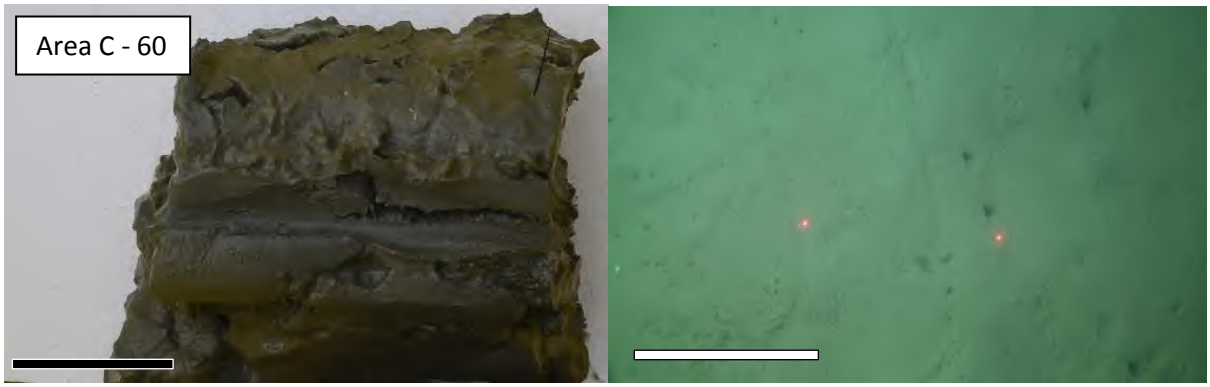

Site C60 physical sample (left), scale = 5 cm; and seafloor image (right), scale = 20 cm.

Figure B-3 (cont): Area C Sediment Sampling Site Images.

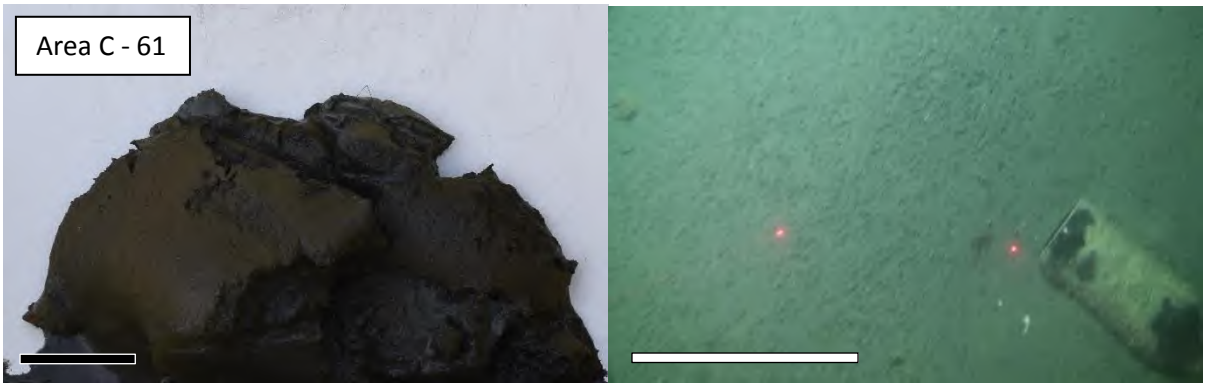

Site C61 physical sample (left), scale = 5 cm; and seafloor image (right), scale = 20 cm.

Site C62 physical sample (left), scale = 5 cm; and seafloor image (right).

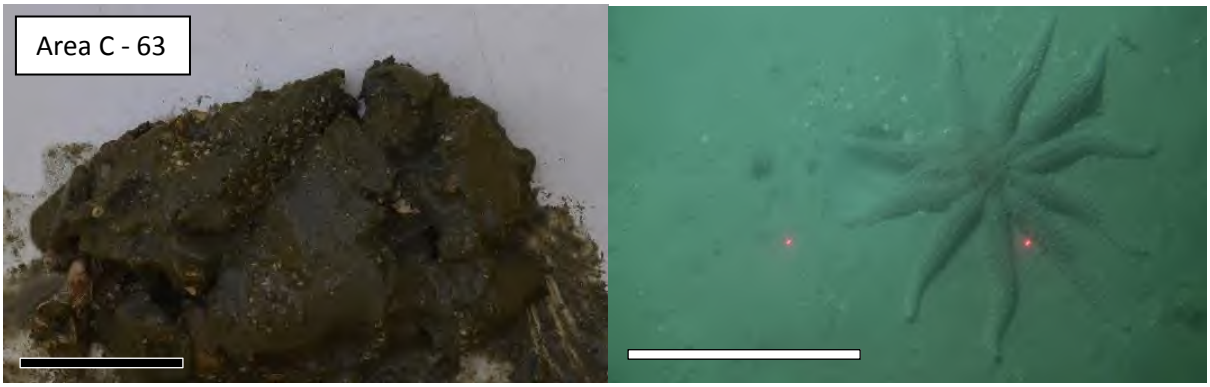

Site C63 physical sample (left), scale = 5 cm; and seafloor image (right), scale = 20 cm.

Figure B-3 (cont): Area C Sediment Sampling Site Images.

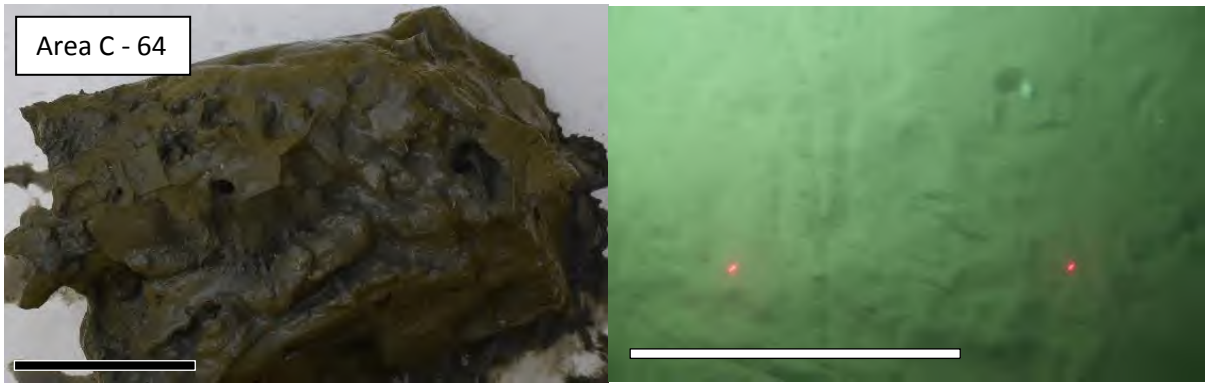

Site C64 physical sample (left), scale = 5 cm; and seafloor image (right), scale = 20 cm.

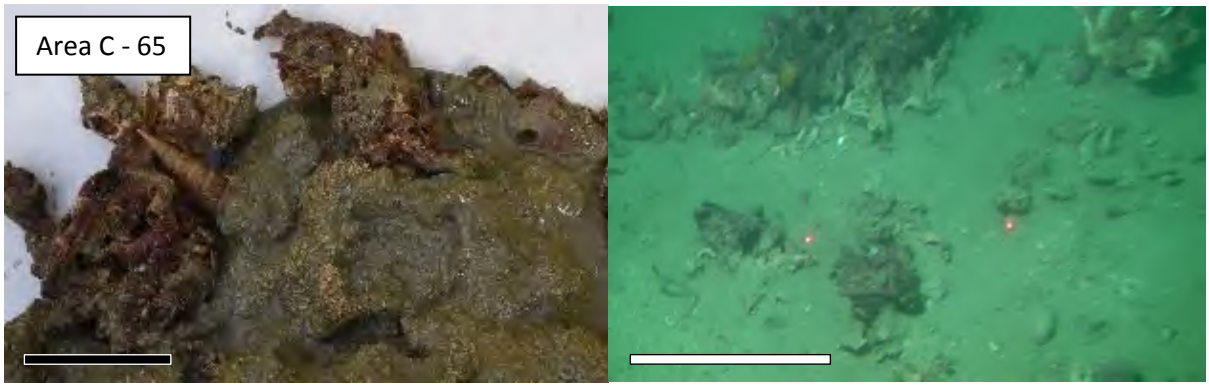

Site C65 physical sample (left), scale = 5 cm; and seafloor image (right), scale = 20 cm.

Site C66 physical sample (left), scale = 5 cm; and seafloor image (right), scale = 20 cm.

Figure B-3 (cont): Area C Sediment Sampling Site Images.

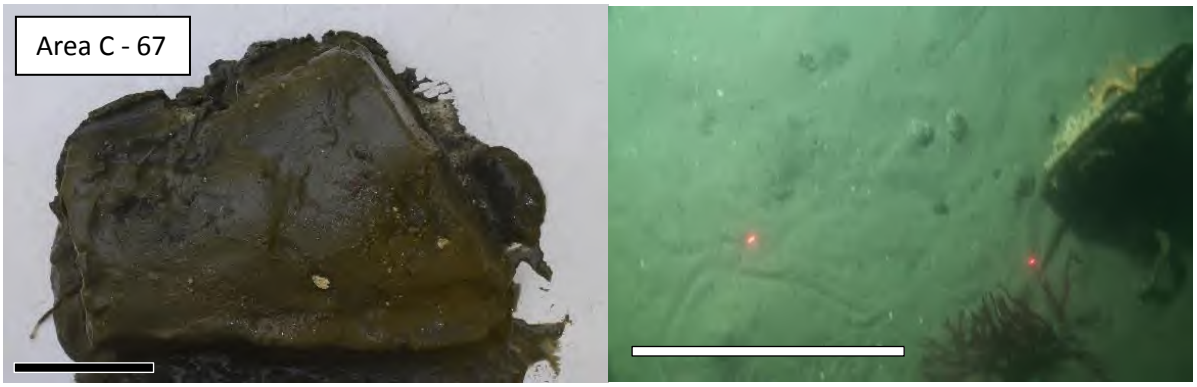

Site C67 physical sample (left), scale = 5 cm; and seafloor image (right), scale = 20 cm.

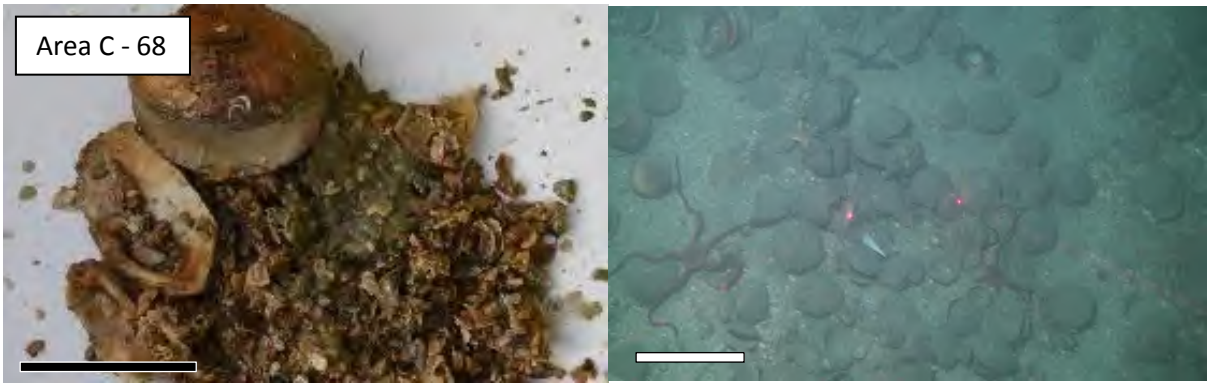

Site C68 physical sample (left), scale = 5 cm; and seafloor image (right), scale = 20 cm.

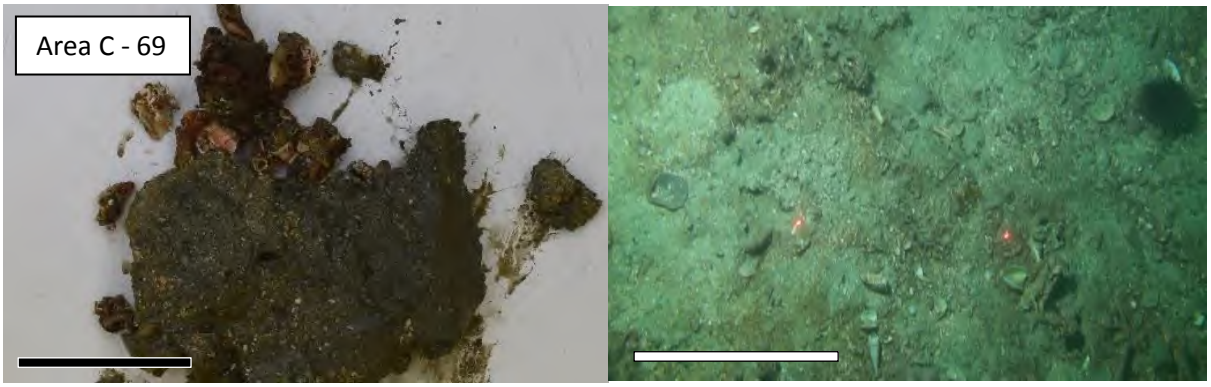

Site C69 physical sample (left), scale = 5 cm; and seafloor image (right), scale = 20 cm.

Figure B-3 (cont): Area C Sediment Sampling Site Images.

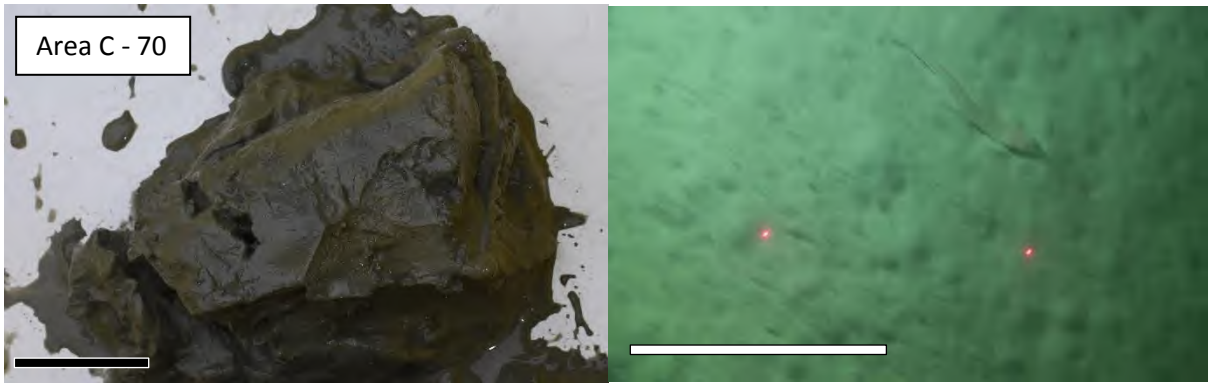

Site C70 physical sample (left), scale = 5 cm; and seafloor image (right), scale = 20 cm.

Site C71 physical sample (left), scale = 5 cm; and seafloor image (right), scale = 20 cm.

Site C72 physical sample (left), scale = 5 cm; and seafloor image (right), scale = 20 cm.

Figure B-3 (cont): Area C Sediment Sampling Site Images.

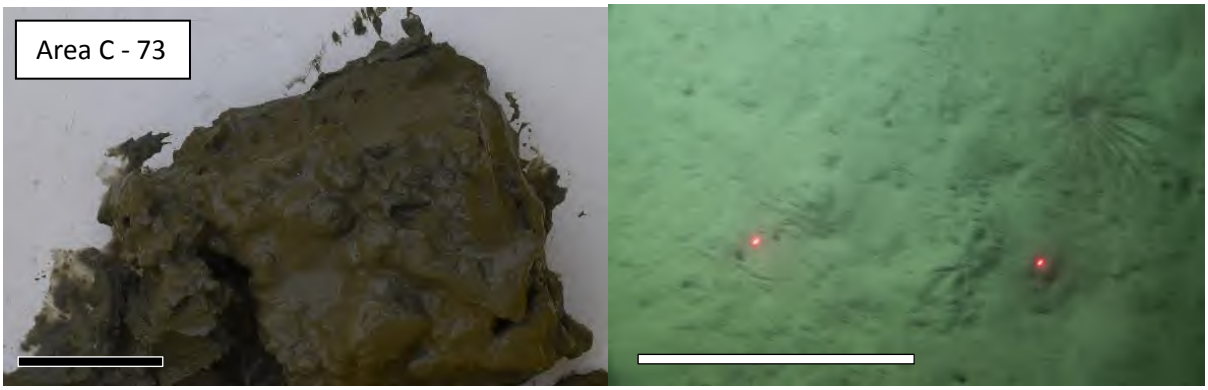

Site C73 physical sample (left), scale = 5 cm; and seafloor image (right), scale = 20 cm.

Figure B-3 (cont): Area C Sediment Sampling Site Images.

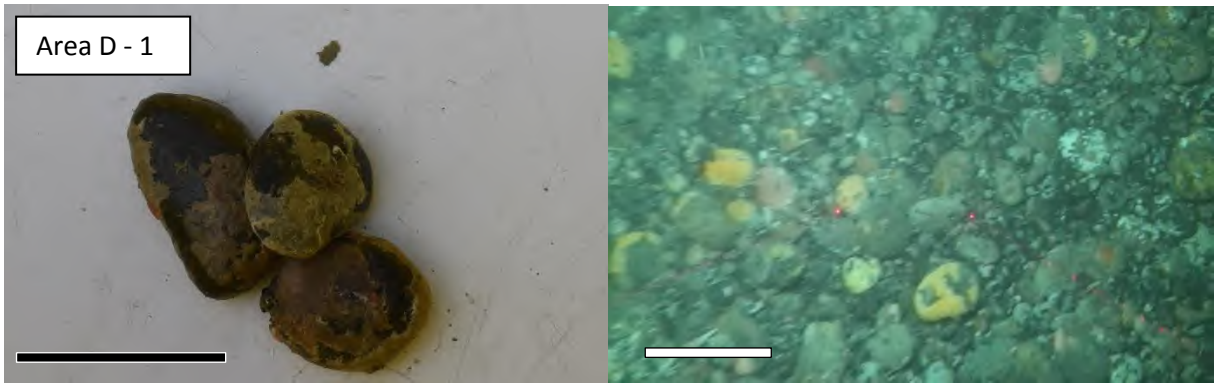

Site D1 physical sample (left), scale = 5 cm; and seafloor image (right), scale = 20 cm.

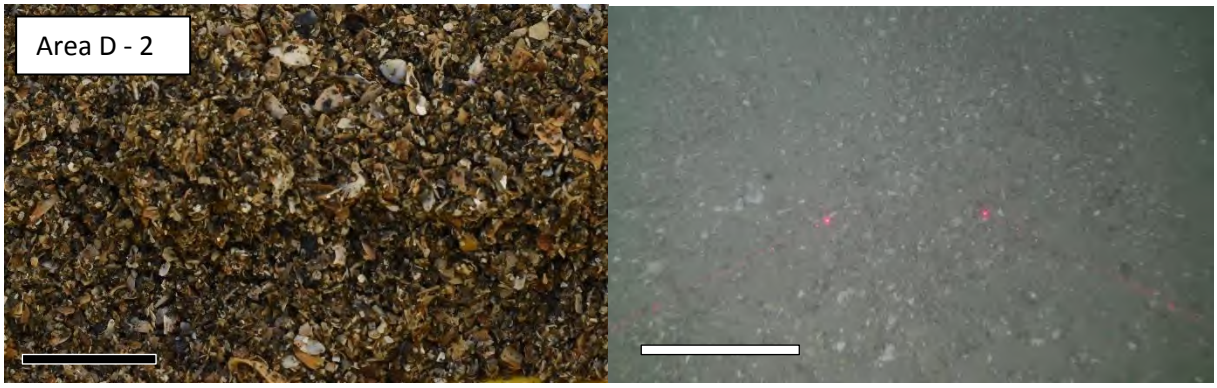

Site D2 physical sample (left), scale = 5 cm; and seafloor image (right), scale = 20 cm.

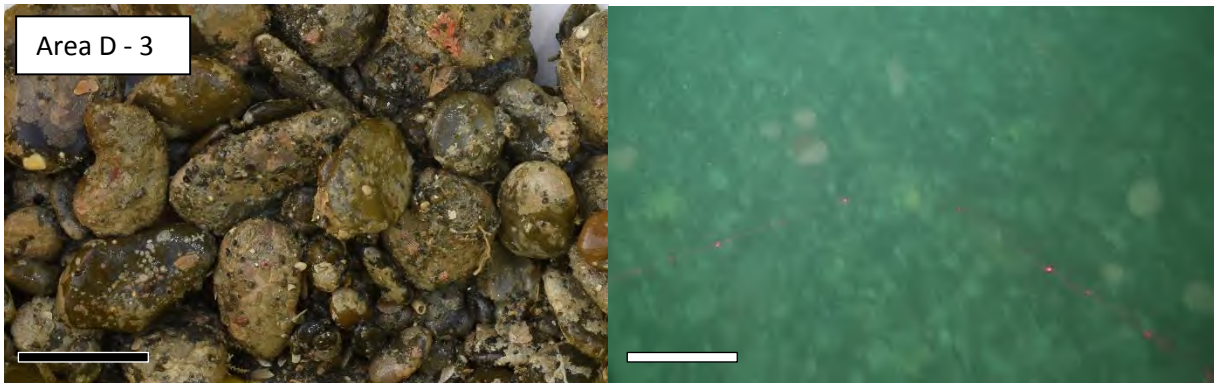

Site D3 physical sample (left), scale = 5 cm; seafloor image (right), scale = 20 cm.

Figure B-4: Area D Sediment Sampling Site Images.

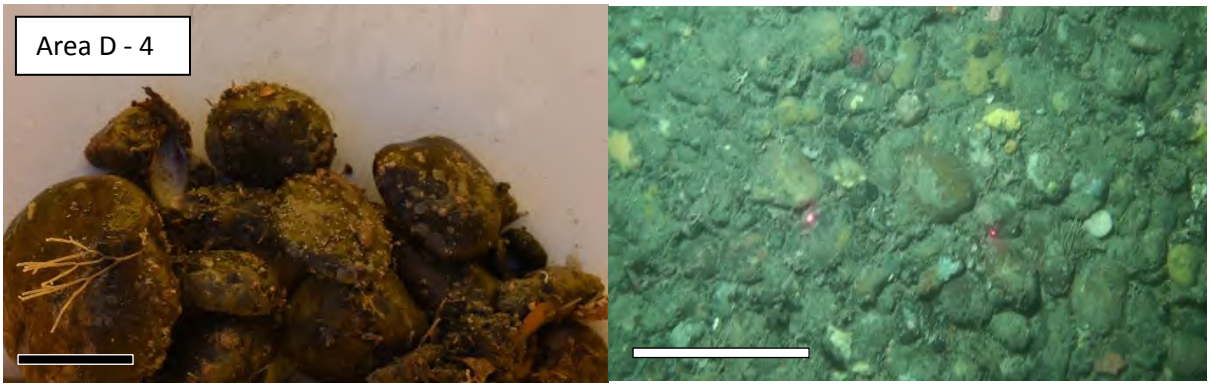

Site D4 physical sample (left), scale = 5 cm; and seafloor image (right), scale = 20 cm.

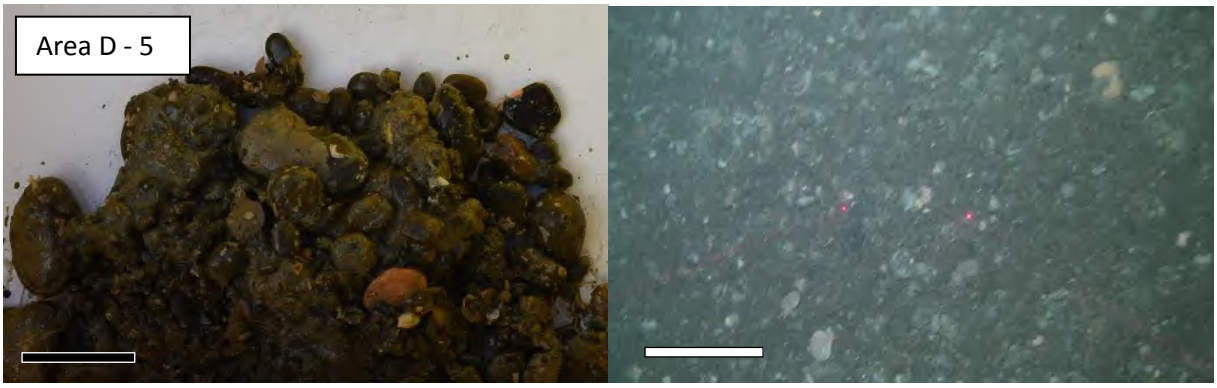

Site D5 physical sample (left), scale = 5 cm; and seafloor image (right), scale = 20 cm.

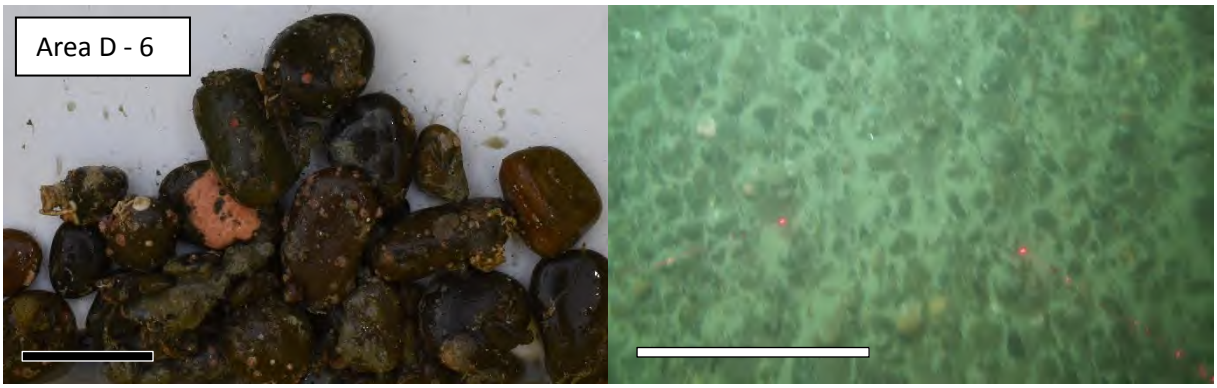

Site D6 physical sample (left), scale = 5 cm; and seafloor image (right), scale = 20 cm.

Figure B-4 (cont): Area D Sediment Sampling Site Images.

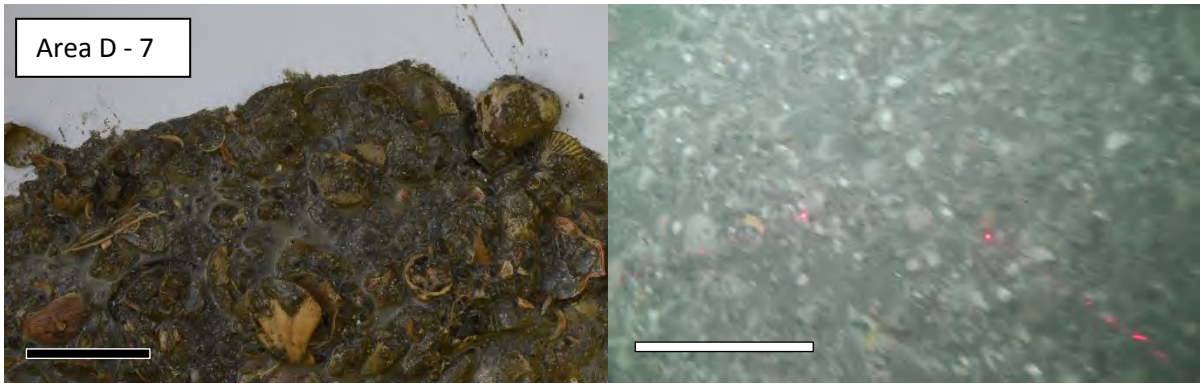

Site D7 physical sample (left), scale = 5 cm; and seafloor image (right), scale = 20 cm.

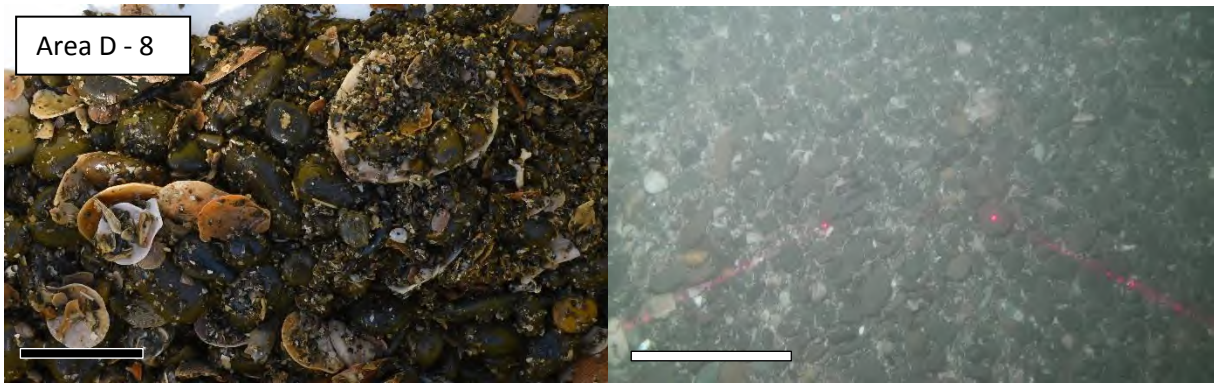

Site D8 physical sample (left), scale = 5 cm; and seafloor image (right), scale = 20 cm.

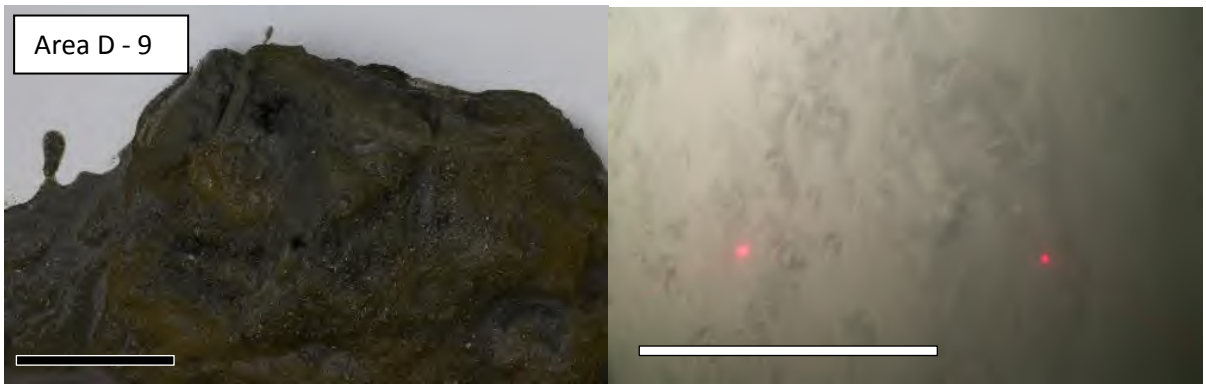

Site D9 physical sample (left), scale = 5 cm; and seafloor image (right), scale = 20 cm.

Figure B-4 (cont): Area D Sediment Sampling Site Images.

Site D10 physical sample (left), scale = 5 cm; and seafloor image (right), scale = 20 cm.

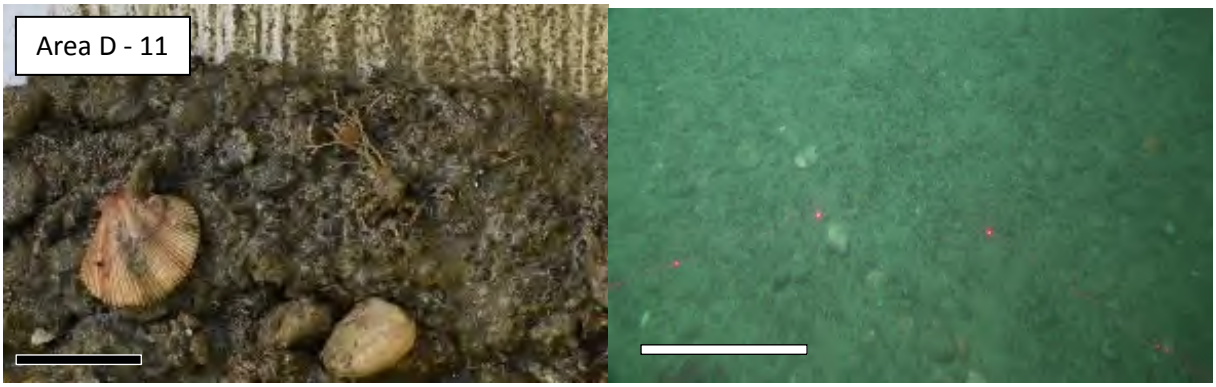

Site D11 physical sample (left), scale = 5 cm; and seafloor image (right), scale = 20 cm.

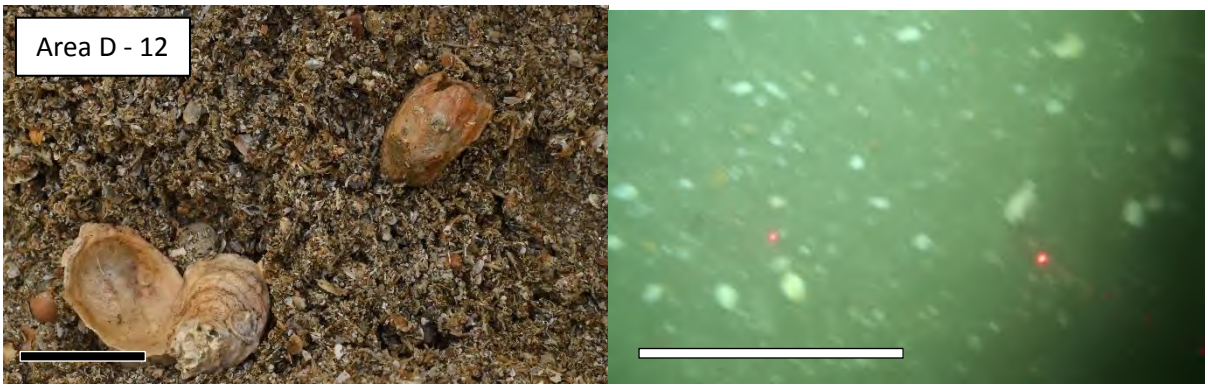

Site D12 physical sample (left), scale = 5 cm; and seafloor image (right), scale = 20 cm.

Figure B-4 (cont): Area D Sediment Sampling Site Images.

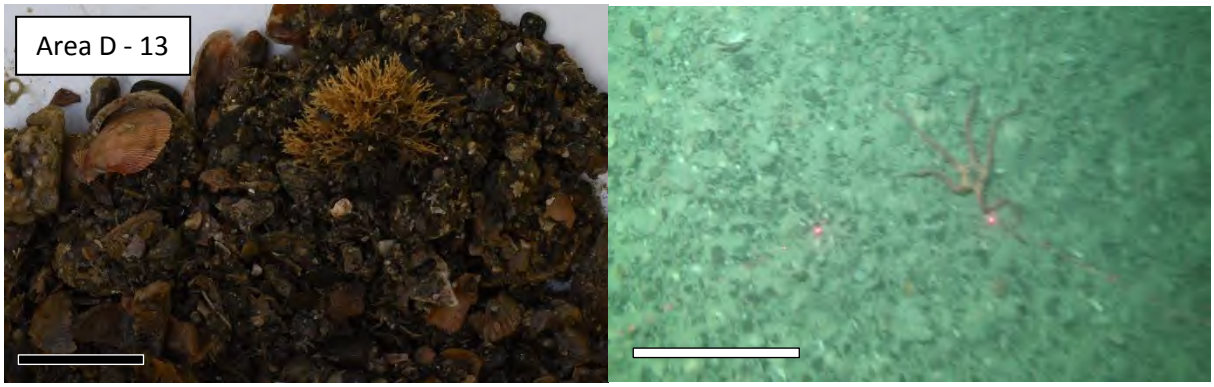

Site D13 physical sample (left), scale = 5 cm; and seafloor image (right), scale = 20 cm.

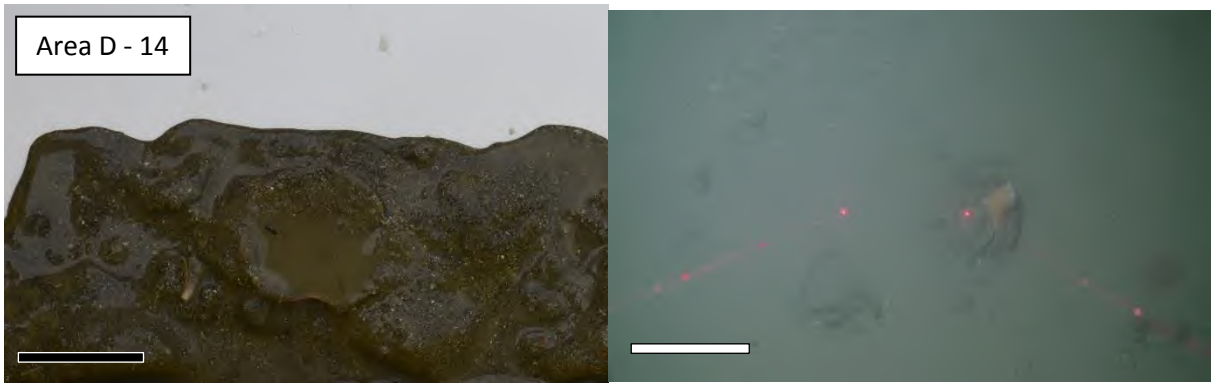

Site D14 physical sample (left), scale = 5 cm; and seafloor image (right), scale = 20 cm.

Site D15 physical sample (left), scale = 5 cm; and seafloor image (right), scale = 20 cm.

Figure B-4 (cont): Area D Sediment Sampling Site Images.

Site D16 physical sample (left), scale = 5 cm; and seafloor image (right), scale = 20 cm.

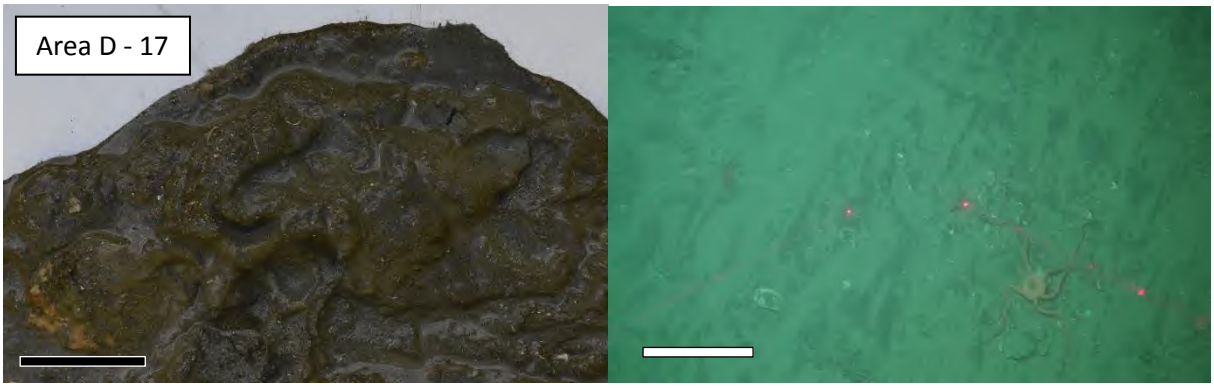

Site D17 physical sample (left), scale = 5 cm; and seafloor image (right), scale = 20 cm.

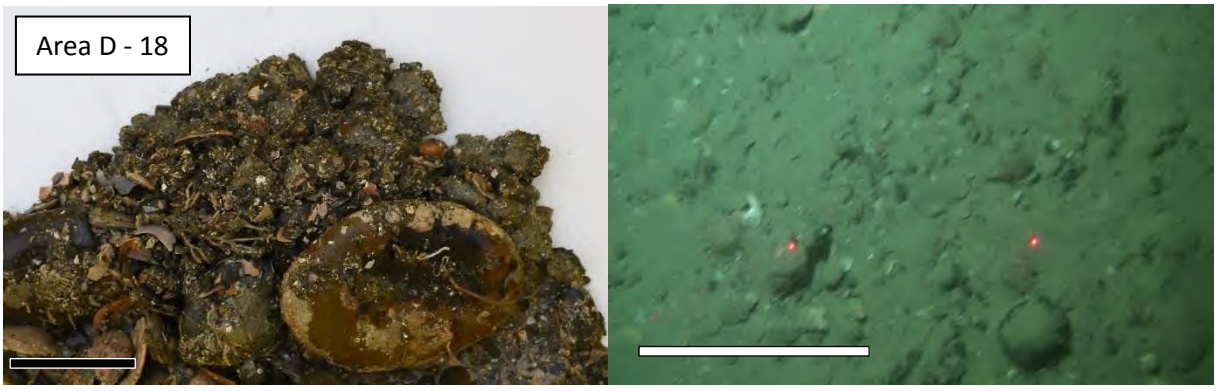

Site D18 physical sample (left), scale = 5 cm; and seafloor image (right), scale = 20 cm.

Figure B-4 (cont): Area D Sediment Sampling Site Images.

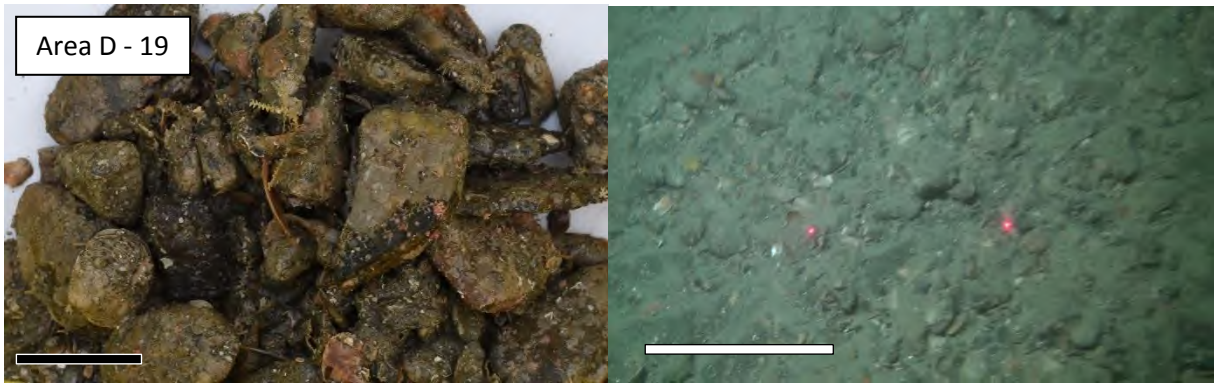

Site D19 physical sample (left), scale = 5 cm; and seafloor image (right), scale = 20 cm.

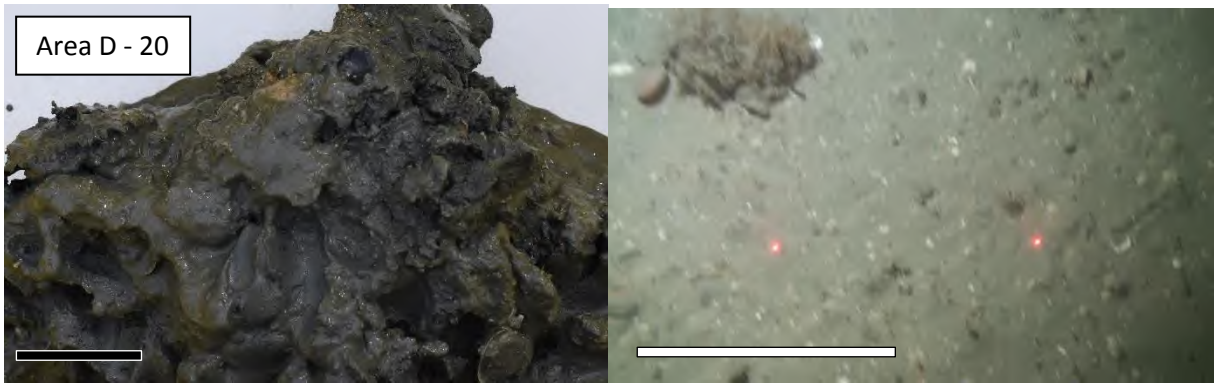

Site D20 physical sample (left), scale = 5 cm; and seafloor image (right), scale = 20 cm.

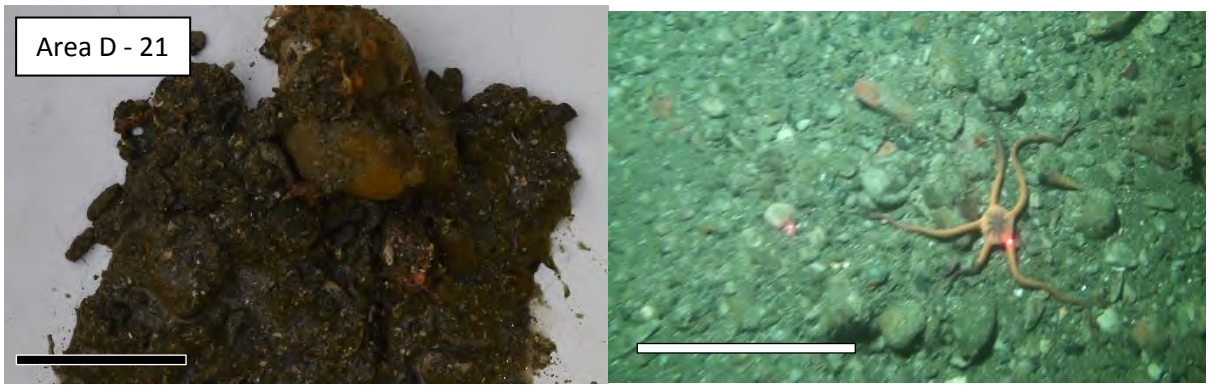

Site D21 physical sample (left), scale = 5 cm; and seafloor image (right), scale = 20 cm.

Figure B-4 (cont): Area D Sediment Sampling Site Images.

Site D22 physical sample (left), scale = 5 cm; and seafloor image (right).

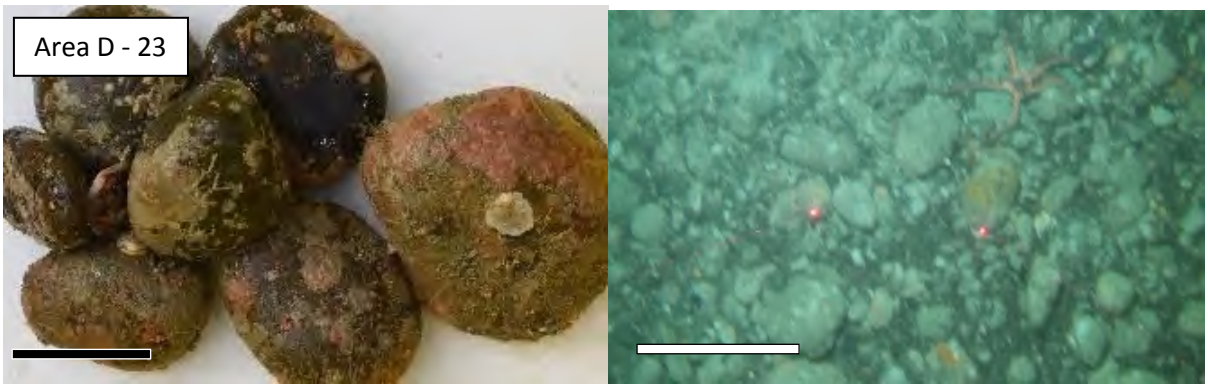

Site D23 physical sample (left), scale = 5 cm; and seafloor image (right), scale = 20 cm.

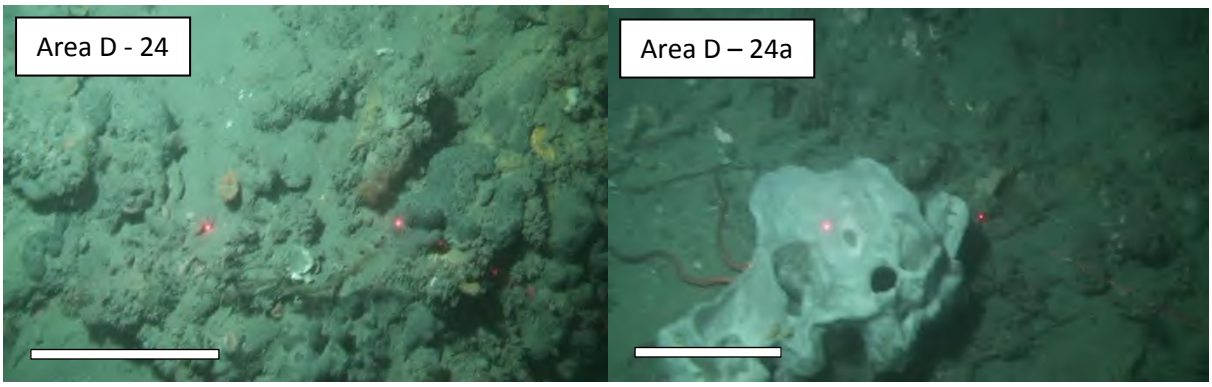

Site D24 seafloor images, scale = 20 cm.

Figure B-4 (cont): Area D Sediment Sampling Site Images.

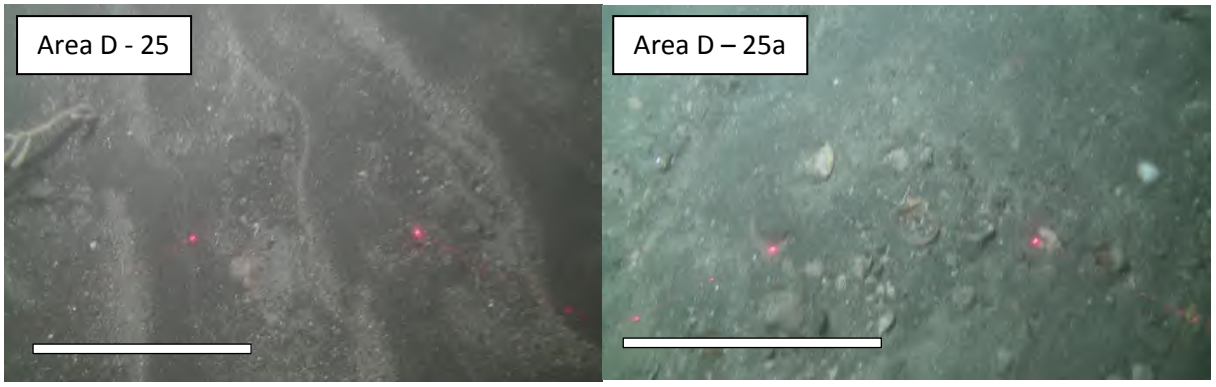

Site D25 seafloor images, scale = 20 cm, compare with D16 and D17.

Site D26 physical sample (left), scale = 5 cm; and seafloor image (right), scale = 20 cm.

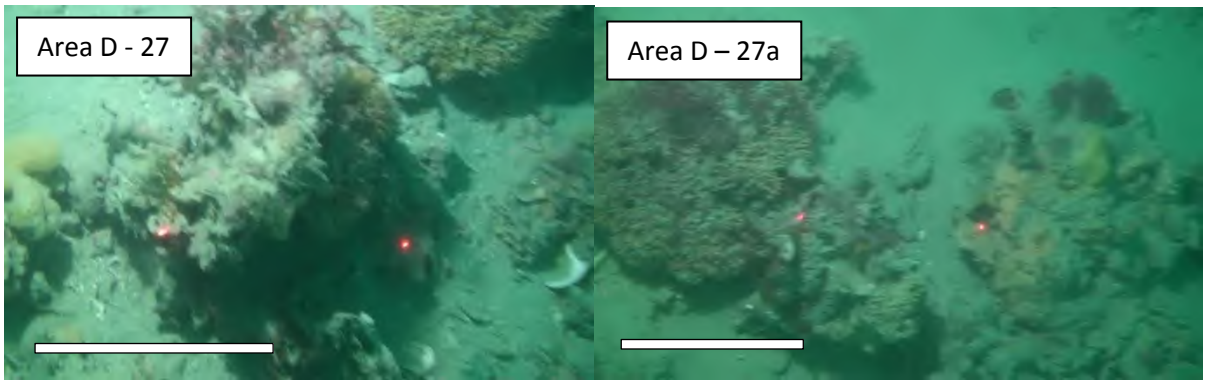

D27 seafloor images, scale = 20 cm.

Figure B-4 (cont): Area D Sediment Sampling Site Images.

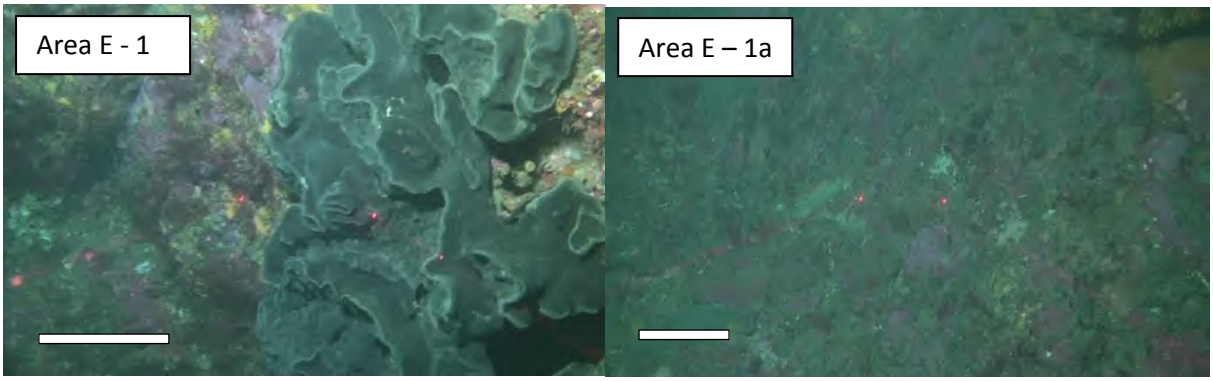

E1 seafloor images, scale = 20 cm.

Figure B-5: Area E Sediment Sampling Site Images.

Appendix C Satellite Derived Bathymetry – EOMAP Methodology

Satellite-Derived Bathymetry and seafloor algorithms and workflows

EOMAP applies physics-based SDB methods which, in contrast to empirical methods, do not require local training data for each location; they are based on physical assumptions and spectral databases. EOMAP uses proprietary software modules known as the Modular Inversion and Processing System (MIP). Briefly described, MIP processes optical satellite and airborne imagery by applying a series of relevant physical and analytical processing steps. These steps are so-called 'actions' which are ordered successively ('job') and controlled by a workflow system (EWS) which tracks and logs the input together with intermediate and final outputs.

Since 1998, a team of physicists, mathematicians and IT experts have systematically developed MIP processors for shallow-water and bathymetry applications[1] within various research programs[2]. This has continued to evolve since 2006 as proprietary EOMAP technology[3]. Within the MIP, radiative transfer modeling of the coupled atmosphere-water systems is based on the Finite Element-Method (FEM) reference model of EOMAP staff Dr. Kiselev. This reference model has 30 years of development history[4, 5], featuring the state-of-the-art algorithms as below. To support efficient production workflows and automated processing, MIP modules and EOMAP pre-/post processors are orchestrated within the Earth observation Workflow System EWS. To derive bathymetry and seafloor properties with the MIP, a number of algorithms and modules are applied, invoked by the EWS. Water depth, water constituents' optical properties, as well as sub-surface and seafloor reflectance are derived in an iterative process, which includes the processes shown in the following figure and described in the following sections.

1 a) Heege, T., Häse, C., Bogner, A., Pinnel, N. (2003): Airborne Multi-spectral Sensing in Shallow and Deep Waters. Backscatter p. 17-19, 1/2003
b) Heege, T., Bogner, A., Pinnel, N. (2004): Mapping of submerged aquatic vegetation with a physically based process chain. Remote Sensing of the Ocean and Sea Ice 2003. Editors: Charles R. Bostater, Jr. &RosaliaSantoleri. Proc. of SPIE Vol. 5233, ISBN: 0-8194-5116-9 pp. 43-50.

2 1998 - 2007, Collaborative research project SFB 454 "Lake Constance Littoral" - research project D3 "Remote sensing of shallow water areas", funded by the DFG (German Research Foundation). Interdisciplinary joint project Univ. Konstanz and DLR. DLR project lead: Dr. T. Heege
2002 - 2005: Development of automated remote sensing tools, supporting management of littoral zones in lakes, part B, BWC21011, supported by BWPLUS. Interdisciplinary joint project DLR and Univ. Hohenheim. DLR lead: Dr. T. Heege
2003 - 2005: High-Tech Offensive Zukunft Bayern project No. 290, Pilotproject Waging-Tachinger See, Limnological Station of the Technical University Munich

3 2008 - 2010: AUKLASS, Development of operational image classification processors for seafloor mapping applications. AUKLASS IBS-3667a/321/7/-TOU-08080003, supported by the Bavarian Ministry of Economy and Infrastructure
2010 - 2013: EU FP7 FRESHMON Downstream project.
2012 - 2015: Apps4GMES: Development of automated bathymetry processor, supported by the Bavarian Ministry of Economy and Infrastructure.
2015 - 2017: EU H2020 Base-plattform: Development of integrated bathymetry services

4 Kisselev, V.; Bulgarelli, B. (2004). Reflection of light from a rough water surface in numerical methods for solving the radiative transfer equation. Journal of Quantitative Spectroscopy and Radiative Transfer 85, 419-435.
B. Bulgarelli, V. Kisselev, L. Roberti (1999): Radiative Transfer in the Atmosphere Ocean System: The Finite-Element Method. Appl. Opt. 38, pp. 1530-1542

5 Kisselev, V.B.; Roberti, L.; Perona, G. (1995), Finite-element algorithm for radiative transfer in vertically inhomogeneous media: numerical scheme and applications. Appl. Opt. , 34, 8460-8471.

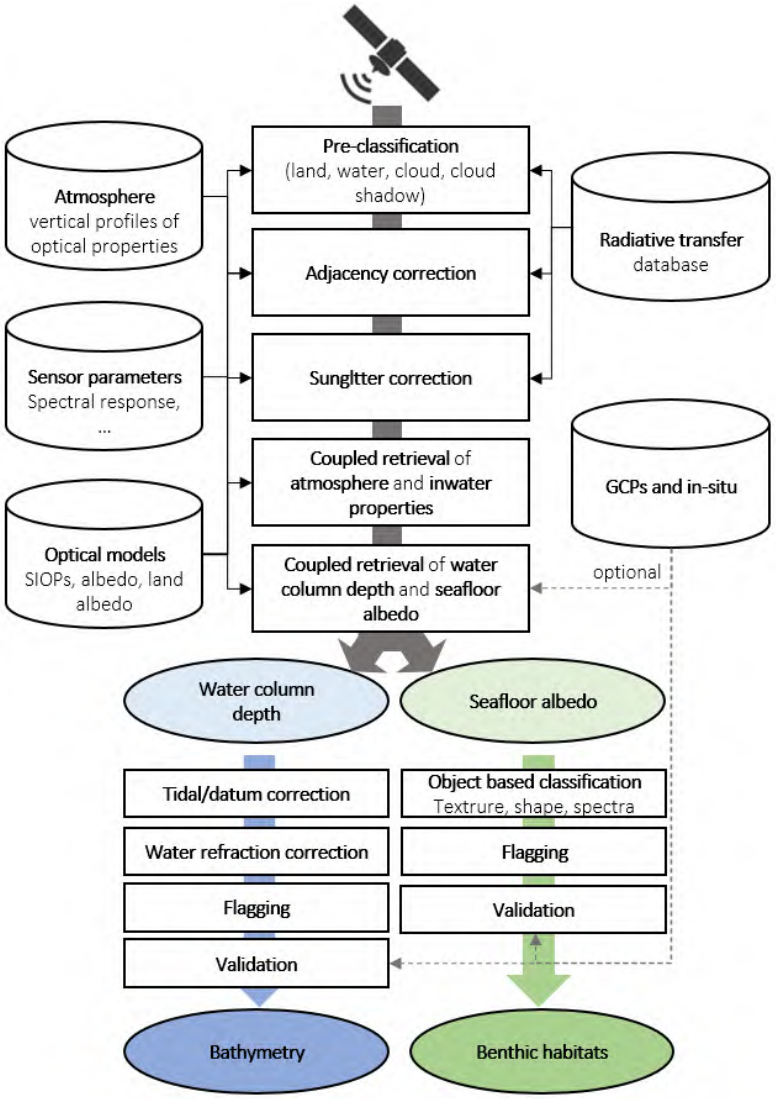

Figure C-1: Schema of EOMAP's workflow for creating (Satellite Derived) bathymetry and benthic information using optical satellite image data. A set of modules area applied to satellite image radiance data which include several steps to minimize negative environmental impacts on the measured spectra. These modules are known as MIP (Modular Inversion Program) which is embedded into the EWS (Earth observation Workflow System) which organizes the modules and the processing.

Satellite data calibration and quality control

All satellite data are calibrated with respect to the standards given by the satellite data provider. On top of this, EOMAP refines the calibration with updated internal recalibration coefficients to account for small calibration changes in time and the higher radiometric requirements for aquatic applications. The resulting calibrated radiances are verified using the EOMAP radiative transfer model incorporated in the MIP. Data noise is reduced using a specific adaptive filter[6] and stripes are filtered to the best extent possible.

6 DE patent DE10050331A1. Increasing signal-to-noise ratio for processing of multichannel digital image data sets using sliding noise filter by matching fine-scale variances.

All optical sensors have so-called stripping effects, which are expressed as small differences in radiance values in the direction of the image recording. These strips are typically not of significance because they have no or very little impact on the final SDB data.

Pre-classification

An automated procedure generates a first pass flagged product, discriminating pixels over water, land and clouds. This pre-classification is used for the following processes but not used for the final flagging of the data, which is done by analyst interpretation (see following sections).

Geo-referencing

Originally the Digital Globe imagery showed an irregular shift of up to 50m against the aerial imagery. The reason for this may be that DigitalGlobe did not use a DTM in order to correctly rectify the satellite imagery, using only the average terrain height within the scene. EOMAP used the orthorectified aerial imagery provided by NIWA to correctly rectify the DigitalGlobe imagery. Several Ground Control Points were selected (based on the Aerial Imagery) in ArcMap and a 2nd degree polynomial transformation was applied.

Adjacency correction

The sensor radiances are corrected for the so-called adjacency effect. This is the increased radiance over water due to contamination of the signal from photons reflected by adjacent land, and their further scattering in the atmosphere. It can be a significant source of error for the water depth retrieval, particularly for coastal areas. This effect strongly depends on the geometry between sun, surface and sensor, as well as land albedo and atmospheric properties. EOMAP's adjacency processor calculates the land albedo from the satellite scene itself, accounting for all the bi-directional effects, atmospheric properties, land albedo and the land cover shape for each pixel. In other words, land-water boundaries outside the satellite image are also accounted for by use of the EOMAP global land-water data base. The result is a radiance image with significantly improved signal data quality for near coastal regions. For further details, please see Kiselev et al.[7].

Correction for sun glint

Scenes that are considerably impacted by sun glitter on the water surface are corrected following the approach of Heege & Fischer 2000[8] for high resolution sensors such as WorldView-2/3/4. Low to intermediate sun glitter noise is corrected with an alternative correction module that is a standard part of the atmospheric correction program (see next paragraph).

Coupled retrieval of atmospheric and in-water optical properties

The coupled retrieval of atmospheric optical thickness and in-water properties is performed by minimizing the mean square deviation of modelled top-of-atmosphere radiances and those measured for all sensor channels[9, 10, 11], while accounting for all bi-directional processes at the air-water-interface

7 Kiselev, V., Bulgarelli, B. and Heege, T., (2015). Sensor independent adjacency correction algorithm for coastal and inland water systems. Remote Sensing of Environment, 157: 85-95. , ISSN 0034-4257, http://dx.doi.org/10.1016/j.rse.2014.07.025

8 Heege, T. & Fischer, J. (2000): Sun glitter correction in remote sensing imaging spectrometry. SPIE Ocean Optics XV Conference, Monaco, Oct 16-20.

9 Sabine Ohlendorf, Andreas Müller, Thomas Heege, Sergio Cerdeira-Estrada and Halina T. Kobryn (2011): "Bathymetry mapping and sea floor classification using multispectral satellite data and standardized physics-based data processing", Proc. SPIE 8175, 817503; doi:10.1117/12.898652

10 Heege, T., Kiselev, V., Wettle, M., Hung N.N. (2014): Operational multi-sensor monitoring of turbidity for the entire Mekong Delta. Int. J. Remote Sensing, Special Issues Remote Sensing of the Mekong, Vol. 35 (8), pp. 2910-2926

11 Richter, R., Heege, T., Kiselev, V., Schläpfer, D. (2014): Correction of ozone influence on TOA radiance. Int. J. of Remote Sensing. Vol. 35(23), pp. 8044-8056, doi: 10.1080/01431161.2014.978041

as well as atmospheric properties. In contrast to other approaches, the output of this process is directly the sub-surface reflectance. In the 3rd generation of the MIP-SDB processors, these calculations are incorporated within the SDB retrieval itself. This step makes use of EOMAP's specific databases for different parameters of the atmosphere, water column absorbers and backscatterers as well as seafloor properties. For each of the satellite image data a specific database of these parameters is created out of spectrally very high-resolution databases (1nm resolution), taking into account the spectral response function and sensor characteristics for each of the used sensors.

Correction for the water column impact and the seafloor albedo

The subsurface reflectance retrieved by the coupled atmospheric and water constituent retrieval [12, 13] retains the spectral properties of the seafloor, depth and the absorption and backscatter occurring within the water column. Having solved for the latter two (see section above), the seafloor properties and water column thickness are iteratively solved in order to account for the effects of different seafloor properties on the water depth calculation. This is done using the WATCOR module 16, 19. In the 1st and 2nd generation of WATCOR, the transformation of sub-surface reflectance to the sea floor albedo is based on equations similar to Albert and Mobley (2003)[14]. The unknown input value of depth is calculated iteratively in combination with the spectral un-mixing of the corresponding bottom reflectance [15,16,17]. The final depth is retrieved for the minimum value of the residual error. EOMAP recently introduced the latest 3rd generation of the water depth retrieval module, which includes a fully-coupled atmospheric -water - seafloor retrieval, based on the physics-based implementation of the reference radiative transfer system Finite Element Method (FEM). This avoids any semi-analytical approximations such as used in earlier versions in order to describe the relation between water-leaving radiance, water and seafloor properties. The main advantage of the newest generation version is to provide significantly improved accuracies of independently retrieved water depth, seafloor properties, together with a full error budget through the whole retrieval process.

Flagging/Masking data

The derived bathymetry information is vetted for areas with bias or where depth is able to be calculated. For this process, EOMAP analyses the uncertainty outputs and also applies a visual quality check by comparing derived bathymetric information with the actual satellite image data. The Qimera/Fledermaus software is used to best identify and delete outliers and biased data in the 3D viewer. Flagging data in this manner requires a high level of expertise, and EOMAP will allocate experienced staff to this task with 5+ years' experience in SDB data processing and analysis. All staff have a university master degree or higher. No data gap of the bathymetric data was interpolated.

12 Heege, T., Kiselev, V., Wettle, M., Hung N.N. (2014): Operational multi-sensor monitoring of turbidity for the entire Mekong Delta. Int. J. Remote Sensing, Special Issues Remote Sensing of the Mekong, Vol. 35 (8), pp. 2910-2926

13 Heege, T., Fischer, J. (2004): Mapping of water constituents in Lake Constance using multispectral airborne scanner data and a physically based processing scheme. Can. J. Remote Sensing, Vol. 30, No. 1, pp. 77-86

14 Albert, A., &Mobley, C. D. 2003. An analytical model for subsurface irradiance and remote sensing reflectance in deep and shallow case-2 waters. Optics Express, 11(22), 2873 -2890.

15 Siermann, J., Harvey, C., Morgan, G., Heege, T. (2014): Satellite derived Bathymetry and Digital Elevation Models (DEM). IPTC International Petroleum Technology Conference 2014, DOI http://dx.doi.org/10.2523/17346-MS, https://www.onepetro.org/conference-paper/IPTC-17346-MS

16 Pinnel, N. 2007. A method for mapping submerged macrophytes in lakes using hyperspectral remote sensing. PhD Dissertation Technische Universität München

17 Cerdeira-Estrada S., Heege, T., Kolb M., Ohlendorf S., Uribe A., Müller A., Garza R., Ressl R., Aguirre R., Marino I., Silva R., Martell, R. (2012): Benthic habitat and bathymetry mapping of shallow waters in Puerto Morelos reefs using remote sensing with a physics based data processing, Proc. IGARSS, p. 1-4

Correction for tidal effects of retrieved water depth

A single vertical tide correction was applied based on tidal information accessed by the nearest tidal station of UK Admiralty. All values rely on Chart Datum (CD).

Date	2014-10-08	2013-12-24	2012-10-30	2010-09-30	2013-01-05	2007-11-24
Station	Okuri Bay	Te Iro Bay, Okuri Bay	Te Iro Bay	Long Island	Long Island	Te Iro Bay
Applied value	0.5m	0.9m	1.3 m	0.7 m	0.5 m	1.4 m

Metadata creation

All of the delivered geodata and bathymetric data come with ISO 19115 conform metadata which represents the standard format for metadata. This includes all relevant information, such as point of contact, tide corrections, processing steps, etc. Metadata are validated through online validation tools by the European Commission and provided as XML files.

Quality control assessment

The quality control and assessment of the SDB data ideally includes two items: an internal QA/QC procedure and a second procedure which includes the validation of the bathymetric results against high quality acoustic data. The internal checks are based on the following mechanisms:

Model settings. The settings of the SDB model were checked and compared against environments with similar water conditions in areas where validation of SDB data was applied.

Analyst expertise. The analyst's experience is also of importance in controlling the SDB model as post-processing the created SDB grids. One of EOMAP's senior experts[18]was in charge of the processing work and regularly discussed the intermediate and final results with the EOMAP SDB team. These multiple checks result in the minimization of uncertainties.

Consistency check Consistency checks, which include double checks of the output data, were done prior to the delivery.

18 Andreas Müller, with 7 years of SDB processing experience

Appendix D Locality Maps

Figure D-1: Locality Map. The major localities are presented here for Queen Charlotte Sound / Tōtaranui and Tory Channel / Kura Te Au Hydrographic Survey (HS51).

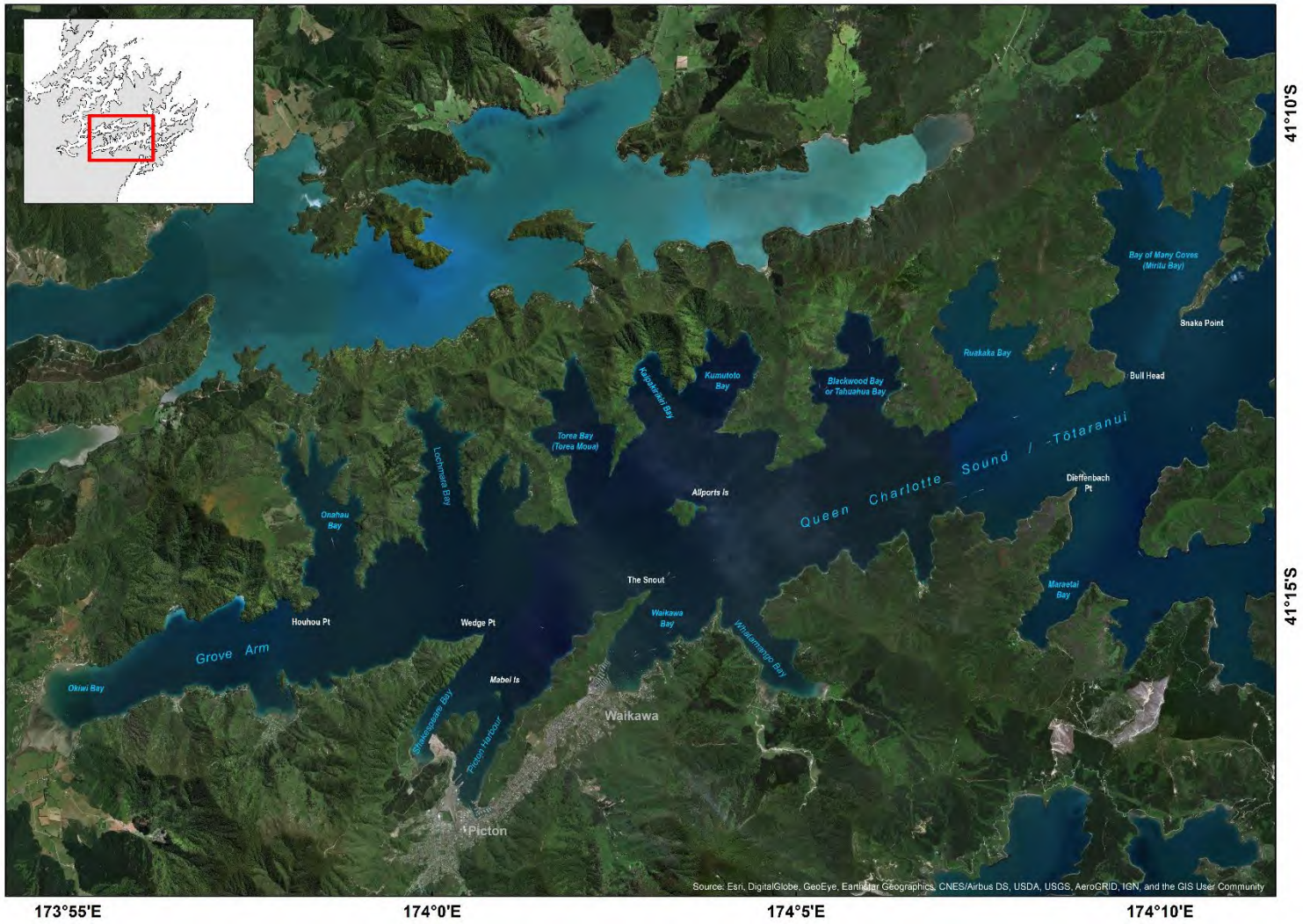

Figure D-2: Locality Map - Inner Queen Charlotte Sound. The major localities are presented here for Inner Queen Charlotte Sound / Tōtaranui Hydrographic Survey (HS51).

Figure D-3: Locality Map - Middle Queen Charlotte Sound. The major localities are presented here for Middle Queen Charlotte Sound / Tōtaranui Hydrographic Survey (HS51).

Figure D-4: Locality Map - Outer Queen Charlotte Sound. The major localities are presented here for Outer Queen Charlotte Sound / Tōtaranui Hydrographic Survey (HS51).

Figure D-5: Locality Map – Tory Channel. The major localities are presented here for Tory Channel / Kura Te Au Hydrographic Survey (HS51).

Appendix E Acknowledgements and Personnel

In a survey of this scale and duration there are many individuals and organisations deserving of formal acknowledgement. None more so than the people and businesses of Picton and the Queen Charlotte Sound region. NIWA thanks you all for embracing us within your community over a year-long field campaign. Your hospitality and support endured long after our work was completed. We acknowledge Te Atiawa o Te Waka-a-Māui, Department of Conservation (DoC) and community members of the Marine Mammal Liaison Group; as well as Land Information New Zealand (LINZ) and Marlborough District Council (MDC). We are also indebted to our three international reviewers, Dr Margaret Dolan (NGU), Dr Vanessa Lucieer (IMAS) and Prof Xavier Lurton (IFREMER) for their constructive criticism and detailed review of our final documents. The following personnel assisted with the field survey of HS51 (Table D-1).

Table E-1: HS51 Survey Personnel.

Staff	Company	Qualification	Position
Mr B.R. Wallen	DML	BSc, IHO Cat A, MNZIS	Relief SIC Nov 2016 – May 2017
Mr D. Stubbing	DML	BSurv, CPHS1, MNZIS, CLM	Initial SIC Oct-Nov 2016
Mr G.J. Cox	DML	IHO Cat A, CPHS1, MNZIS	Backup SIC, Surveyor
Mr K. D. Smith	DML	RPSurv, MNZIS	Contract Manager, Data Processor
Mr C.A. Holmes	DML	IHO Cat A	Surveyor
Mr C. Donselaar	DML	IHO Cat B	Surveyor
Mr B. Waller	DML	BSurv	Surveyor
Mr A. Knyvett	DML	BSurv	Surveyor
Mr D.J. Graham	DML	BSurv	Surveyor
Mr I. Hauman	DML	BSurv	Data Processor
Mr A. Podrumac	DML	MSc (Earth Sciences)	Data Processor
Dr H. Neil	NIWA	PhD (Earth Sciences)	Senior Marine Geologist, Project Director, National Project Manager
Mr S. Wilcox	NIWA	NZCE Electronics and Computer Science	Project Manager and Data Acquisition Operator
Mr J. Hadfield	NIWA	Commercial Launch Master	NIWA Vessels Designated Person Ashore
Mr R. Mitchell	NIWA	Certificate in Occupational Health and Safety level 4 – EMA	HSE Manager
Mr K. Mackay	NIWA	BSc Hons. Geology	Data Acquisition Operator and Data Manager
Mr A. Pallentin	NIWA	Diplom Geologe/Palaeontologe	Data Acquisition Operator
Mr T. Kane	NIWA	MSc. Marine Geology and Geophysics	Data Acquisition Operator and Wader

Staff	Company	Qualification	Position
Mr P. Gerring	NIWA	MSc. Marine Science	Data Acquisition Operator
Mr M. McGlone	NIWA	NZ Offshore Master	RV *Ikatere* Boat Skipper
Mr B. Bennett	NIWA	NZ Offshore Master	RV *Ikatere* Boat Skipper
Mr G. Bennett	NIWA	NZ Coastal Fishing Skipper	RV *Ikatere* Boat Skipper
Mr A. James	NIWA	NZ Coastal Fishing Skipper	RV *Ikatere* Boat Skipper
Mr P. Notman	NIWA	MSc. Hons Marine Biology	RV *Rukuwai* Boat Skipper and Wader
Ms. N. Davey	NIWA	MSc. Hons Marine Biology	Marine Mammal Liaison
Mr N. Eton	NIWA	NZCE Communications and Radar	Electronics Support
Mr J. Forman	NIWA	NZCS. Biology and Microbiology	RV *Rukuwai* Boat Skipper
Mr O. Anderson	NIWA	BSc Hons Zoology	RV *Rukuwai* Boat Skipper
Mr J. Mitchell	NIWA	BSc Geology/Zoology	Field Technician
Dr T Steinmetz	NIWA	PhD (Geoinformatics)	GIS Analyst
Dr A Orpin	NIWA	PhD (Geology)	Internal reviewer
Dr G. Lamarche	NIWA	PhD (Geophysics)	Internal reviewer